

Dear reviewer,

We appreciate your constructive comments for our manuscript. We address your comments point-by-point in the following response.

The manuscript presents results from a modelling exercise to study how the delivery of annual rainfall impacts ecosystems. The Authors used scenarios of given annual rainfall amounts occurring at different rates (and thus different amounts per event) and with different durations of the rainy season; the scenarios are applied to Africa, focusing on biomass productivity (GPP) and soil moisture, which, as I understood, is interpreted to be the key driver of GPP. Even though the manuscript addresses a topic that is likely of interest to the audience of Biogeosciences, it is not well written; there are several grammatical errors and some parts (especially the methods) were not very clear. I have listed below specific comments as they appeared in the text.

Response: Thank you very much for your positive assessment and constructive comments. As this work aims to study the impact of intra-seasonal rainfall variability on ecosystem function (e.g. GPP) and biome distribution, we did use soil moisture pattern to explain the shifts in GPP and biome distribution.

In the revised manuscript, all the coauthors have helped improving the language and presentation. Please refer to the updated manuscript attached at the end of this reply.

- Page 7577, Line 11: it is not clear what the Author meant with ‘second-order climate statistics’.

Response: We change it to “intra-seasonal climate variabilities”.

- P7580, L10-15: the Authors mention here that MAP is given by the product of 3 rainfall characteristics, but in reality they define MAP as a product of 4 parameters, α , λ , T_w , and f_w . I do not think that the term ‘normalized’ used in the context of ‘ f_w ’ is correct here. I think it should also be said here that the rainfall statistics in the wet and dry season are not different (now, this is said at P7592). This part should be better explained.

Response: We realize that the writing in the previous manuscript causes the confusion, and we have clarified this point in the revised manuscript. Please see the following revised text:

“We manipulate rainfall changes through a stochastic weather generator based on a parsimonious model of rainfall processes (Rodriguez-Iturbe et al., 1984). We model the total amount of rainfall during wet season as a product of the three intra-seasonal rainfall characteristics for the wet season, rainfall frequency (λ , event/day), rainfall intensity (α , mm/event), and rainy season length (T_w , days) (More details in section 2.3).”

We actually treat wet and dry season separately for their frequency and intensity, which has been explained in detail in section 2.3. We also revised that section to make it clearer to follow:

“The stochastic rainfall model can be expressed as $MAP = \alpha \lambda T_w / f_w$, and we set f_w to be 0.9, i.e. the period including 90% of total annual rainfall is defined as “rainy season” (exchangeable with “wet season” hereafter). In particular, we first use Markham (1970)’s

approach to find the center of the rainy season, and then extend the same length to both sides of the center until the total rainfall amount in this temporal window (i.e. “rainy season”) is equal to 90% of the total annual rainfall. Rainy season and dry season have their own rainfall frequency and intensity. Two seasons are separately modeled based on the Market Poisson Process. Here we only focus on and manipulate rainy-season rainfall characteristics in our study, as rainy-season rainfall accounts for almost all the meaningful rainfall inputs for plant use. Thus in the following paper, whenever we mention α or λ , we refer to the rainy season.”

- P7580, L19: this line repeats exactly what said 3 lines before.

Response: We revised this part as follows:

“The SEIB-DGVM also allows the development of annual and perennial grasses as well as multiple life cycles of grass at one year based on environmental conditions. Multiple life cycles of tree growth per year are possible in theory but rarely happen in simulations (Sato and Ise, 2012). Soil moisture status is a predominant factor to determine the optimum LAI of the grass layer, which influences maximum daily production and leaf phenology.”

- P7581, L12: what is the rooting depth adopted in the model. Did it vary spatially?

Response: Each plant-functional-type (PFT) in the SEIB-DGVM model has its own inherent rooting depth. Thus rooting depths vary explicitly in space based on the biome distribution, resulted from vegetation dynamics and competition. Different rooting depth also means that each plant simulated in the SEIB-DGVM has different capacity to use soil moisture at different layers of soil. We clarify this point in the revised manuscript.

- P7581, L17: the Authors mention here that ‘other environmental conditions’ affect Lai and so NPP. What are these other conditions? The Authors focus on soil moisture, which is considered the main variable and it is used to interpret the data. However, I think it would be better to report also other variables and explain why their role is not as important as soil moisture.

Response: We tended to be more inclusive and that is why we wrote “other environmental conditions”. In reality, the soil moisture pattern can explain most changes of GPP in woodlands and savannas (Figure 5). The only divergence happens in the tropical forests (Figure 5a and 5b), which is mostly due to the reason that tropical forests in SEIB-DGVM are not water-limited but radiation-limited. Thus, though soil moisture increases with increased rainfall frequency in tropical forests (Figure 5a), GPP instead decreases due to increased cloudiness (Figure 5b), as we have already discussed in Section 3.1 (specifically Pattern 1.3).

For the relevant text, we have changed it as follows:

“Soil moisture status is the predominant factor to determine LAI of the grass layer, which influences maximum daily productivity and leaf phenology. When LAI exceeds 0 for 7 continuous days, dormant phase of perennial grass layer changes into growth phase. While when LAI falls below 0 for 7 continuous days, growth phase switches to dormant phase (Sato et al, 2007).”

- P7582, L3-5: please, re-phrase this part.

Response: This part has been revised as follows:

“Two plant function types (PFTs) of tropical woody species are simulated by the SEIB-DGVM in Africa: tropical evergreen trees and tropical deciduous trees. The distribution of these two woody types is largely determined by hydro-climatic environments in the model. Tropical evergreen trees only develop in regions where water resources are sufficient all year around, so they can maintain leaves for all seasons; otherwise, tropical deciduous trees could survive and dominate the landscape as they can shed leaves if there is no sufficient water supply in its root zone during the dry season (Sato and Ise, 2012).”

- P5782, L11: how were 30 years used to drive the 2000-year warm-up period?

Response: We repeatedly use the 30-year climate forcing for 2000 years for the spin-up period. We have clarified this point in the revised manuscript.

- P7583: daily rainfall is generated using a marked Poisson process with frequency of daily rainfall and daily rainfall depths exponentially distributed. According to Fig. 1, it seems that this approximation is not realistic. I think the Authors should justify this assumption.

Response: We recognize the reviewer’s concern, though we are afraid that there is a misunderstanding here. Figure 1 provides the spatial patterns of rainfall frequency, intensity and rainy season length, and these spatial patterns do not reflect the temporal feature of the rainfall distribution at a single point.

The Market Poisson process has been validated and widely used as a stochastic rainfall model in the past (see the following references [1]-[4] have been cited in the manuscript too). Thus, we feel that citing these references may be sufficient here for the methods, and we have also clarified the text to make it easier to follow.

References:

[1] Rodr ́guez-Iturbe, I. and Porporato, A.: Ecohydrology of Water-Controlled Ecosystems: Soil Moisture And Plant Dynamics, Cambridge University Press, Cambridge, United Kingdom, 2004.

[2] Porporato, A., Laio, F., Ridolfi, L., and Rodr ́guez-Iturbe, I.: Plants in water-controlled ecosystems: active role in hydrologic processes and response to water stress – III. Vegetation water stress, *Adv. Water Resour.*, 24, 725–744, 2001.

[3] Rodr ́guez-Iturbe, I., Gupta, V. K., and Waymire, E.: Scale considerations in the modeling of temporal rainfall, *Water Resour. Res.*, 20, 1611–1619, 1984.

[4] Rodr ́guez-Iturbe, I., Porporato, A., Ridolfi, L., Isham, V., and Cox, D. R.: Probabilistic modeling of water balance at a point: the role of climate, soil and vegetation, *P. Roy. Soc. A-Math. Phys.*, 10 455, 3789–3805, 1999.

- P7584, L28: from P7583 L6-7 and L14, it looks like T_w is a stochastic variable; how was the fix value defined in Exp 1 simulations? Specifically, in sections 3.2 and 3.3 the Authors refer to values of T_w (not its statistics) and comment on the large impact that this parameter has on the results. This is an important point and it needs to be clear how this parameter was determined in

order to understand the results.

Response: Thanks for pointing this out. We have revised the relevant text as follows:

“The stochastic rainfall model can be expressed as $MAP = \alpha \lambda Tw / fw$, and we set fw to be 0.9, i.e. the period including 90% of total annual rainfall is defined as “rainy season” (exchangeable with “wet season” hereafter). In particular, we first use Markham (1970)’s approach to find the center of the rainy season, and then extend the same length to both sides of the center until the total rainfall amount in this temporal window (i.e. “rainy season”) is equal to 90% of the total annual rainfall. Rainy season and dry season have their own rainfall frequency and intensity. Two seasons are separately modeled based on the Market Poisson Process. Here we only focus on and manipulate rainy-season rainfall characteristics in our study, as rainy-season rainfall accounts for almost all the meaningful rainfall inputs for plant use. Thus in the following paper, whenever we mention α or λ , we refer to the rainy season.”

Also see:

“All the necessary parameters to fit for the stochastic rainfall (including the mean and variance of rainfall frequency, intensity and length of wet and dry seasons) were derived from the satellite-gauge-merged rainfall measurement from TRMM 3b42V7 (Huffman et al., 2007) for the period of 1998 to 2012, based on the above assumptions for the rainfall process. Specifically, we applied our definition of “rainy season” to each year of the TRMM rainfall data for per pixel, and calculated the mean and variance of the “rainy season length”, using which we fitted the beta distribution for Tw . For rainfall frequency and intensity, we lumped all the wet or dry season rainfall record together to derive their parameters.”

- P7586, L6-7: rainfall intensity is defined as 1 mm, which is a depth. It should be 1mm day⁻¹ or it should be referred to as rainfall depth per event.

Response: We revised the unit for rainfall intensity as: mm/event; the unit for rainfall frequency as: events/day. Thanks for pointing this out.

- P7587, L13-16: this phrase was not clear to me. Please, re-phrase.

Response: We revised the text as follows:

“The relationship of GPP sensitivity to MAP and rainfall intensity (Fig. 6c) is complex and has no clear patterns as previous ones, mostly because the GPP sensitivity space that most pixels cluster (Fig. A4c) also contains large uncertainties (Fig. A4d, shown as large variance in the data). Thus we will not over-interpret the pattern in Fig. 6c.”

- P7588, L3: how is s^* defined?

Response: We put the following text under the Equation (2) in the revised manuscript:

“Figure 2 provides a schematic diagram of “water stress factor” from the SEIB-DGVM, and we also include an approximated linear model that has been widely adopted elsewhere (e.g. Milly, 1992; Porporato et al., 2001). The linear model uses an extra variable S^* , so called “critical point” of soil moisture: when $S > S^*$, there is no water stress (water stress factor =1); and when $S < S^*$, water stress factor linearly decreases with the decrease of S . Though SEIB-DGVM adopts a quadratic form for “water stress factor”, it essentially functions

similarly as the linear model, such that S^* distinguishes two soil moisture regimes that below which there is a large sensitivity of water stress to soil moisture status, and above which there is little water stress. Understanding how this “water stress factor” functions is the key to explain the following results.”

- P7591, L24: I do not think that the term ‘understand’ is correct here. Considering the limitations of the model, the model is used for interpretation more than understanding.

Response: We accept the reviewer’s suggestion, and change “understand” to be “interpret”.

- P7592, L11-12: I would erase the word ‘still’ (‘: : in reality they have seasonal variations’).

Response: We accept the reviewer’s suggestion and have made the corresponding revision.

- P7593, L12: a rainfall frequency of 0.35 day⁻¹ is not very low.

Response: We change to the following text:

“We identify that negative GPP sensitivity with increased rainfall frequency is possible at very low MAP range (~400 mm year⁻¹) with relatively low rainfall frequency (<0.35 events/day) (Fig. 6a)”.

- P7594, L15-16: I thought α and λ also described the dry season. This is confusing.

Response: We agree that our text is confusing and we made the changes to clarify it.

In the rainfall model, we have wet season (including 90% of the total annual rainfall) and dry season (having 10% of the total annual rainfall). Wet season and dry season have their own rainfall frequency and intensity, derived from the TRMM rainfall data. In the experiments we only apply the changes of rainfall frequency/intensity for wet season, while always use the climatological value for dry season. For example, if we need to increase rainfall frequency by 10% in one experiment, we only apply the change to the wet-season rainfall frequency, and keep the dry-season rainfall frequency unchanged, and then we use the Market Poisson Process to simulate the daily rainfall for wet and dry season separately.

Thus when we use “rainfall frequency” and “rainfall intensity” in the manuscript, we refer to the values during wet-season, as dry-season rainfall characteristics are fixed at the climatological values. Besides, dry-season also only accounts for 10% of the total rainfall, and has little importance for the ecosystem changes.

We have clarified this point in the revised manuscript as follows:

“The stochastic rainfall model can be expressed as $MAP = \alpha \lambda T_w / f_w$, and we set f_w to be 0.9, i.e. the period including 90% of total annual rainfall is defined as “rainy season” (exchangeable with “wet season” hereafter). In particular, we first use Markham (1970)’s approach to find the center of the rainy season, and then extend the same length to both sides of the center until the total rainfall amount in this temporal window (i.e. “rainy season”) is equal to 90% of the total annual rainfall. Rainy season and dry season have their own rainfall frequency and intensity. Two seasons are separately modeled based on the Market Poisson Process. Here we only focus on and manipulate rainy-season rainfall

characteristics in our study, as rainy-season rainfall accounts for almost all the meaningful rainfall inputs for plant use. Thus in the following paper, whenever we mention α or λ , we refer to the rainy season.”

- Fig. 1: panel b: rainfall intensity should be depth. Panels e-h do not look like histograms; how were they normalized?

Response: Thanks for pointing this out. They are normalized histogram that the areas of the histogram should be added up to 1, but we forgot to provide the bins of x-axis for each data in the figure caption. We attached the bins for the histogram in the revised manuscript:

“e-f: Normalized histograms of the rainfall characteristics in two savanna regions of West and Southwest Africa. e-MAP (bin width for the x-axis: 100 mm/year); f-rainfall intensity (bin width for the x-axis: 1 mm/event); g-rainfall frequency (bin width for the x-axis: 0.1 event/day); h-rainy season length (bin width for the x-axis: 20 days).”

- Fig. 2: I would remove this figure.

Response: We accept the reviewer’s suggestion and have removed this figure in the revised manuscript.

- Fig. 3: this figure is not very useful. The linearized model and s^* are not used here.

Response: We decide to keep this figure as it helps the explanations of the hydrological mechanism. We also added the explanation of S^* under the Equation (2):

“Figure 2 provides a schematic diagram of “water stress factor” from the SEIB-DGVM, and we also include an approximated linear model that has been widely adopted elsewhere (e.g. Milly, 1992; Porporato et al., 2001). The linear model uses an extra variable S^* , so called “critical point” of soil moisture: when $S > S^*$, there is no water stress (water stress factor =1); and when $S < S^*$, water stress factor linearly decreases with the decrease of S . Though SEIB-DGVM adopts a quadratic form for “water stress factor”, it essentially functions similarly as the linear model, such that S^* distinguishes two soil moisture regimes that below which there is a large sensitivity of water stress to soil moisture status, and above which there is little water stress. Understanding how this “water stress factor” functions is the key to explain the following results.”

Also, I believe that this is not a water stress factor as defined in Porporato et al. (2001), but is more a reduction function for transpiration. The water stress is lower at high soil moisture and increases as soil moisture decreases.

Response: The reviewer’s assessment is correct that Equation (1) and (2) provide a reduction function for transpiration; what we are saying here is that this concept is similar as Porporato et al. (2001), which is basically the reversed form of Equation (2).

We clarified this point in the revised manuscript.

Fig. 6: it would be nice to have more explanation in the text on how this figure is generated.

Response: We have added the following text in the revised manuscript:

“Figure 6 further shows the difference of simulated GPP as a function of MAP and a perturbed rainfall characteristic in the corresponding experiment, to explore how MAP and

these rainfall characteristics affect the simulated GPP. We term Figure 6 as “GPP sensitivity space”, and “positive GPP sensitivity” means that GPP changes at the same direction with MAP or rainfall characteristics, and vice versa for “negative GPP response”. These “GPP sensitivity spaces” are generated based on the aggregated mean GPP in each bin of the rainfall properties. The bin size for MAP, rainfall frequency, rainfall intensity and rainy season length are 100 mm/year, 0.05 event/day, 1 mm/event and 15 days respectively. We also provide the standard error (SE) of GPP in each bin to assess the uncertainties of the “GPP

sensitivity spaces”, with higher SE meaning larger uncertainties. $SE = \frac{\sigma}{\sqrt{n}}$, where σ and n refer to the standard deviation of GPP values and the sample size in each bin respectively.”

Again, thank you very much for taking your precious time in reviewing our manuscript and providing constructive comments! Please let us know whether you are satisfied with our responses, and we will try our best to address any extra concerns and suggestions.

Best wishes,

Kaiyu Guan, on behalf of all the authors

The attached files:

- 1) revised manuscript with all the editing marks
- 2) final revised manuscript without any marks

1 **Continental-scale impacts of intra-seasonal rainfall variability**
2 **on simulated ecosystem responses in Africa**

3
4 Kaiyu Guan^{1,2*}, Stephen P. Good³, Kelly K. Caylor¹, Hisashi Sato⁴, Eric F. Wood¹, and
5 Haibin Li⁵

6
7 ¹Department of Civil and Environmental Engineering, Princeton University, Princeton,
8 NJ, USA

9 ²Department of Environmental & Earth System Science, Stanford University, Stanford,
10 CA 94025, USA

11 ³Department of Geology and Geophysics, University of Utah, Salt Lake City, UT
12 84112, USA

13 ⁴Graduate School of Environmental Studies, Nagoya University, D2-1(510) Furo-cho,
14 Chikusa-ku, Nagoya-city, Aichi 464-8601, Japan

15 ⁵Department of Earth and Planetary Sciences, Rutgers University, Piscataway, NJ
16 08854, USA

Formatted: Font: 12 pt

17
18 *Corresponding author:

19 Kaiyu Guan

20 Department of Environmental & Earth System Science,
21 Stanford University, Stanford, CA 94025, USA

22 Phone: 609-647-1368, Fax: 650-498-5099

23 Email: kaiyug@stanford.edu

24
25 Running title: Ecological Impacts of Intra-Seasonal Rainfall Variability

26
27 Submitted to *Biogeosciences*

28

29 **Abstract:**

30 Climate change is expected to ~~result in an increase change of~~ intra-seasonal rainfall
31 variability, ~~which has arisen~~ arising from ~~concurrent~~ shifts in rainfall frequency,
32 intensity and seasonality. ~~These intra-seasonal C~~ changes in intra-seasonal rainfall
33 ~~variability~~ are likely to have important ecological impacts ~~for on~~ terrestrial
34 ecosystems. ~~Yet, and~~ quantifying these impacts across biomes and large climate
35 gradients is ~~required largely missing~~. This gap hinders our ability to for a better
36 ~~prediction of~~ ecosystem services and their responses to climate change, esp. for arid
37 and semi-arid ecosystems. Here we use a synthetic weather generator and an
38 ~~independently validated~~ advanced vegetation dynamic model (SEIB-DGVM) to
39 virtually conduct a series of “rainfall manipulation experiments” to study how
40 changes in the intra-seasonal rainfall variability affect continent-scale ecosystem
41 responses across Africa. We generated different rainfall scenarios with fixed total
42 annual rainfall but shifts in: i) frequency vs. intensity, ii) rainy season length ~~seasonality~~
43 vs. frequency, iii) intensity vs. rainy seasonality ~~season length~~. These scenarios were
44 fed into ~~the~~ SEIB-DGVM to investigate changes in biome distributions and ecosystem
45 productivity. We find a loss of ecosystem productivity with increased rainfall
46 frequency and decreased intensity at very low rainfall regimes (<400 mm/year) and
47 low frequency (<0.3 ~~day⁻¹ event/day~~); beyond these very dry regimes, most
48 ecosystems benefit from increasing frequency and decreasing intensity, except in the
49 wet tropics (>1800 mm/year) where radiation limitation prevents further productivity
50 gains. This finding result reconciles seemingly contradictory findings in previous field
51 studies ~~on the direction of~~ rainfall frequency/intensity impacts on ecosystem
52 productivity. We also find that changes in rainy season length can yield more dramatic
53 ecosystem responses compared with similar percentage changes in rainfall frequency
54 or intensity, with the largest impacts in semi-arid woodlands. This study demonstrates
55 that not all rainfall regimes are ecologically equivalent, and that intra-seasonal rainfall
56 characteristics play a significant role in influencing ecosystem function and structure
57 through controls on ecohydrological processes. Our results also suggest that shifts in
58 rainfall seasonality have potentially large impacts on terrestrial ecosystems,

59 ~~something that~~ and these understudied impacts should be explicitly examined in future
60 studies of climate impacts.

61 **Keywords:** rainfall frequency, rainfall intensity, rainfall seasonality, biome
62 distribution, Gross Primary Production (GPP), Africa

63

64

65 **1. Introduction**

66 Due to increased water holding capacity in the atmosphere as a consequence of global
67 warming (O’Gorman and Schneider, 2009), rainfall is projected to ~~vary~~ change in
68 intensity and frequency across much of the world (Easterling et al., 2000; Trenberth et
69 al., 2003; Chou et al., 2013), in conjunction with complex shifts in rainfall seasonality
70 (Feng et al., 2013; Seth et al., 2013). ~~These changes possibly~~ is indicates a large
71 increase in the frequency of extreme events and variability in rainfall (Easterling et al.,
72 2000; Allan and Soden, 2008), and many of these changes may be accompanied with
73 little changes in total annual rainfall (Knapp et al., 2002; Franz et al., 2010).
74 Meanwhile, regions sharing similar mean climate state may have very different
75 intra-seasonal ~~dynamics~~ variabilities, and the ecological significance of intra-seasonal
76 ~~climate variabilities~~ second-order climate statistics has been largely overlooked
77 previously in terrestrial biogeography (Good and Caylor, 2011). For example,
78 ecosystems in West Africa and Southwest Africa (Figure 1) share similar total annual
79 rainfall, but West Africa has much more intense rainfall events within a much shorter
80 rainy season, while Southwest Africa has a longer and less intense rainy season. The
81 same amount of total rainfall can come in very different ways, which may cause
82 distinctive ecological-ecosystem responses and landscapestructure. Understanding the
83 impacts of these regional differences in intra-seasonal rainfall variability and their
84 possible future changes on terrestrial ecosystems is critical for maintaining ecosystem
85 services and planning adaptation and mitigation strategies for ecological and social
86 benefits (Anderegg et al., 2013).

87

88 [insert Figure 1]

89

90 The changes in intra-seasonal rainfall characteristics, specifically frequency,
91 intensity and seasonality, have critical significance to ecosystem productivity and
92 structure (Porporato et al., 2001; Weltzin et al., 2003; Williams and Albertson, 2006;
93 Good and Caylor, 2011; Guan et al., 2014), but previous studies on this topic
94 (summarized in Table 1) have their limitations in the following aspects. First, existing

Formatted: Font color: Black

Formatted: Font: 12 pt, Not Bold, Font color: Black

Formatted: Font color: Black

95 relevant field studies ~~on this topic~~ mostly focus on a single ecosystem, *i.e.* grasslands,
96 and subsequently only low rainfall regimes have been examined to date (mostly below
97 800mm/year, see Table 1). Grasslands have the largest sensitivity to hydrological
98 variabilities among all natural ecosystems (Scanlon et al., 2005; Guan et al., 2012),
99 however inferences drawn from a single ecosystem are limited in scope and difficult
100 to apply to other ecosystems ~~and rainfall regimes~~. Second, even within grasslands,
101 different studies have seemingly contradictory findings (see Table 1), and there is a
102 lack of a comprehensive framework to resolve these inconsistencies. Specifically,
103 whether increased rainfall intensity with decreased rainfall frequency has positive
104 (Knapp et al., 2002; Fay et al., 2003; Robertson et al., 2009; Heisler-White et al., 2009)
105 or negative impacts (Heisler-White et al., 2009; Thomey et al., 2011) on grassland
106 productivity is still under debateable. Third, previous relevant studies mostly focus on
107 the impacts of rainfall frequency and intensity (Table 1 and Rodríguez-Iturbe and
108 Porporato, 2004), and largely ~~neglect-overlook~~ the possible changes in rainfall
109 seasonality. Rainfall frequency and intensity mostly describe rainfall characteristics
110 within the rainy season, but do not account for the impacts of interplay between rainy
111 season length and dry season length (Guan et al., 2014). For ecosystems
112 predominately controlled by water availability, rainy season length constrains the
113 temporal niche for active plant physiological activities (van Schaik et al., 1993;
114 Scholes and Archer, 1997), and large variations in rainfall seasonality can lead to
115 significant shifts in biome distribution found from paleoclimate pollen records (e.g.
116 Vincens et al., 2007). Given changes in rainfall seasonality have been found in various
117 tropical regions (Feng et al., 2013) and have been projected in future climate (Biasutti
118 and Sobel, 2009; Shongwe et al., 2009; Seth et al., 2013), studies investigating their
119 impacts on terrestrial ecosystems are relatively rare, and very few field studies are
120 designed to address this aspect (Table 1, Bates et al., 2006; Svejcar et al., 2003; Chou
121 et al., 2008). Finally, there is an increasing trend of large-scale studies addressing
122 rainfall variability and ecological responses using satellite remote sensing (Fang et al.,
123 2005; Zhang et al., 2005; Good and Caylor, 2011; Zhang et al., 2013; Holmgren et al.,
124 2013) and flux network data (Ross et al., 2012). These large-scale studies are able to

125 expand analyses to more types of ecosystems and different climate conditions, and
126 provide valuable observation-based insights. However there are very few theoretical
127 modeling works to corroborate this effort. All these above issues call for a
128 comprehensive modeling study to investigate different aspects of intra-seasonal
129 rainfall variability on terrestrial ecosystems spanning large environmental gradients
130 and various biomes.

131 In this paper, we aim to study ecological impacts of intra-seasonal rainfall
132 variability on terrestrial ecosystems. In particular, we design virtual “rainfall
133 manipulation experiments” to concurrently shift intra-seasonal rainfall characteristics
134 without changing total annual rainfall. We focus on the impacts of these different
135 rainfall scenarios on ecosystem productivity (e.g. Gross Primary Production, GPP)
136 and biome distributions in the African continent, simulated by an advance
137 independently validated dynamic vegetation model SEIB-DGVM (Sato and Ise, 2012).
138 Previous modeling approaches in this topic (Gerten et al., 2008; Hély et al., 2006)
139 designed various rainfall scenarios by rearranging (halving, doubling or shifting) the
140 rainfall amount based on the existing rainfall observations. In contrast to these
141 approaches, we design a weather generator based on a stochastic rainfall model
142 (Rodríguez-Iturbe et al., 1999), which allows us to implement a series of experiments
143 by synthetically varying two of the three rainfall characteristics (rainfall intensity,
144 rainfall frequency, and rainy season length) while fixing total annual rainfall at the
145 current climatology. We choose Africa as our test-bed mostly because the following
146 two reasons: (1) the rainfall regimes and biomes have large gradients varying from
147 extremely dry grasslands to highly humid tropical evergreen forests, ~~and thereby~~
148 ~~provide a large pool of different biomes~~; (2) Africa is a continent usually assumed to
149 have few temperature constraints (Nemani et al., 2003), which will help to isolate the
150 impacts of precipitation from temperature, as one challenge in attributing climatic
151 controls on temperate ecosystems or Mediterranean ecosystems is the superimposed
152 influences from both temperature and precipitation. The overarching science question
153 we will address is: **How do African ecosystems respond to possible changes in**
154 **intra-seasonal rainfall variability (i.e. rainfall frequency, intensity and rainy**

155 **season length)?**

156

157 [insert Table 1]

158

159 **2. Materials and Methods:**

160 **2.1 Methodology overview**

161 Table 1 summarizes previous field-based rainfall manipulation experiments, such as

162 ~~the one that Knapp et al. (2002) did in a grassland~~ that concurrently increasing rainfall
163 frequency and decreasing rainfall intensity while fixing total rainfall ~~for a grassland.~~

164 The central idea of our study is to design similar rainfall manipulation experiments
165 but test them virtually in the model domain across large environment gradients. ~~We~~

166 ~~manipulate rainfall changes through a weather generator based on a parsimonious~~
167 ~~stochastic rainfall model (Rodriguez-Iturbe et al., 1984). We model the total amount~~

168 ~~of rainfall during rainy season as a product of the three intra-seasonal rainfall~~
169 ~~characteristics for the rainy season, rainfall frequency (λ , event/day), rainfall intensity~~

170 ~~(α , mm/event), and rainy season length (T_w , days) (More details in section 2.3). We~~
171 ~~manipulate rainfall changes through a stochastic weather generator based on a~~

172 ~~parsimonious model of rainfall processes: statistically for the daily rainfall record, the~~
173 ~~mean annual precipitation (MAP) is a product of the three rainfall characteristics for~~

174 ~~the wet season, rainfall frequency (λ , day⁻¹), rainfall intensity (α , mm), and rainy~~
175 ~~season length (T_w , days), normalized by f_w (the fraction of wet season rainfall to the~~

176 ~~MAP) to account for the contribution from dry season rainfall ($MAP = \alpha \lambda T_w / f_w$).~~
177 Thus it is possible to simultaneously perturb two of the rainfall characteristics away

178 from their climatological values while preserving the mean annual precipitation (MAP)
179 unchanged (Figure 2). We then feed these different rainfall scenarios into a

180 well-validated dynamic vegetation model (SEIB-DGVM, section 2.2) to study
181 simulated ecosystem responses. Detailed experiments design is described in section

182 2.5.

183

184 [insert Figure 2]

Formatted: Font color: Black

Formatted: Font: 12 pt, Not Bold, Font color: Black

Formatted: Font: Not Bold, Font color: Black

Formatted: Font: 12 pt, Not Bold, Font color: Black

Formatted: Font: Not Bold, Font color: Black

Formatted: Font: 12 pt, Not Bold, Font color: Black

Formatted: Font: Not Bold, Font color: Black

Formatted: Font: 12 pt, Not Bold, Font color: Black

Formatted: Font: Not Bold, Font color: Black

Formatted: Font: 12 pt, Not Bold, Font color: Black

Formatted: Font: Not Bold, Font color: Black

Formatted: Font: 12 pt, Not Bold, Font color: Black

Formatted: Font color: Black

185

186 **2.2 SEIB-DGVM model and its performances in Africa**

187 We use a well-validated vegetation dynamic model SEIB-DGVM (Sato et al., 2007)
188 as the tool to study ecosystem responses to different rainfall variabilities. This model
189 follows the traditional “gap model” concept (Shugart, 1998) to explicitly simulate the
190 dynamics of ecosystem structure and function for individual plants ~~the dynamics of~~
191 ~~fine scale ecosystem structure and function for~~ at a set of virtual vegetation patches,
192 and uses results at these virtual patches as a surrogate to represent large-scale
193 ecosystem states. Thus individual trees are simulated from establishment, having
194 competition with other plants, to death, which creates “gaps” in which for different
195 plant function types (PFTs) to other plants to occupy and develop. ~~The~~ SEIB-DGVM
196 includes mechanical-based and empirical-based algorithms for land physical
197 processes, plant physiological processes, and plant dynamic processes. ~~The~~
198 SEIB-DGVM contains algorithms that explicitly involve the mechanisms of
199 plant-related water stress (~~Figure 3~~ Figure 2; Sato and Ise, 2012). With S similar
200 concepts to previous studies (e.g. Milly, 1992; Porporato et al., 2001), the current
201 ~~SEIB model~~ SEIB-DGVM implements a continuous “water stress factor” (Equation 2)
202 based on the soil moisture status (Equation 1), scaling from 0 (most stressful) to 1
203 (with no stress), which then acts to scale the stomatal conductance for plant
204 transpiration and carbon assimilation.

$$205 \quad stat_{water} = (S - S_w) / (S_f - S_w) \quad (\text{Equation 1})$$

$$206 \quad \text{Water stress factor} = 2 * stat_{water} - stat_{water}^2 \quad (\text{Equation 2})$$

207 where S, S_w and S_f refer to the fraction of volumetric soil water content within the
208 rooting depth, at the wilting point, and at field capacity, respectively. Figure 2
209 provides a schematic diagram of “water stress factor” from the SEIB-DGVM, and we
210 also include an approximated linear model that has been widely adopted elsewhere
211 (e.g. Milly, 1992; Porporato et al., 2001). The linear model uses an extra variable S*,
212 so called “critical point” of soil moisture: when S>S*, there is no water stress (water
213 stress factor =1); and when S<S*, water stress factor linearly decreases with the
214 decrease of S. Though SEIB-DGVM adopts a quadratic form for “water stress factor”.

215 it essentially functions similarly as the linear model, such that S^* distinguishes two
216 soil moisture regimes that below which there is a large sensitivity of water stress to
217 soil moisture status, and above which there is little water stress. Understanding how
218 this “water stress factor” functions is the key to explain the following results.

219

220 [insert Figure 2]

221

222 ~~The~~ SEIB-DGVM also allows ~~the~~ development of annual and perennial grasses as
223 well as multiple life cycles of grass at one year based on environmental conditions ~~;~~
224 ~~and m~~Multiple life cycles of tree growth per year are possible in theory but rarely
225 happen in simulations (Sato and Ise, 2012). Soil moisture status is the predominant
226 factor to determine LAI of the vegetation layer, which influences maximum daily
227 productivity and leaf phenology. In particular, life cycles of grass are under prominent
228 control of soil moisture status. The previously defined “water stress factor” and other
229 environmental conditions co-determine the optimum LAI of the grass layer, which
230 influences maximum daily NPP and the leaf phenology. When optimum LAI exceeds
231 0 for preceding 7 continuous days, the dormant phase of perennial vegetation layer
232 changes into the growth phase; ~~w~~While when optimum LAI falls below 0 for
233 preceding 7 continuous days, the growth phase changes switches into to the dormant
234 phase (Sato et al, 2007). SEIB-DGVM also explicitly simulates ~~the~~ light conditions
235 and light competitions among different PFTs in the landscape based on its simulated
236 its simulation of 3D canopy structure and radiative transfer scheme (Sato et al, 2007).

237

238 [insert Figure 3]

239

240 ~~The~~ SEIB-DGVM has been tested both globally (Sato et al., 2007) and regionally
241 for various ecosystems (Sato et al., 2010; Sato, 2009; Sato and Ise, 2012), ~~which~~
242 whose simulated results compared favorably with ground observations and satellite
243 remote sensing measurements in terms of for ecosystem composition, structure and
244 function. In particular, ~~the~~ SEIB-DGVM has been successfully validated and

Formatted: Font: Not Bold

Formatted: Font: Not Bold

Formatted: Font: Not Bold

245 demonstrated its ability in simulating ecosystem structure and function in the African
246 continent (Sato and Ise, 2012). Two plant function types (PFTs) of tropical woody
247 species are simulated by SEIB-DGVM in Africa: tropical evergreen trees and tropical
248 deciduous trees. The distribution of these two woody types in the simulation is largely
249 determined by hydro-climatic environments. Tropical evergreen trees only develop in
250 regions where water resources are sufficient all year around, so they can maintain
251 leaves for all seasons; otherwise, tropical deciduous trees could survive and dominate
252 the landscape as they can shed leaves if there is no sufficient water supply in its root
253 zone during the dry season (Sato and Ise, 2012). For woody species, two plant
254 function types (PFTs) of tropical woody species are modeled in Africa: tropical
255 evergreen trees and tropical deciduous trees, which distinguish in their phenology,
256 with the former having leaves all year around, and the latter shedding leaves during
257 dry season, which is mostly controlled by root zone moisture status (Sato and Ise,
258 2012). Trees and grasses coexist in a cell, with the floor of a virtual forest
259 monopolized by one of the two grass PFTs, C₃ or C₄ grass. T, the dominating grass
260 type of which type is determined at the end of each year by air temperature,
261 precipitation, and CO₂ partial pressure (Sato and Ise, 2012).

Formatted: Font: Not Bold

Formatted: Font: Not Bold

262 ~~The SEIB model~~SEIB-DGVM was run at a ~~one degree~~1° ~~spatial resolution and~~
263 at a ~~the~~ daily ~~temporal resolution~~step. It was spun-up for 2000 years driven by the
264 observed climate (1970-2000) repeatedly for the soil carbon pool to reach steady state,
265 followed by 200 years simulation driven by the forcings based on the experiment
266 design in Section 2.4. Because our purpose is to understand the direct impacts of
267 intra-seasonal rainfall variability, we turned off the fire component of ~~the SEIB~~
268 ~~model~~SEIB-DGVM to exclude fire-mediated feedbacks in the results. Though we are
269 fully aware of the important role of fire in interacting with rainfall seasonality and
270 ~~thus in their influenceing on~~ African ecosystems ~~productivity and structures~~ (Bond et
271 al., 2005; Lehmann et al., 2011; Staver et al., 2012), studying these interactions is
272 beyond the scope of this work. For the similar reason, we fixed the atmospheric CO₂
273 concentration at 380 ppmv to exclude possible impacts of CO₂ fertilization effects.

Formatted: Font: Times New Roman

274

275 2.3 Synthetic weather generator

276 The synthetic weather generator used here ~~consists of~~ has two major components: i) to
277 stochastically generate daily rainfall based on a stochastic rainfall model, and ii) to
278 conditionally sample all other environmental variables from historical records to
279 preserve the covariance among climate ~~forcing~~ forcing ~~foreing inputs~~ variables.

280 The stochastic rainfall model can be ~~statistically~~ expressed as $MAP = \alpha \lambda T_w / f_w$,
281 and we set f_w to be 0.9, i.e. the period including 90% of total annual rainfall is defined
282 as “~~wet~~ wet season” (exchangeable with “~~rainy~~ wet season” hereafter). In particular,
283 we first use Markham (1970)’s approach to find the center of the rainy season, and
284 then extend the same length to both sides of the center until the total rainfall amount
285 in this temporal window (i.e. “rainy season”) is equal to 90% of the total annual
286 rainfall. Rainy season and dry season have their own rainfall frequency and intensity.
287 Two seasons are separately modeled based on the Market Poisson Process. Here we
288 only focus on and manipulate rainy-season rainfall characteristics in our study, as
289 rainy-season rainfall accounts for almost all the meaningful rainfall inputs for plant
290 use. Thus in the following paper, whenever we mention α or λ , we refer to those
291 during the rainy season.

292 The “~~wet season~~” and “~~dry season~~” rainfall time series are ~~respectively modeled~~
293 ~~using the Marked Poisson Process~~. In this rainfall model, any day can be either rainy
294 or not, and a rainy day is counted as one rainy event; rainfall events occur as a
295 Poisson Process, with the parameter $1/\lambda$ (unit: days/event) being the mean intervals
296 between rainfall events, and rainfall intensity α for each rainfall event following an
297 exponential distribution, with α being the mean rainfall intensity per event
298 (Rodríguez-Iturbe et al., 1999). The wet season length is modeled as a beta
299 distribution bounded from 0 to 1, scaled by 365 days. All the necessary parameters to
300 fit for the stochastic rainfall model ~~climatological values of these rainfall~~
301 ~~characteristics~~ (including the mean and variance of rainfall frequency, intensity and
302 length of wet and dry seasons) were derived from the satellite-gauge-merged rainfall
303 measurement from TRMM 3b42V7 (Huffman et al., 2007) for the period of 1998 to
304 2012, based on the above assumptions for the rainfall process. Specifically, we

305 ~~applied our definition of “rainy season” to each year of the TRMM rainfall data for~~
306 ~~per pixel, and calculated the mean and variance of the “rainy season length”, using~~
307 ~~which we fitted the beta distribution for T_w . For rainfall frequency and intensity, we~~
308 ~~lumped all the wet or dry season rainfall record together to derive their parameters.~~
309 ~~The ~~the~~ two steps of the synthetic weather generator are described ~~as~~ below:~~

310 **Step 1:** Model the daily rainfall following the Marked Poisson process described
311 above. In particular, for a specific year, we first stochastically generate the wet season
312 length by sampling from the beta distribution, and the dry season length is determined
313 accordingly. Then we generate the daily rainfall for wet and dry season respectively.

314 **Step 2:** Based on the simulated daily rainfall time series in Step 1, we conditionally
315 sample temperature, wind, and humidity from the Global Meteorological Forcing
316 Dataset (GMFD, Sheffield et al., 2006), as well as cloud fraction and soil temperature
317 from the Climate Forecast System Reanalysis (CFSR) from National Centers for
318 Environmental Prediction (NCEP) (Saha et al., 2010). ~~To sample for a specific day, all~~
319 ~~the historical record within a 21-day time window centered at that specific day makes~~
320 ~~up a sampling pool. For each day, a sample is randomly drawn from a pool that covers~~
321 ~~all the historical record within a 21-day time window centered at the sampling day.~~
322 From the sampling pool, we ~~find-choose~~ the day such that the historical rainfall
323 amount of the chosen day is within (100-30)% to (100+30)% of the simulated daily
324 rainfall amount. We then draw all ~~other-the~~ environmental variables ~~(except rainfall)~~
325 on that sampled day to the new climate forcing. If we can find a sample from the pool
326 ~~based on the above rule~~, this sampling is called “successful”. When there is more than
327 one suitable sample, we randomly select one. When there is no suitable sample, we
328 randomly select one day within the pool. The mean “successful” rate for all the
329 ~~experiments and ensembles and all the experiments a~~cross Africa is 83%.

330 ~~The GMFD data (Sheffield et al., 2006) blends reanalysis data with observations~~
331 ~~and disaggregates in time and space, and is available from 1948 to 2008, with~~
332 ~~1.0 degree spatial resolution and daily temporal resolution. The CFSR data (Saha et~~
333 ~~al., 2010) provides cloud fraction and simulated soil temperature from three soil~~
334 ~~layers for the SEIB model. The CFSR version that we used is from 1979 to 2010, and~~

335 ~~the original 0.3 degree spatial resolution and 6 hourly temporal resolution are~~
336 ~~aggregated to 1.0 degree and daily.~~

337 —To test the validity of the synthetic weather generator, we ran ~~the SEIB~~
338 ~~model~~SEIB-DGVM using the historical climate record ($S_{\text{climatology}}$) and the synthetic
339 forcing (S_{control}), with the latter generated using the weather generator based on the
340 rainfall characteristics derived from the former. Figure S1 shows that the ~~SEIB~~
341 ~~model~~SEIB-DGVM simulations driven by these two different forcings generate
342 similar biome distributions with a Cohen's Kappa coefficient of 0.78 (Cohen, 1960),
343 and similar GPP patterns in Africa, with the linear fits of annual GPP as:
344 $GPP(S_{\text{control}}) = 1.03 \times GPP(S_{\text{climatology}}) + 0.215$ ($R^2 = 0.89$, $P < 0.0001$). Both biome and
345 GPP patterns are consistent with observations (Sato and Ise, 2012). These results
346 provide confidence in using the synthetic weather generator and SEIB-DGVM to
347 conduct the further study.

348

349 **2.4 Experiment design**

350 Three experiments are designed as follows, ~~and are shown in the conceptual diagram~~
351 ~~(Figure 2)~~:

352 **Exp 1** (Perturbation of rainfall frequency and intensity, ~~and the experiment is~~ termed
353 as $S_{\lambda-\alpha}$ hereafter, ~~with S referring “Scenario”~~) Simulations forced by the synthetic
354 forcings with varying λ and α simultaneously for wet season (20% increases of λ and
355 corresponding decreases of α to make MAP unchanged; 20% decreases of λ and
356 corresponding increases of α to make MAP unchanged; no change for dry season
357 rainfall characteristics), while fixing T_w at the current climatology;

358 **Exp 2** (Perturbation of rainfall frequency and rainy season length, termed as $S_{T_w-\lambda}$)
359 Simulations forced by the synthetic forcing with varying T_w and λ simultaneously for
360 wet season (20% increases of T_w and corresponding decreases of λ to make MAP
361 unchanged; 20% decreases of T_w and corresponding increases of λ to make MAP
362 unchanged; no change for dry season characteristics), while fixing α at the current
363 climatology;

364 **Exp 3** (Perturbation of rainy season length and intensity, termed as $S_{T_w-\alpha}$) Simulations

365 forced by the synthetic forcing with varying T_w and α simultaneously for wet season
366 (20% increases of T_w and corresponding decreases of α to make MAP unchanged;
367 20% decreases of T_w and corresponding increases of α to make MAP unchanged; no
368 change for dry season characteristics), while fixing λ at the current climatology.

369 Because λ and T_w have bounded ranges ($\lambda \sim [0, 1]$ and $T_w \sim [0, 365]$), if the ~~se two~~
370 ~~variables after perturbation~~ ~~updated value~~ exceeds the range, we would force the
371 ~~new updated~~ ~~ir~~ value to be the lower or upper bound, and rearrange the other
372 ~~corresponding variable~~ ~~rainfall characteristic~~ to ensure MAP unchanged. Each rainfall
373 scenario has six ensemble realizations of synthetic climate forcings to account for the
374 stochasticity of our synthetic weather generator.
375 ~~For example in Exp 1, if after 10% increase the updated λ is larger than 1, we would~~
376 ~~force the updated λ to be 1, and recalculate the changes in α to keep MAP the same as~~
377 ~~before. All the scenarios have six ensemble runs differentiated in their synthetic~~
378 ~~forcings to account for the stochasticity of the synthetic weather generator.~~

379

380 **3. Results**

381 We present the differences in simulated biome distributions of the three experiments
382 (i.e. $S_{\lambda-\alpha}$, $S_{T_w-\lambda}$, $S_{T_w-\alpha}$) in ~~Figure 4~~ Figure 3, ~~(and Figure S2 and S3 for their spatial~~
383 ~~patterns are shown in Figure S2 and S3).~~ ~~and the 4~~ Differences in simulated annually
384 averaged soil moisture and GPP for each experiment are shown in Figure 5 Figure 4
385 and 6. These differences ~~indicate~~ represent the simulated ecosystem sensitivity to the
386 slight perturbation ~~away from the current climatology~~ of intra-seasonal rainfall
387 characteristics deviating from the current climatology. ~~We present the differences~~
388 ~~between +20% and -20% changes in each experiment. We also assessed shifts of +/-~~
389 ~~10%, and found that these responses are similar with only smaller magnitudes and~~
390 ~~thus not shown here. To further explore how MAP and these rainfall characteristics~~
391 affect the simulated GPP, Figure 6 Figure 5 shows plots the difference ~~in~~ of simulated
392 GPP as a function of mean annual precipitation MAP and the climatological value of a
393 perturbed rainfall characteristic in the corresponding experiment. We term Figure 5 as
394 “GPP sensitivity space”, and “positive GPP sensitivity” means that GPP changes at

395 the same direction with MAP or rainfall characteristics, and vice versa for “negative
396 GPP response”. These “GPP sensitivity spaces” are generated based on the aggregated
397 mean GPP in each bin of the rainfall properties. The bin size for MAP, rainfall
398 frequency, rainfall intensity and rainy season length are 100 mm/year, 0.05 event/day,
399 1 mm/event and 15 days respectively. We also provide the standard error (SE) of the
400 “GPP sensitivity spaces” in each bin to assess their uncertainties, with higher SE
401 meaning larger uncertainties. ~~paired with the standard error (SE) between~~
402 ~~simulations to indicate the uncertainty of the result, as $SE = \sigma / \sqrt{n}$, where σ and n~~
403 refer to the standard deviation of GPP values and the sample size in each bin
404 respectively. ~~Thus changes in GPP and their associated standard errors are calculated~~
405 ~~for each climatological bin; where the bin size for MAP, rainfall frequency, rainfall~~
406 ~~intensity and rainy season length are 100 mm/year, 0.05 day⁻¹, 1 mm and 15 days~~
407 ~~respectively. We recognize that there are large heterogeneity in soil texture, altitude~~
408 ~~and other factors which can influence simulation results at local scale, and using the~~
409 ~~current approach essentially lumps these factors and highlights the impacts from our~~
410 ~~interested variables (i.e. rainfall characteristics). A series of illustrations in Figure~~
411 ~~7Figure 6 were generalized from the simulated time series, and will be~~ used to
412 explain the underlying mechanisms.

413

414 [insert ~~Figure 4~~Figure 3; ~~Figure 5~~Figure 4; ~~Figure 6~~Figure 5]

415

416 3.1 Ecosystem sensitivity to rainfall frequency and intensity (Experiment $S_{\lambda-\alpha}$)

417 Experiment $S_{\lambda-\alpha}$ assesses ecosystem responses after increasing rainfall frequency λ
418 and decreasing rainfall intensity α ($\lambda \uparrow, \alpha \downarrow$) under a fixed total annual rainfall. The ~~The~~
419 experiment $S_{\lambda-\alpha}$ shows that the simulated biome distributions, after increasing rainfall
420 frequency λ and decreasing its intensity α ($\lambda \uparrow, \alpha \downarrow$) under a fixed total annual rainfall,
421 have small differences in the low rainfall regime (around 500 mm/year, Figure 4a),
422 with show that a small portion of regions ~~converting are converted~~ from woodland to
423 grassland at low rainfall regime (~500 mm/year), corresponding to a decrease of GPP

Formatted: Not Superscript/ Subscript

424 ~~in these regions indicating a negative impact of increasing rainfall frequency when~~
425 ~~total rainfall is very low.~~ In the high rainfall regime (around 1500 mm/year, ~~Figure~~
426 ~~4~~~~Figure 3a~~), increasing rainfall frequency significantly converts tropical evergreen
427 forests into woodlands. In the intermediate rainfall regime (600-1000 mm/year), there
428 ~~are is~~ little changes in biome distributions. We further check the spatial patterns of
429 differences in annual mean soil moisture and annual total GPP (~~Figure 5~~~~Figure 4a~~ and
430 5b). We find that GPP increases with increasing rainfall frequency across most of the
431 Africa continent, except in ~~the~~ very dry end (in the southern and eastern Africa) ~~as~~
432 ~~well as and the~~ very wet regions (in central Africa and northeastern Madagascar). This
433 GPP pattern mostly mirrors the soil moisture change ~~in woodlands and grasslands~~
434 (~~Figure 5~~~~Figure 4b~~), except the wet tropics, where the changes of soil moisture and
435 GPP are ~~in the reversed signs~~.

436 ~~Figure 6~~~~Figure 5a~~ shows the GPP sensitivity as a function of MAP and the
437 climatological rainfall frequency, and we find three major patterns ~~stand out~~:

438 **Pattern 1.1:** Negative GPP sensitivity shows up in the very dry end of MAP regime
439 (MAP < 400 mm/year) and with ~~very~~ ~~relatively~~ low rainfall frequency ($\lambda < 0.3$
440 ~~day⁻¹event/day~~), i.e. GPP decreases with more frequent but less intense rainfall in this
441 low rainfall ~~regime range, without changes in the total rainfall amount~~.

442 **Pattern 1.2:** Across most rainfall ~~range regimes~~ (MAP from 400 mm/year to 1600
443 mm/year), increasing frequency of rainfall (and simultaneously decreasing rainfall
444 intensity) lead to positive GPP sensitivity. This positive GPP sensitivity peaks at the
445 low range of rainfall frequency (~ 0.35 ~~day⁻¹event/day~~) and around the MAP of 1000
446 mm/year.

447 **Pattern 1.3:** At the high range of MAP (>1800 mm/year) with low rainfall frequency
448 (~ 0.4 ~~day⁻¹event/day~~), GPP decreases with increased rainfall frequency.

449 ~~The relationship of GPP sensitivity to MAP and rainfall intensity (Fig. 6c) has no~~
450 ~~clear patterns as previous ones, mostly because the GPP sensitivity space (Fig. A4c)~~
451 ~~contains large uncertainties (Fig. A4d, shown as large variance in the data). Thus we~~
452 ~~will not over-interpret the pattern in Fig. 6c. The GPP sensitivity with respect to MAP~~
453 ~~and rainfall intensity (Figure 6c) contains more uncertainties and shows more~~

Formatted: Font: Not Bold

454 ~~complex patterns, mostly because the space that most pixels cluster (Figure S4c) also~~
455 ~~has large variance (Figure S4d). Thus we will not over interpret the pattern in Figure~~
456 ~~6e.~~

457 ~~Illustrative time series in Figure 7a and 7b explain the above~~ Pattern 1.1 and
458 ~~Pattern 1.2 can be explained by the illustrative time series in Figure 6a and 6b,~~
459 ~~respectively. Figure 7~~Figure 6a shows that when rainfall events are small and very
460 infrequent, increasing rainfall frequency while decreasing intensity would cause more
461 frequent downcrossings of soil moisture at the wilting point S_w , which subsequently
462 would reduce the effective time of carbon assimilation and plant growth (i.e. when
463 soil moisture is below S_w , plants would be in the extreme water stress and slow down
464 or stop physiological activity). ~~It is worth noting that t~~This case only happens where
465 MAP is very low with low frequency, ~~where and~~ the biome is predominantly
466 grasslands, which explains why negative changes in soil moisture and GPP in Figure
467 4a and 4b are distributed in those regions. the spatial patterns of negative soil moisture
468 and GPP sensitivity in Figure 5a and 5b. This result also corroborates the field
469 findings of the negative impacts from increasing rainfall frequency in Heisler-White
470 et al.(2009) and Thomey et al. (2011) at low rainfall regimes.

471 ~~Figure 7~~Figure 6b ~~explains~~ provides the hydrological mechanism for the positive
472 sensitivity of soil moisture and GPP with increasing rainfall frequency over the most
473 African continent (Pattern 1.2). Once individual rainfall event has enough intensity
474 and rainfall ~~events are frequent~~ frequency is enough, downcrossings of S_w would not
475 easily happen. ~~;~~ Instead, the accumulative rainy-season soil moisture becomes the
476 dominant control of plant growth, and water stress (shaded areas between S_w and S^* ,
477 Porporato et al., 2001) becomes the dominant source of growth stress for plants; and
478 increasing rainfall frequency has can lead to a significant decrease in this type of plant
479 water stress increase of soil moisture for plant water use (Figure 4a and 4b). This
480 conclusion drawn from our numerical modeling is consistent with previous findings in
481 Rodríguez-Iturbe and Porporato (2004) based on stochastic modeling. We also find
482 that this positive impact-GPP sensitivity reaches to its maximum in the intermediate
483 total rainfall (~1000 mm/year) and relatively low rainfall frequency (~0.35

484 ~~day⁻¹event/day~~), indicating that in these regimes increasing rainfall frequency could
485 most effectively ~~decrease~~ increase plant water stress ~~soil moisture for plant water use~~
486 and create marginal benefits of GPP to the increased rainfall frequency. Further
487 increase in ~~Either too~~-large total annual rainfall ~~or too high or~~ rainfall frequency may
488 uplift soil moisture status in general, which would reduce the sensitivity to water
489 stress with fewer downcrossings of soil moisture critical point S^* ; and once the soil
490 moisture is always ample (i.e. above S^*), the changes in either MAP or rainfall
491 frequency would not alter plant water stress.

492 Pattern 1.3 also shows a negative GPP sensitivity, but its mechanism is different
493 from the previous case of Pattern 1.1. There is another negative GPP sensitivity
494 shown in Pattern 1.3, but the mechanism is different from the previous negative GPP
495 case. In regions with total rainfall usually more than 1800 mm/year, SEIB-simulated
496 tropical forests exhibit radiation-limitation rather than water-limitation during wet
497 season. Increase of rainfall frequency at daily scale would enhance cloud fraction and
498 suppress plant productivity in these regions (Graham et al., 2003). Thus even though
499 soil moisture still increases (~~Figure 5~~Figure 4a), GPP decreases with increased rainfall
500 frequency. This mechanism also explains why tropical evergreen forests shrink its
501 area with increased rainfall frequency (~~Figure 4~~Figure 3a).

502 It is worth noting that the magnitude of GPP changes due to rainfall frequency
503 and intensity is relatively small in most of the woodlands, but can be relatively large
504 for drylands with MAP below 600 mm/year (up to 10-20% of annual GPP). This
505 pattern also explains why only modest changes in biome distribution ~~happen~~ for the
506 transitional area between woodlands and grasslands in $S_{\lambda-\alpha}$ (~~Figure 4~~Figure 3a).

507

508 [insert ~~Figure 7~~Figure 6]

509

510 **3.2 Ecosystem sensitivity to rainfall seasonality and frequency (Experiment $S_{TW-\lambda}$)**

511 ~~The~~ experiment $S_{TW-\lambda}$ assesses ecosystem responses after increasing rainy season
512 length and decreasing rainfall frequency (i.e. $T_w \uparrow, \lambda \downarrow$) under a fixed total annual
513 rainfall. T ~~shows that~~ the simulated biome distribution, ~~after increasing rainy season~~

514 ~~length and decreasing rainfall frequency (i.e. $T_w \uparrow$, $\lambda \downarrow$) under a fixed total annual~~
515 ~~rainfall, shows a gain of~~ ~~has an increase of~~ area in tropical evergreen forests, ~~which~~
516 ~~are~~ converted from woodlands. ~~The northern Africa has~~, an area increase of
517 woodlands converted from grasslands ~~in the northern Africa~~, and African Horn region
518 ~~has~~ a small expansion of grasslands into woodlands ~~in the African Horn region~~
519 ~~(Figure 4~~ Figure 3b). ~~Figure 5~~ Figure 4c and 4d show that increasing rainy season
520 length T_w and decreasing frequency λ would significantly increase annual mean soil
521 moisture and GPP (up to 30%) in most woodland area, ~~meanwhile decreased soil~~
522 moisture and GPP are found in the southern and eastern Africa, ~~and~~ ~~tropical~~
523 evergreen forests ~~show regions have~~ little response. We further explore the GPP
524 sensitivity space in ~~Figure 6~~ Figure 5e and 5g, and find the following interesting
525 robust patterns (based on small standard errors shown in Figure 5f and 5h):
526 ~~, which are mostly robust due to the small standard errors shown in Figure 6f and 6h:~~
527 **Pattern 2.1:** The negative GPP sensitivity tends to happen where MAP is mostly
528 below 1000 mm/year with long rainy season length ($T_w > 150$ days) and low rainfall
529 frequency ($\lambda < 0.35$ ~~day⁻¹event/day~~), ~~which is a unique rainfall regime that sporadically~~
530 ~~spread rain events for a long rainy season.~~
531 **Pattern 2.2:** When MAP and rainfall frequency are ~~both larger than certain~~
532 ~~ranges~~ large enough ($MAP > 1000$ mm/year and $\lambda > 0.4$ ~~day⁻¹event/day~~), decreasing λ
533 while increasing ~~trading the decrease of λ for the increase of~~ T_w would significantly
534 increase GPP. The maximum positive GPP sensitivity happens ~~in the rainfall regime~~
535 ~~with the~~ at the intermediate MAP range (1100-1500 mm/year) and the high rainfall
536 frequency ($\lambda \sim 0.7$ ~~day⁻¹event/day~~).

537 **Pattern 2.3:** There exists an “optimal rainy season length” for relative changes in
538 ecosystem productivity ~~at across large different~~ MAP ranges (the white area between
539 the red and blue space in ~~Figure 6~~ Figure 5e). For the same MAP, any deviation of T_w
540 from the “optimal rainy season length” would reduce GPP. longer than this length,
541 rainy season lengthening would decrease GPP; while shorter than this length, rainy
542 season lengthening would increase GPP. This “optimal rainy season length” follows
543 an increasing trendes with MAP until 1400 mm/year.

Formatted: Not Superscript/ Subscript

Formatted: Not Superscript/ Subscript

544 ~~Figure 7~~Figure 6c explains the hydrological mechanism for the negative GPP
545 sensitivity in Pattern 2.1. In the situation with low MAP and infrequent rainfall events,
546 decreasing rainfall frequency ~~to and~~ expanding rainy season length (i.e. $T_w \uparrow$, $\lambda \downarrow$)
547 would lead to longer ~~interval~~ time b between rainfall events and possibly longer
548 excursions below S_w , which would ~~restrain~~ disrupt continuous plant growth and have
549 detrimental effects on ecosystem productivity. It is worth noting that long rainy season
550 in dryland (~~Figure 6~~Figure 5e) is usually accompanied with low rainfall frequency
551 (~~Figure 6~~Figure 5g). The southern African drygrasslands (south of 15°S) typically fall
552 in this category, and these regions thus have negative GPP sensitivity (~~Figure 5~~Figure
553 4c and 4d), accompanied by a small biome conversion from; ~~these regions also~~
554 ~~correspond to the small biome conversion from~~ woodlands to grasslands in the low
555 range of MAP (<300 mm/year) as shown in (~~Figure 4~~Figure 3b).

556 ~~Figure 7~~Figure 6d explains the hydrological mechanisms for the positive GPP
557 sensitivity in Pattern 2.2, ~~which shows that~~ When rainfall is ample enough to
558 maintain little or no water stress during rainy season, increasing the interval of rainfall
559 events may introduce little additional water stress but can significantly extend the
560 growing season. This situation mostly happens in woodlands, where limited water
561 stress exists during growing ~~rainy~~ season, and dry season length is the major
562 constraint for plant growth. Thus the increase of rainy season length extends the
563 temporal niche for plant growth, and ~~significantly modifies the biome distribution,~~
564 ~~which~~ leads to a significant woodland expansion ~~large wood encroachment~~ to
565 grasslands and as well as ~~also~~ an expansion of tropical evergreen forests ~~conversion~~
566 ~~of woodlands to tropical evergreen forests, as shown into woodlands~~ (~~Figure 4~~Figure
567 3b).

568 The little GPP sensitivity in tropical evergreen forest regions is mostly attributed
569 to the long rainy season length ~~already existed~~ in this ~~type of~~ ecosystem. Thus further
570 increasing T_w may reach to its saturation (365 days) and ~~has thus have~~ little impact to
571 ecosystem productivity. This also explains why the magnitude of GPP sensitivity is
572 much smaller at high MAP range than at the intermediate MAP range. Similar reason
573 ~~also explains why the GPP sensitivity has the maximum response in the intermediate~~

Formatted

Formatted: Font: Times New Roman

Formatted

574 ~~MAP range rather than the high MAP range, at which GPP sensitivity has been~~
575 ~~saturated.~~

576 The finding of “optimal rainy season length” across different rainfall regimes
577 (~~Figure 6~~Figure 5e) is consistent with our previous empirical finding about the similar
578 pattern of “optimal rainy season length” for tree fractional cover in Africa derived
579 based on a satellite remote sensing product (Guan et al., 2014). The existence of
580 “optimal rainy season length” ~~Two distinctive GPP sensitivities separated by the~~
581 ~~“optimal rainy season length”, with this optimal length increasing with MAP,~~ fully
582 demonstrates the importance to explicitly consider the non-linear impacts of rainy
583 season length on ecosystem productivity under climate change, which has been
584 largely overlooked before.

585

586 3.3 Ecosystem sensitivity to rainfall seasonality and intensity ($S_{T_w-\alpha}$)

587 ~~The results of the e~~Experiment $S_{T_w-\alpha}$ have many similarities with those of $S_{T_w-\lambda}$,
588 including the similar changes in biome distributions (~~Figure 4~~Figure 3), soil moisture
589 and GPP patterns (~~Figure 5~~Figure 4e and 4f). We further find that the GPP sensitivity
590 space with MAP and rainy season length for $S_{T_w-\alpha}$ (~~Figure 6~~Figure 5j) is also similar
591 with that ~~of for~~ $S_{T_w-\lambda}$ (~~Figure 6~~Figure 5e). One new pattern-finding is that rainfall
592 intensity has little impacts on ~~the GPP sensitivity~~, as the contour lines in ~~Figure~~
593 ~~6~~Figure 5k are mostly parallel with y-axis (i.e. rainfall intensity); ~~in other words, the~~
594 ~~trade-off between T_w and α is mostly a function of MAP and T_w , but not α , and the~~
595 ~~largest marginal effects happen in the intermediate range of MAP, similar as in $S_{T_w-\lambda}$.~~

596 Figure 7Figure 6e and 6f explain the governing hydrological mechanisms for the
597 patterns of $S_{T_w-\alpha}$, which also have many similarities with $S_{T_w-\lambda}$. For the negative case
598 (~~Figure 7~~Figure 6e), decreasing rainfall intensity to extend and increasing rainy season
599 length in the very low MAP regime may ~~possibly~~ lead to more downcrossings of S_w
600 and interrupt continuous plant growth. The positive case (~~Figure 7~~Figure 6e) is similar
601 as that in ~~Figure 7~~Figure 6d, i.e. the repartitioning of excessive ~~rainy wet-season water~~
602 rainfall to the dry season for an extended growing period would significantly benefit
603 plant growth and possible increase tree fraction cover.

604

605 **4. Discussion**

606 In this paper we provide a new modeling approach to systematically ~~understand~~
607 ~~interpret~~ the ecological impacts from changes in intra-seasonal rainfall characteristics
608 (i.e. rainfall frequency, rainfall intensity and rainy season length) across biomes and
609 climate gradients in the African continent.

610

611 **4.1 Limitation of the methodology**

612 Though ~~the-our~~ modeling framework ~~that-we-used~~ is able to characterize the diverse
613 ecosystem responses to the shifts in different rainfall characteristics, it nevertheless
614 has its limitations. The current rainfall model only deals with the case of single rainy
615 season per year, and approximates the case of double rainy seasons per year to be ~~the~~
616 single rainy season case. This assumption may induce unrealistic synthetic rainfall
617 patterns in the equatorial dryland regions, in particular the Horn of Africa. ~~T~~, thus the
618 ~~resulting-simulated~~ sensitivity of these regions may be less reliable. We also assume
619 that rainfall frequency and intensity are homogenous throughout wet ~~and-dry~~ seasons
620 ~~(or dry seasons)s~~, but in reality they ~~still~~ have seasonal variations. We only consider
621 rainy season length for rainfall seasonality, and neglect the possible temporal phase
622 change; ~~actually-in reality~~, rainfall seasonality change usually has length and phase
623 shifts in concert. These rainfall-model-related limitations can be possibly overcome by
624 simulating smaller intervals of rainfall processes (e.g. each month has their own α and
625 λ) rather than simulating the whole wet or dry season using one fixed set of α and λ .
626 Besides, only using one ecosystem model also means that the simulated ecosystem
627 sensitivity can be model-specific. ~~Though magnitudes or thresholds for the~~
628 ~~corresponding patterns may vary depending on different models, we argue that ;~~
629 ~~though-we-believe~~ the qualitative results for the GPP sensitivity patterns (e.g. ~~Figure~~
630 ~~5Figure 4~~ and ~~Figure-6Figure 5~~) should ~~mostly~~ hold as the necessary ecohydrological
631 processes have been incorporated in ~~the SEIB-DGVM, magnitudes or thresholds in~~
632 ~~these patterns may vary depending on different models. For example, GPP in tropical~~
633 ~~evergreen forests (Figure 5b and Figure 6a) is less sensitive to radiation limitation as~~

634 ~~shown in satellite based observation than in the SEIB simulation in Africa (Guan et al.,~~
635 ~~2013).~~ We also recognize that to exclude fire impacts in the current simulation may
636 bring some ~~eaveats limitation in interpreting the results for this study,~~ as evidence
637 shows that many savanna regions can be bistable due to fire effects (Staver et al 2011;
638 Hirota et al 2011; Higgins and Scheiter 2012; also see for a possible rebuttal in Hanan
639 et al, 2013). ~~and e~~ Changes in rainfall regimes ~~may~~ not only have direct effects on
640 vegetation productivity, but can also indirectly ~~effects affect ecosystems~~ through
641 ~~influeneing its interactions with~~ fire regimes, ~~and with~~ rapid biome shifts ~~may be being~~
642 ~~a possible a~~ consequence. These feedbacks can be important in situations ~~where when~~
643 ~~the changes in the~~ growing season length ~~changes, which~~ are related to fuel loads, fuel
644 moisture dynamics and hence fire intensity (Lehmann et al., 2011). Quantifying these
645 fire-rainfall feedbacks will be the important future direction to pursue.

646

647 **4.2 Clarifying the impacts of rainfall frequency and intensity on ecosystem** 648 **productivity**

649 In this ~~modeling study, we provide a plausible answer to possibly resolve paper we~~
650 ~~have resolved~~ the previous debate about whether increasing rainfall intensity (or
651 equivalently decreasing rainfall frequency, i.e. $\lambda \downarrow$, $\alpha \uparrow$) has positive or negative
652 impacts on above-ground primary productivity ~~with under~~ a fixed annual rainfall total.
653 We identify that negative GPP sensitivity with increased rainfall frequency is possible
654 at very low MAP range (~ 400 mm/year) with ~~very relatively~~ low rainfall frequency
655 (< 0.35 ~~day⁻¹ event/day~~) (Figure ~~6~~ Figure 5a), due to the increased downcrossings of
656 soil moisture wilting point, which restricts plant growth (Figure ~~7~~ Figure 6a). ~~Our This~~
657 derived MAP threshold (~400 mm/year) ~~to distinguish different GPP sensitivities with~~
658 ~~rainfall frequency~~ is consistent with our meta-analysis based on the previous field
659 studies (Table 1), which shows a threshold of MAP at 340 mm/year separates positive
660 and negative impacts of more intense rainfall on ANPP ~~aboveground net primary~~
661 production (ANPP). Our findings are also consistent with ~~another other~~ studies about
662 increased tree encroachments with increased rainfall intensity in ~~very~~ low rainfall
663 regime (< 544 mm/year, Kulmatiski and Beard, 2013), which essentially follows the

664 same mechanism as identified in ~~Figure 7~~Figure 6a.

665 In addition, we thoroughly investigated the ecosystem responses across ~~all the a~~
666 ~~wide ranges~~ of ~~annual~~ rainfall in Africa, ~~and w~~We find that beyond the very low
667 rainfall range (below 400 mm/year), most grasslands and woodlands would benefit
668 from increasing rainfall frequency, which also corroborate the previous large-scale
669 findings about the positive effects of increased rainfall frequency (and decreased
670 rainfall intensity) for tree fractions across the African continent (Good and Caylor,
671 2011). The only exception happens at the very wet end of MAP (~1800mm/year)
672 where cloud-induced radiation-limitation may suppress ecosystem productivity with
673 increased rainfall frequency. We also find that changes in rainfall frequency and
674 intensity mostly ~~aff~~ect grassland-dominated savannas (changes of GPP up to 20%),
675 and the corresponding effects are much smaller in woodlands and have little impact
676 on woodland distribution. Though this work is only based on a single model, it
677 provides a primary assessment for understanding of interactive changes between λ and
678 α in ecosystem functioning, ~~which and~~ expands ~~the analysis to the full spectra of a~~
679 ~~wide range of annual~~ rainfall ~~ranges conditions~~ compared with previous studies (e.g.
680 Porporato et al., 2004).

681

682 4.3 Ecological importance of rainy season length

683 The results involving rainy season length (i.e. $S_{T_w-\lambda}$ and $S_{T_w-\alpha}$) ~~have fully demonstrated~~
684 ~~provide evidence for~~ the ecological importance of rainfall seasonality. The magnitudes
685 of changes in soil moisture, GPP and biome distribution in $S_{T_w-\lambda}$ and $S_{T_w-\alpha}$ are much
686 larger than those of $S_{\lambda-\alpha}$, with almost one order of magnitude difference. These
687 disproportional impacts ~~of of~~ T_w indicate that slight changes in rainy season length
688 could modify biome distribution and ecosystem function more dramatically compared
689 with the same percentage changes in rainfall frequency and intensity. We also notice
690 that $S_{T_w-\lambda}$ and $S_{T_w-\alpha}$ have similar results, ~~which~~This ~~is~~ because that both λ and α
691 describe rainfall characteristics within wet season, while T_w describes rainfall
692 characteristics of both dry season and wet season. Cautions are required that our
693 simplified treatment rainy season length may overestimate its importance, and we did

694 ~~not consider the rainfall phase information here.~~ –

695 Given the importance of rainy season length, its ecological impacts under climate
696 change are largely understudied, though substantial shifts in rainfall seasonality have
697 been projected in both Sahel and South Africa (Biasutti and Sobel, 2009; Shongwe et
698 al., 2009; Seth et al., 2013). Here we only address the rainfall seasonality in terms of
699 its length, and future changes in rainfall seasonality may modify their phase and
700 magnitude in concert. The climate community has focused on the increase of extreme
701 rainfall events (Field et al., 2012), which could be captured by the changes in λ or α
702 towards heavier tails in their distribution. However, explicit and systematic
703 assessments and projection on rainfall seasonality changes (including both phase and
704 magnitude) are still limited even in the latest Intergovernmental Panel on Climate
705 Change (IPCC) synthesis reports (Field et al., 2012; Stocker et al., 2013). More
706 detailed studies related to these changes and their ecological implications are required
707 for future hydroclimate-ecosystem research.

708

709 **4.4 Not all rainfall regimes are ecologically equivalent**

710 As Figure 1 gives a convincing example that the same total annual rainfall may arrive
711 in a very different way, our results further demonstrate that ecosystems respond
712 differently to the changes in ~~these~~ intra-seasonal rainfall variability. For example, with
713 similar MAP, ~~drylands in~~ West Africa and Southwest Africa ~~can have~~ reversed
714 responses to the same changes in intra-seasonal rainfall variability. As shown in the
715 experiments of $S_{T_w-\lambda}$ and $S_{T_w-\alpha}$, increasing T_w while decreasing λ or α generates
716 slightly positive soil moisture and GPP sensitivity in West Africa (~~Figure 5~~Figure 4c
717 and 4d), but would cause relatively large GPP decrease in Southwest Africa. The
718 prior hydroclimate conditions of these two regions can explain these differences: West
719 Africa has much shorter rainy season with more intense rainfall events; ~~which is~~
720 ~~totally contrary to~~in contrast, Southwest Africa, ~~which~~ has a long rainy season but
721 many small and sporadic rainfall events. As a result, under a fixed annual rainfall total,
722 slightly increasing rainy season and meanwhile decreasing rainfall intensity would
723 benefit plant growth in West Africa, but the same change would lengthen dry spells in

724 Southwest Africa and bring negative effects to the ecosystem productivity. We further
725 deduce that the rainfall use efficiency (RUE, defined as the ratio of plant net primary
726 production ~~and to~~ total rainfall amount) in these two drylands could be different: West
727 Africa may have lower RUE, and the intense rainfall could lead to more
728 infiltration-excess runoff, and thus less water would be used by plants; while
729 Southwest Africa can have higher RUE, because its sporadic and feeble rainfall events
730 would favor grass to fully take the advantage of the ephemerally existed water
731 resources. This conclusion is partly supported by Martiny et al. (2007) based on
732 satellite remote sensing. We further hypothesize that landscape geomorphology in
733 these two drylands may be different and therefore reflect distinctive rainfall
734 characteristics. More bare soil may exist in West Africa grasslands due to
735 intense-rainfall-induced erosion, while Southwest Africa may have more grass
736 fraction and less bare soil fraction. Testing these interesting hypotheses is beyond the
737 scope of this paper, but is worthy the further exploration.

738

739

740 **Acknowledgements:**

741 K. Guan and E. F. Wood acknowledge the financial supports from the NASA NESSE
742 fellowship. S.P. Good and K. K. Caylor acknowledge the financial supports from the
743 National Science Foundation through the Grant EAR-0847368. The authors thank
744 Ignacio Rodríguez-Iturbe for his valuable inputs and discussion.

745

746

747 **References:**

- 748 Anderegg, L. D. L.; Anderegg, W. R. L. & Berry, J. A. (2013), 'Not all droughts are
749 created equal: translating meteorological drought into woody plant mortality', *Tree*
750 *Physiology* **33**, 701-712.
- 751
- 752 Bates, J.; Svejcar, T.; Miller, R. & Angell, R. (2006), 'The effects of precipitation
753 timing on sagebrush steppe vegetation', *Journal of Arid Environments* **64**, 670-697.
- 754
- 755 Biasutti, M. & Sobel, A. H. (2009), 'Delayed Sahel rainfall and global seasonal cycle in
756 a warmer climate', *Geophysical Research Letters* **36**, L23707.
- 757
- 758 Bond, W. J.; Woodward, F. I. & Midgley, G. F. (2005), 'The Global Distribution of
759 Ecosystems in a World without Fire', *New Phytologist* **165**(2), 525-537.
- 760
- 761 Easterling, D. R.; Meehl, G. A.; Parmesan, C.; Changnon, S. A.; Karl, T. R. & Mearns,
762 L. O. (2000), 'Climate Extremes: Observations, Modeling, and Impacts', *Science* **289**,
763 2068-2074.
- 764
- 765 Fang, J.; Piao, S.; Zhou, L.; He, J.; Wei, F.; Myneni, R. B.; Tucker, C. J. & Tan, K.
766 (2005), 'Precipitation patterns alter growth of temperate vegetation', *Geophysical*
767 *Research Letters* **32**, L21411.
- 768
- 769 Fay, P. A.; Carlisle, J. D.; Knapp, A. K.; Blair, J. M. & Collins, S. L. (2003),
770 'Productivity responses to altered rainfall patterns in a C4-dominated grassland',
771 *Oecologia* **137**, 245-251.
- 772
- 773 Feng, X.; Porporato, A. & Rodriguez-Iturbe, I. (2013), 'Changes in rainfall seasonality
774 in the tropics', *Nature Climate Change*.
- 775
- 776 Field, C.; Barros, V.; Stocker, T.; Qin, D.; Dokken, D.; Ebi, K.; Mastrandrea, M.; Mach,
777 K.; Plattner, G.-K.; Allen, S.; Tignor, M. & Midgley, P., ed. (2012), *IPCC, 2012:*
778 *Managing the Risks of Extreme Events and Disasters to Advance Climate Change*
779 *Adaptation. A Special Report of Working Groups I and II of the Intergovernmental*
780 *Panel on Climate Change*, Cambridge University Press, Cambridge, UK, and New
781 York, NY, USA.
- 782
- 783 Franz, T. E.; Caylor, K. K.; Nordbotten, J. M.; Rodríguez-Iturbe, I. & Celia, M. A.
784 (2010), 'An ecohydrological approach to predicting regional woody species distribution
785 patterns in dryland ecosystems', *Advances in Water Resources* **33**(2), 215-230.
- 786
- 787 Gerten, D.; Luo, Y.; Maire, G. L.; Parton, W. J.; Keough, C.; Weng, E.; Beier, C.; Ciais,
788 P.; Cramer, W.; Dukes, J. S.; Hanson, P. J.; Knapp, A. A. K.; Linder, S.; Nepstad, D.;
789 Rustad, L. & Sowerby, A. (2008), 'Modelled effects of precipitation on ecosystem
790 carbon and water dynamics in different climatic zones', *Global Change Biology* **14**,

791 2365-2379.
792
793 Good, S. P. & Caylor, K. K. (2011), 'Climatological determinants of woody cover in
794 Africa', *Proceedings of the National Academy of Sciences of United States of America*
795 **108(12)**, 4902-4907.
796
797 Graham, E. A.; Mulkey, S. S.; Kitajima, K.; Phillips, N. G. & Wright, S. J. (2003),
798 'Cloud cover limits net CO₂ uptake and growth of a rainforest tree during tropical
799 rainy seasons', *Proceedings of the National Academy of Sciences of the United States*
800 *of America* **100(2)**, 572-576.
801
802 ~~Guan, K.; Wolf, A.; Medvigy, D.; Caylor, K.; Pan, M. & Wood, E. (2013), 'Seasonal~~
803 ~~coupling of canopy structure and function in African tropical forests and its~~
804 ~~environmental controls', *Ecosphere* **4(3)**.~~
805
806 Guan, K.; Wood, E. F. & Caylor, K. K. (2012), 'Multi-sensor derivation of regional
807 vegetation fractional cover in Africa', *Remote Sensing of Environment* **124**, 653-665.
808
809 Guan, K.; Wood, E. F.; Medvigy, D.; Pan, M.; Caylor, K. K.; Sheffield, J.; Kimball, J.;
810 Xu, X. & Jones, M. O. (2014), 'Terrestrial hydrological controls on vegetation
811 phenology of African savannas and woodlands', *Journal of Geophysical Research*.
812
813 Hanan, N. P.; Tredennick, A. T.; Prihodko, L.; Bucini, G. & Dohn, J. (2013), 'Analysis
814 of stable states in global savannas: is the CART pulling the horse?', *Global Ecology and*
815 *Biogeography* **23(3)**, 259-263.
816
817 Harper, C. W.; Blair, J. M.; Fay, P. A.; Knapp, A. K. & Carlisle, J. D. (2005), 'Increased
818 rainfall variability and reduced rainfall amount decreases soil CO₂ flux in a grassland
819 ecosystem', *Global Change Biology* **11**, 322-334.
820
821 Heisler-White, J. L.; Blair, J. M.; Kelly, E. F.; Harmony, K. & Knapp, A. K. (2009),
822 'Contingent productivity responses to more extreme rainfall regimes across a grassland
823 biome', *Global Change Biology* **15(12)**, 2894-2904.
824
825 Hély, C.; Bremond, L.; Alleaume, S.; Smith, B.; Sykes, M. T. & Guiot, J. (2006),
826 'Sensitivity of African biomes to changes in the precipitation regime', *Global Ecology*
827 *and Biogeography* **15**, 258-270.
828
829 Hirota, M.; Holmgren, M.; Nes, E. H. V. & Scheffer, M. (2011), 'Global Resilience of
830 Tropical Forest and Savanna to Critical Transitions', *Science* **334**, 232-235.
831
832 Higgins, S. I. & Scheiter, S. (2012), 'Atmospheric CO₂ forces abrupt vegetation shifts
833 locally, but not globally', *Nature* **488**, 209-212.
834

835 Holmgren, M.; Hirota, M.; van Nes, E. H. & Scheffer, M. (2013), 'Effects of
836 interannual climate variability on tropical tree cover', *Nature Climate Change*.
837
838 Huffman, G. J.; Bolvin, D. T.; Nelkin, E. J.; Wolff, D. B.; Adler, R. F.; Bowman, K. P.
839 & Stocker, E. F. (2007), 'The TRMM Multisatellite Precipitation Analysis (TMPA):
840 Quasi-Global, Multiyear, Combined-Sensor Precipitation Estimates at Fine Scales',
841 *Journal of Hydrometeorology* **8**, 38-55.
842
843 Knapp, A. K.; Fay, P. A.; Blair, J. M.; Collins, S. L.; Smith, M. D.; Carlisle, J. D.;
844 Harper, C. W.; Danner, B. T.; Lett, M. S. & McCarron, J. K. (2002), 'Rainfall
845 Variability, Carbon Cycling, and Plant Species Diversity in a Mesic Grassland', *Science*
846 **298**, 2202-2205.
847
848 Kulmatiski, A. & Beard, K. H. (2013), 'Woody plant encroachment facilitated by
849 increased precipitation intensity', *Nature Climate Change*.
850
851 Lehmann, C. E. R.; Archibald, S. A.; Hoffmann, W. A. & Bond, W. J. (2011),
852 'Deciphering the distribution of the savanna biome', *New Phytologist* **191**, 197-209.
853
854 [Markham, C. \(1970\), 'Seasonality of precipitation in the United States', *Annals of the*](#)
855 [*Association of American Geographers* **60\(3\)**, 593-597.](#)
856
857
858 Martiny, N.; Camberlin, P.; Richard, Y. & Philippon, N. (2006), 'Compared regimes of
859 NDVI and rainfall in semi-arid regions of Africa', *International Journal of Remote*
860 *Sensing* **27(23)**, 5201-5223.
861
862 Miranda, J.; Armas, C.; Padilla, F. & Pugnaire, F. (2011), 'Climatic change and rainfall
863 patterns: Effects on semi-arid plant communities of the Iberian Southeast', *Journal of*
864 *Arid Environments* **75**, 1302-1309.
865
866 Nemani, R. R.; Keeling, C. D.; Hashimoto, H.; Jolly, W. M.; Piper, S. C.; Tucker, C. J.;
867 Myneni, R. B. & Running, S. W. (2003), 'Climate-Driven Increases in Global
868 Terrestrial Net Primary Production from 1982 to 1999', *Science* **300**, 1560-1563.
869
870 O'Gorman, P. A. & Schneider, T. (2009), 'The physical basis for increases in
871 precipitation extremes in simulations of 21st-century climate change', *Proceedings of*
872 *the National Academy of Sciences of the United States of America* **106(35)**,
873 14773-14777.
874
875 Porporato, A.; Daly, E. & Rodríguez-Iturbe, I. (2004), 'Soil Water Balance and
876 Ecosystem Response to Climate Change', *American Naturalist* **164(5)**, 625-632.
877
878 Porporato, A.; Laio, F.; Ridolfi, L. & Rodríguez-Iturbe, I. (2001), 'Plants in

Formatted: Font: (Asian) 宋体

879 water-controlled ecosystems: active role in hydrologic processes and response to water
880 stress - III. Vegetation water stress', *Advances in Water Resources* **24(7)**, 725-744.
881
882 Robertson, T. R.; Bell, C. W.; Zak, J. C. & Tissue, D. T. (2009), 'Precipitation timing
883 and magnitude differentially affect aboveground annual net primary productivity in
884 three perennial species in a Chihuahuan Desert grassland', *New Phytologist* **181**,
885 230-242.
886
887 Rodríguez-Iturbe, I.; Gupta, V. K. & Waymire, E. (1984), 'Scale Considerations in the
888 Modeling of Temporal Rainfall', *Water Resource Research* **20(11)**, 1611-1619.
889
890 Rodríguez-Iturbe, I. & Porporato, A. (2004), *Ecohydrology of Water-Controlled*
891 *Ecosystems: Soil Moisture And Plant Dynamics*, Cambridge University Press.
892
893 Rodríguez-Iturbe, I.; Porporato, A.; Ridolfi, L.; Isham, V. & Cox, D. R. (1999),
894 'Probabilistic Modelling of Water Balance at a Point: The Role of Climate, Soil and
895 Vegetation', *Proceedings: Mathematical, Physical and Engineering Sciences* **455**,
896 3789-3805.
897
898 Ross, I.; Misson, L.; Rambal, S.; Arneth, A.; Scott, R. L.; Carrara, A.; Cescatti, A. &
899 Genesio, L. (2012), 'How do variations in the temporal distribution of rainfall events
900 affect ecosystem fluxes in seasonally water-limited Northern Hemisphere shrublands
901 and forests?', *Biogeosciences* **9**, 1007-1024.
902
903 Saha, S.; Moorthi, S.; Pan, H.-L.; Wu, X.; Wang, J.; Nadiga, S.; Tripp, P.; Kistler, R.;
904 Woollen, J.; Behringer, D.; Liu, H.; Stokes, D.; Grumbine, R.; Gayno, G.; Wang, J.;
905 Hou, Y.-T.; Chuang, H.-Y.; Juang, H.-M. H.; Sela, J.; Iredell, M.; Treadon, R.; Kleist,
906 D.; Delst, P. V.; Keyser, D.; Derber, J.; Ek, M.; Meng, J.; Wei, H.; Yang, R.; Lord, S.;
907 Dool, H. V. D.; Kumar, A.; Wang, W.; Long, C.; Chelliah, M.; Feng, Y.; Huang, B.;
908 Schemm, J.-K.; Ebisuzaki, W.; Lin, R.; Xie, P.; Chen, M.; Zhou, S.; Higgins, W.; Zou,
909 C.-Z.; Liu, Q.; Chen, Y.; Han, Y.; Cucurull, L.; Reynolds, R. W.; Rutledge, G. &
910 Goldberg, M. (2010), 'The NCEP Climate Forecast System Reanalysis', *Bulletin of the*
911 *American Meteorological Society* **91**, 1015-1057.
912
913 Sato, H. (2009), 'Simulation of the vegetation structure and function in a Malaysian
914 tropical rain forest using the individual-based dynamic vegetation model SEIB-DGVM',
915 *Forest Ecology and Management* **257**, 2277-2286.
916
917 Sato, H. & Ise, T. (2012), 'Effect of plant dynamic processes on African vegetation
918 responses to climate change: analysis using the spatially explicit individual-based
919 dynamic global vegetation model (SEIB-DGVM)', *Journal of Geophysical Research*
920 **117**, G03017.
921
922 Sato, H.; Itoh, A. & Kohyama, T. (2007), 'SEIB-DGVM: A new Dynamic Global

923 Vegetation Model using a spatially explicit individual-based approach', *Ecological*
924 *Modelling* **200(3-4)**, 279-307.

925

926 Sato, H.; Kobayashi, H. & Delbart, N. (2010), 'Simulation study of the vegetation
927 structure and function in eastern Siberian larch forests using the individual-based
928 vegetation model SEIB-DGVM', *Forest Ecology and Management* **259**, 301-311.

929

930 Scanlon, T. M.; Caylor, K. K.; Manfreda, S.; Levin, S. A. & Rodriguez-Iturbe, I. (2005),
931 'Dynamic response of grass cover to rainfall variability: implications for the function
932 and persistence of savanna ecosystems', *Advances in Water Resources* **28**, 291-302.

933

934 Shugart, H. H. (1998), 'Terrestrial ecosystems in changing environments', Cambridge
935 University Press, United Kingdom.

936

937 van Schaik, C. P.; Terborgh, J. W. & Wright, S. J. (1993), 'The Phenology of Tropical
938 Forests: Adaptive Significance and Consequences for Primary Consumers', *Annual*
939 *Review of Ecology and Systematics* **24**, 353-377.

940

941 Scholes, R. J. & Archer, S. R. (1997), 'Tree-Grass Interactions in Savannas', *Annual*
942 *Review of Ecology and Systematics* **28**, 517-544.

943

944 Seth, A.; Rauscher, S. A.; Biasutti, M.; Giannini, A.; Camargo, S. J. & Rojas, M. (2013),
945 'CMIP5 Projected Changes in the Annual Cycle of Precipitation in Monsoon Regions',
946 *Journal of Climate* **26**, 7328-7351.

947

948 Sheffield, J.; Goteti, G. & Wood, E. F. (2006), 'Development of a 50-Year
949 High-Resolution Global Dataset of Meteorological Forcings for Land Surface
950 Modeling', *Journal of Climate* **19**, 3088-3111.

951

952 Shongwe, M. E.; van Oldenborgh, G. J.; van den Hurk, B. J. J. M.; de Boer, B.; Coelho,
953 C. A. S. & van Aalst, M. K. (2009), 'Projected Changes in Mean and Extreme
954 Precipitation in Africa under Global Warming. Part I: Southern Africa', *Journal of*
955 *Climate* **22**, 3819-3837.

956

957 Staver, A. C.; Archibald, S. & Levin, S. A. (2011), 'The Global Extent and
958 Determinants of Savanna and Forest as Alternative Biome States', *Science* **334**,
959 230-232.

960

961 Stocker, T. F.; Qin, D.; Plattner, G.-K.; Tignor, M.; Allen, S. K.; Boschung, J.; Nauels,
962 A.; Xia, Y.; Bex, V. & Midgley, P. M., ed. (2013), *IPCC, 2013: Climate Change 2013:*
963 *The Physical Science Basis. Contribution of Working Group I to the Fifth Assessment*
964 *Report of the Intergovernmental Panel on Climate Change*, Cambridge University
965 Press, Cambridge, United Kingdom and New York, NY, USA..

966

967 Svejcar, T.; Bates, J.; Angell, R. & Miller, R. (2003), 'The influence of precipitation
968 timing on the sagebrush steppe ecosystem. In: Guy, McPherson, Jake, Weltzin (Eds.),
969 Changing Precipitation Regimes & Terrestrial Ecosystems. University of Arizona Press,
970 Tucson, AZ 237pp.'. .
971
972 Thomey, M. L.; Collins, S. L.; Vargas, R.; Johnson, J. E.; Brown, R. F.; Natvig, D. O. &
973 Friggens, M. T. (2011), 'Effect of precipitation variability on net primary production
974 and soil respiration in a Chihuahuan Desert grassland', *Global Change Biology* **17**,
975 1505-1515.
976
977 Trenberth, K. E.; Dai, A.; Rasmussen, R. M. & Parsons, D. B. (2003), 'The Changing
978 Character of Precipitation', *Bulletin of American Meteorological Society* **84**, 1205-1217.
979
980 Vincens, A.; Garcin, Y. & Buchet, G. (2007), 'Influence of rainfall seasonality on
981 African lowland vegetation during the Late Quaternary: pollen evidence from Lake
982 Masoko, Tanzania', *Journal of Biogeography* **34**, 1274-1288.
983
984 Weltzin, J. F.; Loik, M. E.; Schwinning, S.; Williams, D. G.; Fay, P. A.; Haddad, B. M.;
985 Harte, J.; Huxman, T. E.; Knapp, A. K.; Lin, G.; Pockman, W. T.; Shaw, M. R.; Small,
986 E. E.; Smith, M. D.; Smith, S. D.; Tissue, D. T. & Zak, J. C. (2003), 'Assessing the
987 Response of Terrestrial Ecosystems to Potential Changes in Precipitation', *BioScience*
988 **53(10)**, 941-952.
989
990 Williams, C. A. & Albertson, J. D. (2006), 'Dynamical effects of the statistical
991 structure of annual rainfall on dryland vegetation', *Global Change Biology* **12**,
992 777-792.
993
994 Zhang, X.; Friedl, M. A.; Schaaf, C. B.; Strahler, A. H. & Liu, Z. (2005), 'Monitoring
995 the response of vegetation phenology to precipitation in Africa by coupling MODIS
996 and TRMM instruments', *Journal of Geophysical Research* **110**, D12103.
997
998 Zhang, Y.; Moran, M. S.; Nearing, M. A.; Campos, G. E. P.; Huete, A. R.; Buda, A. R.;
999 Bosch, D. D.; Gunter, S. A.; Kitchen, S. G.; McNab, W. H.; Morgan, J. A.; McClaran,
1000 M. P.; Montoya, D. S.; Peters, D. P. & Starks, P. J. (2013), 'Extreme precipitation
1001 patterns and reductions of terrestrial ecosystem production across biomes', *Journal of*
1002 *Geophysical Research: Biogeosciences* **118**, 148-157.
1003

Table 1. Summary of previous representative studies on assessing the impacts of rainfall characteristics (i.e. rainfall frequency, intensity and seasonality) on the structure and function of terrestrial ecosystem.

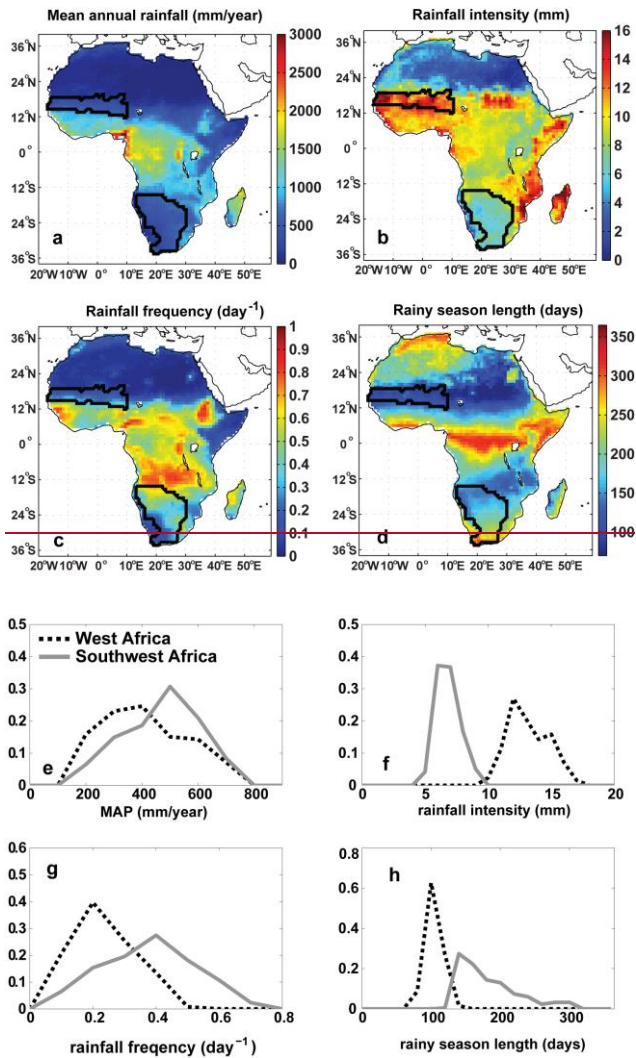
Focus: frequency (freq); intensity (int); seasonality (sea); variation (CV).

Methods: Field Experiments (Field); Remote Sensing (RS); Flux Tower (Flux).

Major Conclusion: increasing rainfall intensity (or decreasing frequency) has positive impacts (int+); increasing intensity (or decreasing frequency) has negative impacts (int-); increasing rainfall CV has positive impacts (CV+); increasing rainfall CV has negative impacts (CV-).

| Focus | Methods | Spatial Scale | Time scale | MAP (mm/year) | Ecosystem type | Major Conclusion | Reference |
|-----------|---------|----------------------------|--------------------------|-------------------|---------------------------------|--|-----------------------|
| freq; int | RS | Africa continent | intra-annual climatology | [0,3000] | Africa all | (int-) woody cover | Good and Caylor, 2011 |
| freq; int | RS | US | | [163,1227] | US | (int-) ANPP greatest in arid grassland (16%) and Mediterranean forest (20%) and less for mesic grassland and temperate forest (3%) | Zhang et al., 2013 |
| freq; int | RS | Pan-tropics (35°N to 15°S) | inter-annual | [0,3000] | Tropical ecosystems | (CV+) wood cover in dry tropics; (CV-) wood cover in wet tropics | Holmgren et al., 2013 |
| freq; int | RS | Northern China | intra-annual | [100,850] | temperate grassland and forests | (int-) NDVI for temperate grassland and broadleaf forests, not for coniferous forest | Fang et al., 2005 |
| freq; int | Flux | Northern Hemisphere | intra-annual | [393±155,906±243] | shrubland and forest | (int-) GPP, RE and NEP | Ross et al., 2012 |
| seas | RS | Africa continent | climatology | [0,3000] | Africa all | rainy season onset and offset controls vegetation growing season | Zhang et al., 2005 |
| freq; int | Field | plot (Kansas, USA) | intra-annual | 615 | grassland | (int-) ANPP | Knapp et al., 2002 |

| | | | | | | | |
|----------------------------|-------|--|---------------------|-----------|----------------------|---|--|
| (fix MAP) | | | | | | | |
| freq; int | Field | plot (Kansas, USA) | intra-annual | 835 | grassland | (int-) ANPP | Fay et al., 2003 |
| (fix MAP) | | | | | | | |
| increase seasonal rainfall | Field | plot(Texas, USA) | intra-annual | 365 | grassland | (int-) ANPP | Robertson et al., 2009 |
| freq; int | Field | plot (Kansas, USA) | intra-annual | [320,830] | grassland | (int-)ANPP for MAP=830mm/yr; (int+)ANPP for MAP=320mm/yr | Heisler-White et al., 2009 |
| freq; int | Field | plot(New Mexico, USA) | intra-annual | 250 | grassland | (int+) ANPP | Thomey et al., 2011 |
| freq; int | Field | Plot(Kansas, USA) | intra-annual | 834 | grassland | (int-) soil CO2 flux | Harper et al., 2005 |
| (fix MAP) | | | | | | | |
| freq; int | Field | plot(Kruger National Park, South Africa) | intra-annual | 544 | sub-tropical savanna | (int+) wood growth; (int-) grass growth | Kulmatiski and Beard, 2013 |
| sea | Field | plot(Oregon, USA) | intra-annual | [140,530] | grassland | impact biomass and bare soil fraction | Bates et al., 2006; Svejcar et al., 2003 |
| (fix MAP) | | | | | | | |
| sea | Field | | | | | | |
| freq; int; MAP | Field | plot(South Africa) | intra-annual | [538,798] | grassland | (int-) ANPP | Swemmer et al., 2007 |
| MAP; sea | Field | plot(Spain) | intra-/inter-annual | 242 | grassland | Mediterranean dryland ecosystem has more resilience for intra- and inter-annual changes in rainfall | Miranda et al., 2008 |



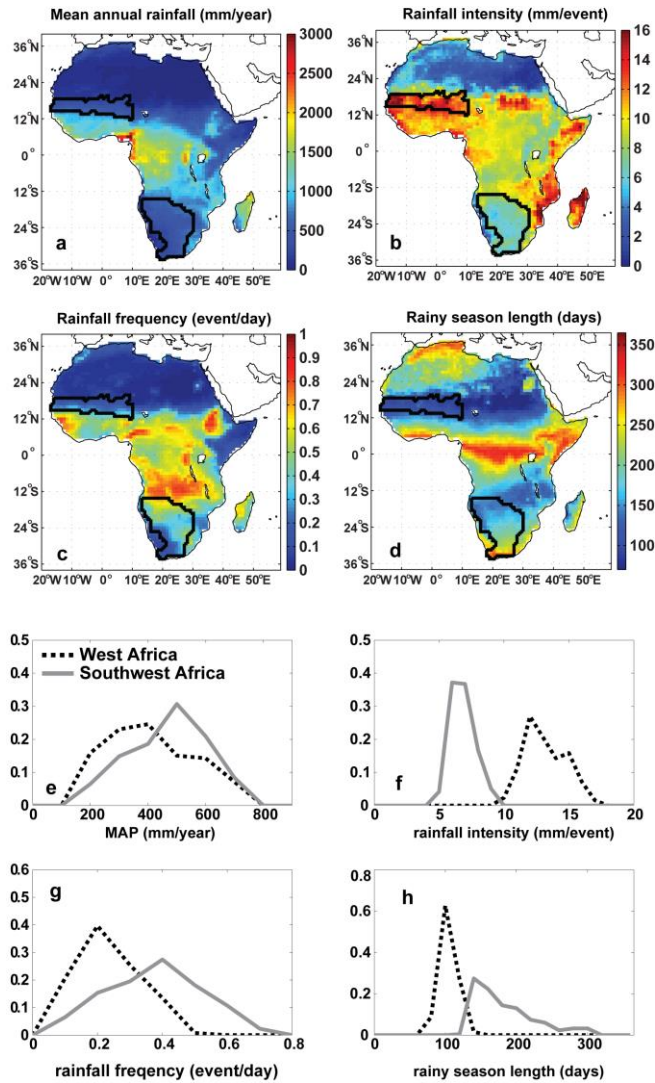


Figure 1. a-b: Spatial pattern of the rainfall characteristics in Africa: a-MAP; b-rainfall intensity; c-rainfall frequency; d-rainy season length. The black-line identified areas refer to two savanna regions in West and Southwest Africa. e-f: Normalized histograms of the rainfall characteristics in two savanna regions of West and Southwest Africa. e-MAP (bin width for the x-axis: 100 mm/year); f-rainfall intensity (bin width for the x-axis: 1 mm/event); g-rainfall frequency (bin width for the x-axis: 0.1 event/day); h-rainy season length (bin width for the x-axis: 20 days).--

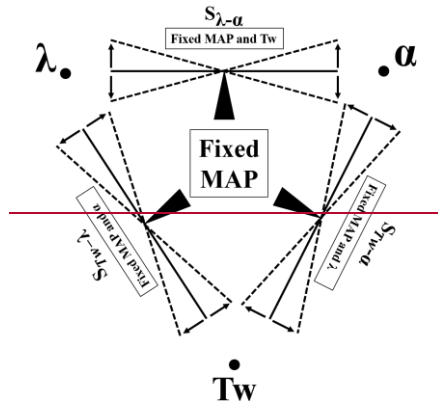


Figure 2. Conceptual diagram of the experiment designs for three experiments ($S_{\lambda-\alpha}$, $S_{Tw-\lambda}$, $S_{Tw-\alpha}$).

Formatted: Centered

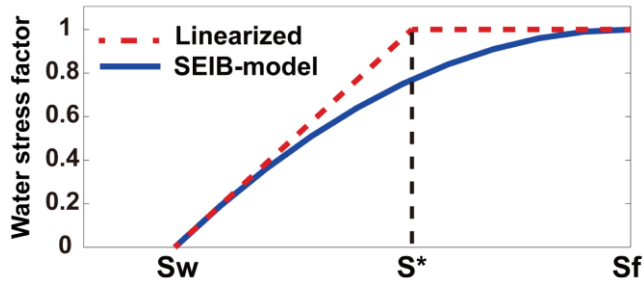


Figure 2. Schematic diagram of water stress factor ranging from 0 (most stressful) to 1 (no stress), which acts to reduce transpiration and carbon assimilation. The red dotted line is based on Porporato et al. (2001) with a reversed sign, and the SEIB-model SEIB-DGVM has a nonlinear implementation (blue solid line, Sato and Ise, 2012).

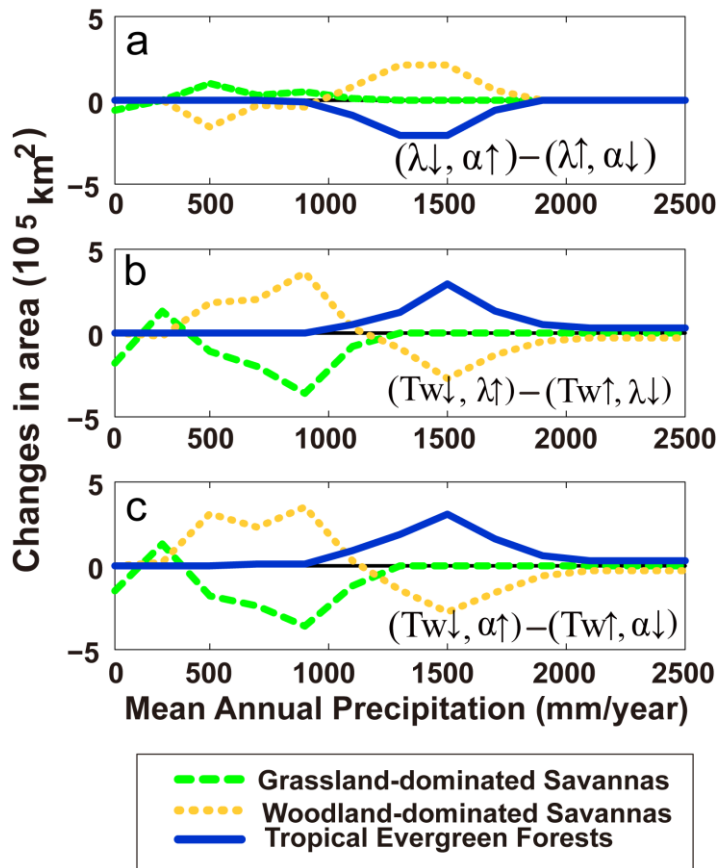


Figure 3. Differences in simulated dominated biomes in the three experiments (i.e. $S_{\lambda-\alpha}$, $S_{Tw-\lambda}$, $S_{Tw-\alpha}$).

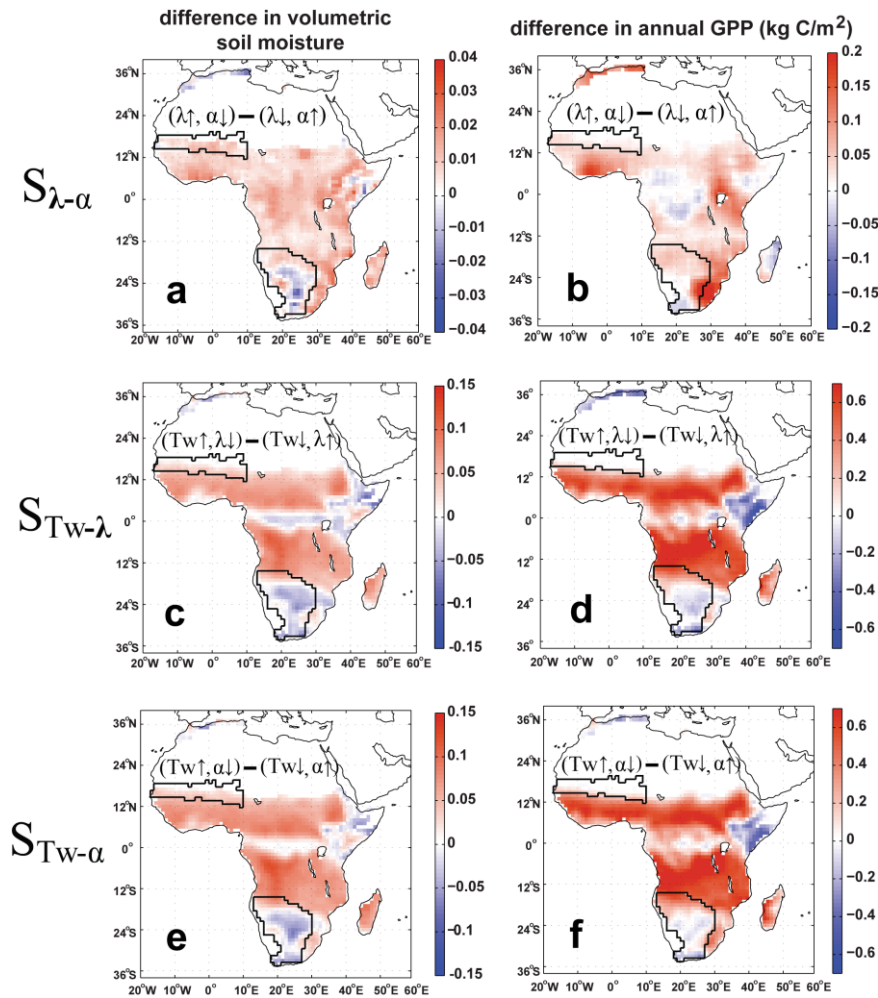
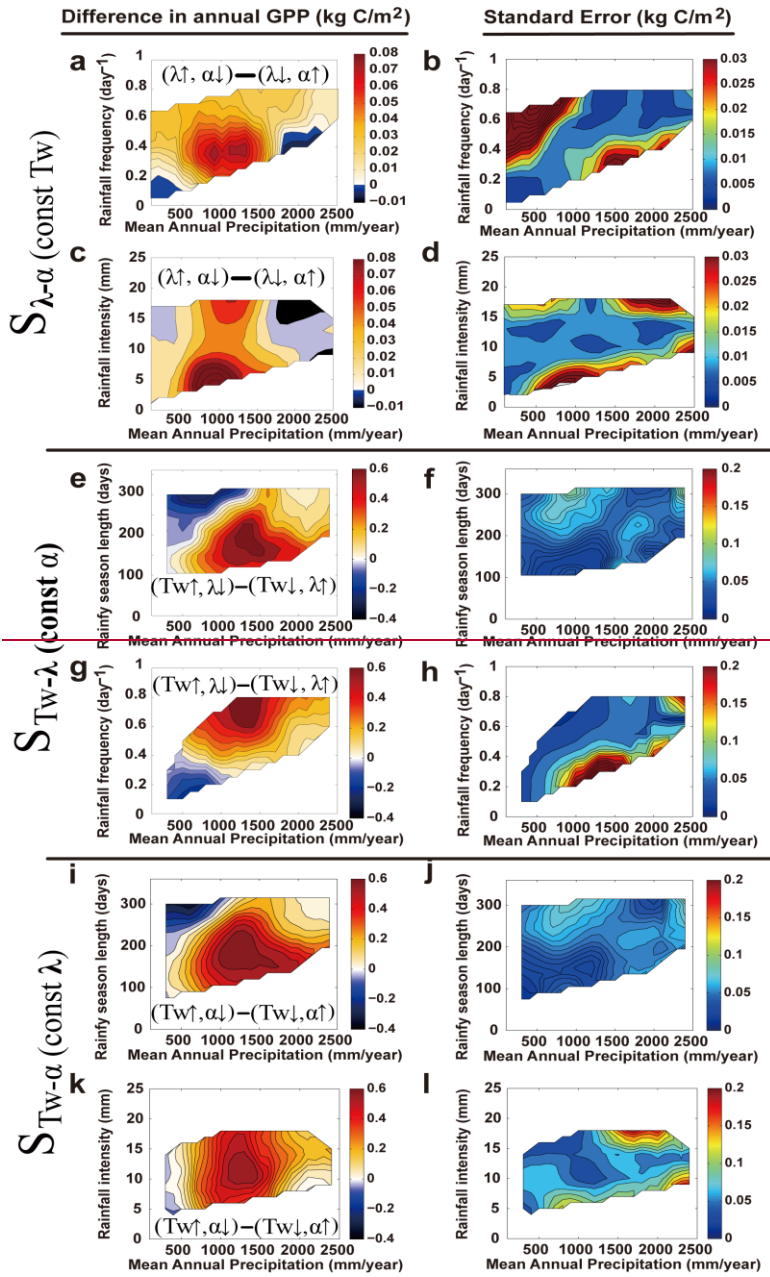
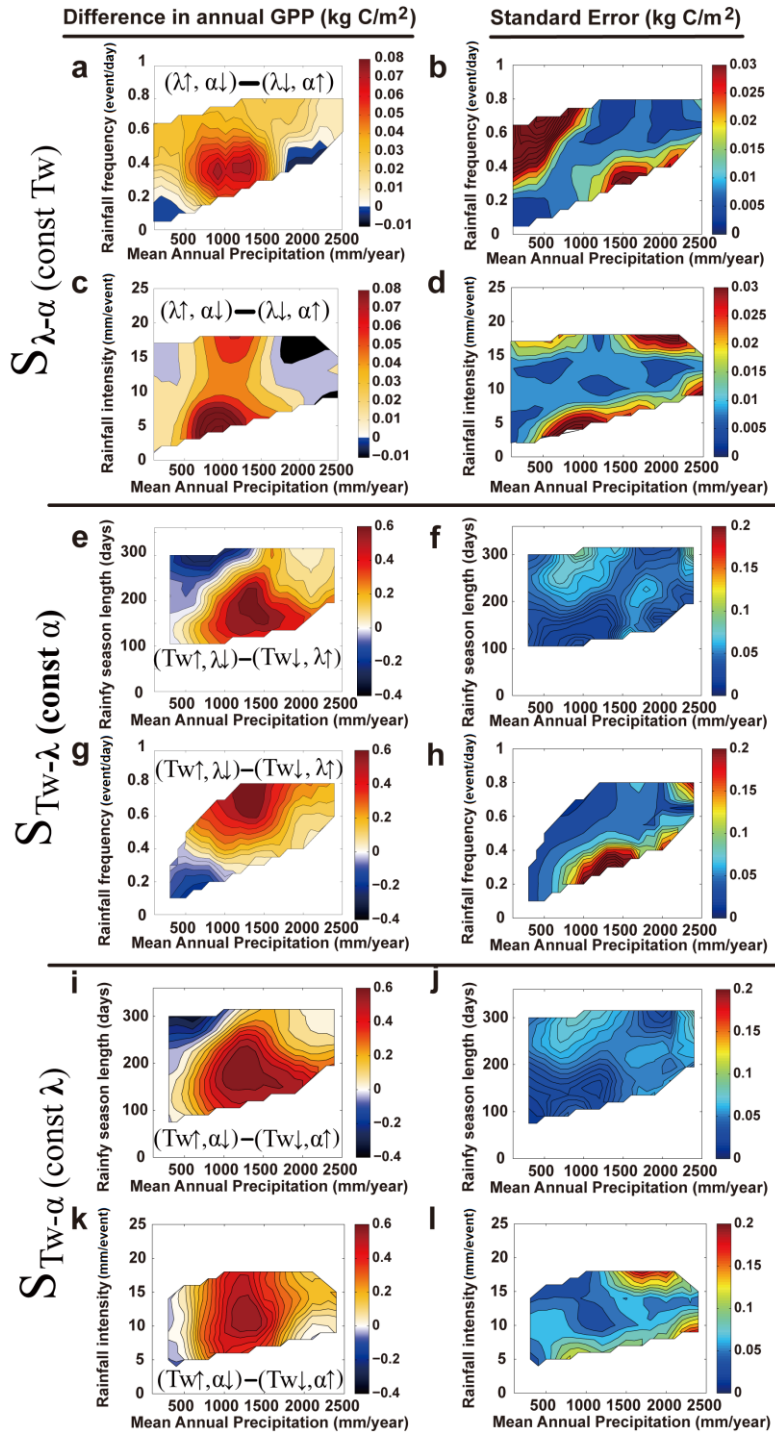


Figure 4. Simulated changes in annual mean soil moisture (0-500mm, first column) and annual mean GPP (second column) for different experiments. Please note that the scales of $S_{\lambda-\alpha}$ is much smaller than those of $S_{TW-\lambda}$ and $S_{TW-\alpha}$. The two areas with black boundaries in each panel are West African grassland and Southwest African grassland associated with Figure 1. The spatial patterns shown here are smoothed by 3*3 smoothing window from the raw data.





~~Figure 6~~ **Figure 5.** Differences in simulated annual GPP as a function of mean annual precipitation and one of the perturbed rainfall characteristics in all the three experiments (i.e. $S_{\lambda-\alpha}$, $S_{TW-\lambda}$, $S_{TW-\alpha}$) in the left column. The right column shows the correspondent standard errors (SE, calculated as $SE = \frac{\sigma}{\sqrt{n}}$, where σ refers to the standard deviation within each bin, n is the sample size in each bin, and n and σ are shown in Figure S4), with larger values associated with more uncertainties and requires more caution in interpretation. The contours are based on the binned values, with for each 100 mm/year in MAP, each 0.05 ~~day~~⁻¹event/day in rainfall frequency, each 1 ~~mm~~mm/event in rainfall intensity and each 15 day in rainy season length.

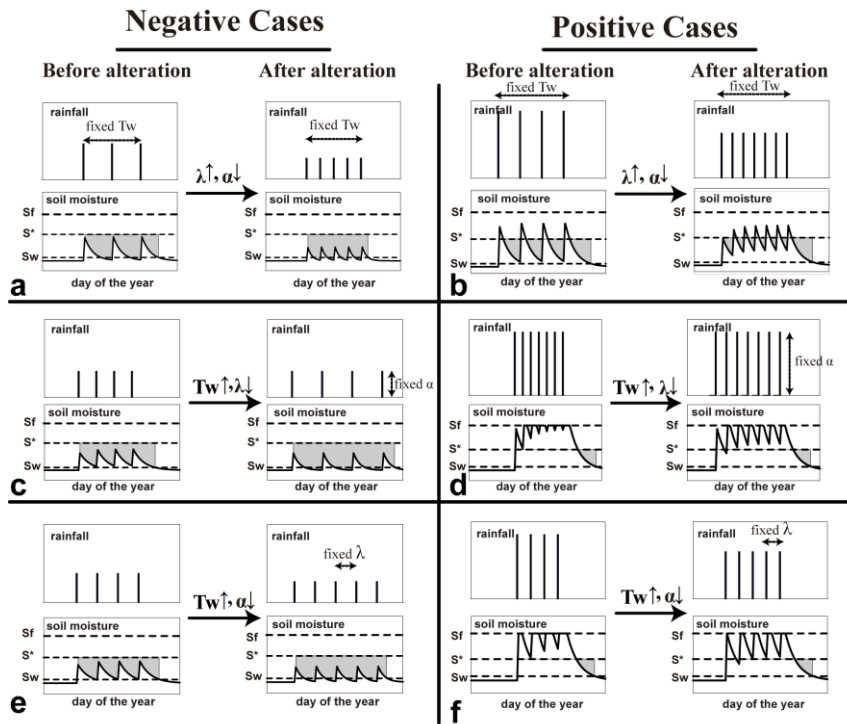


Figure 6. Illustrative time series for hydrological controls on plant root-zone soil moisture dynamics for all the experiments, and these illustrations are generalized based on the simulated time series from the experiments. Both negative and positive cases are shown, and cases with directly hydrological controls are shown (i.e. cloud-induced negative impacts in tropical forests are not shown). The cumulative shaded areas refer to “plant water stress” defined by Porporato et al. (2001).

Supplementary materials:

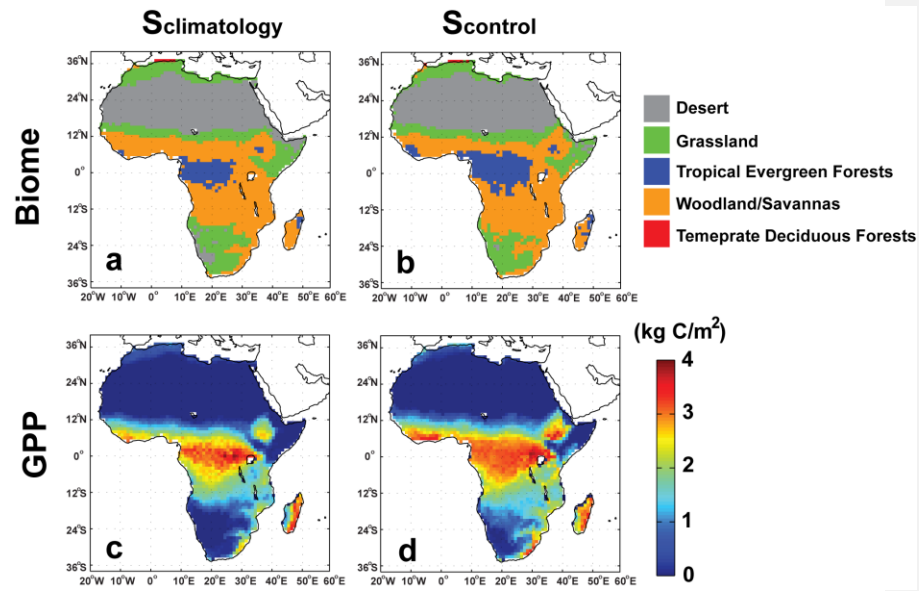


Figure S1. Comparison of biomes and annual GPP between $S_{climatology}$ and $S_{control}$ to test the validity of the synthetic weather generator. The biome definition follows Sato and Ise (2012).

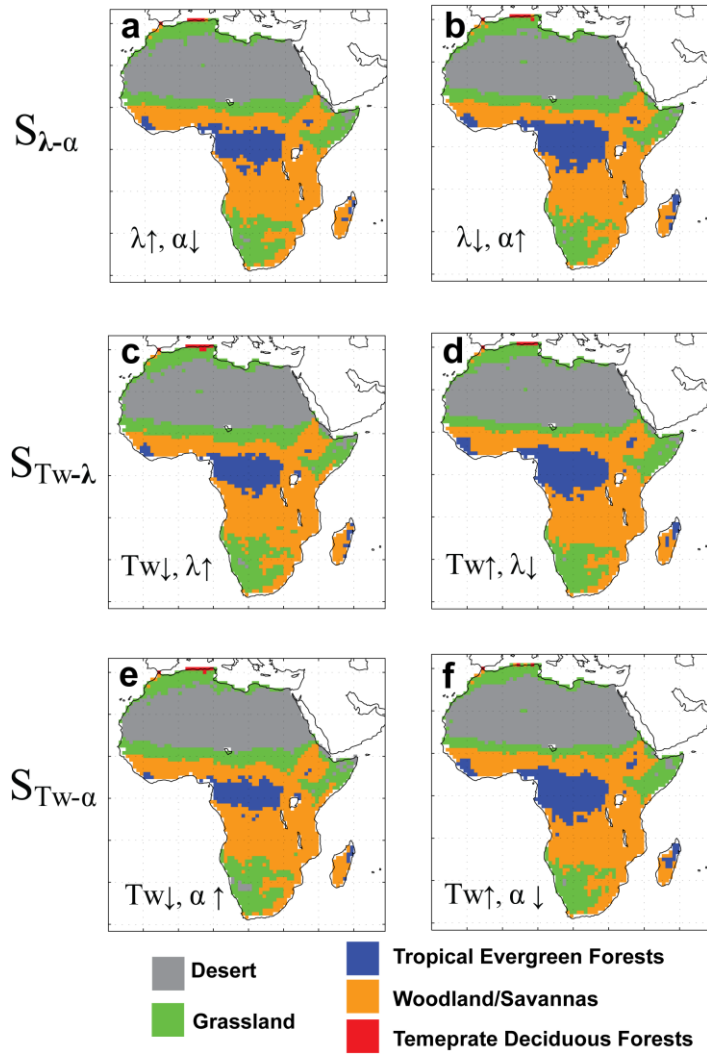


Figure S2. Simulated biomes for different experiments.

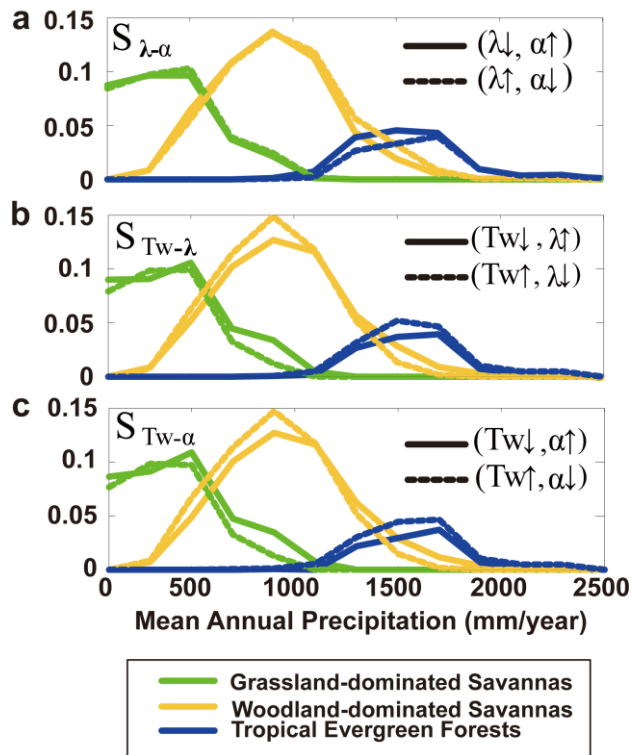
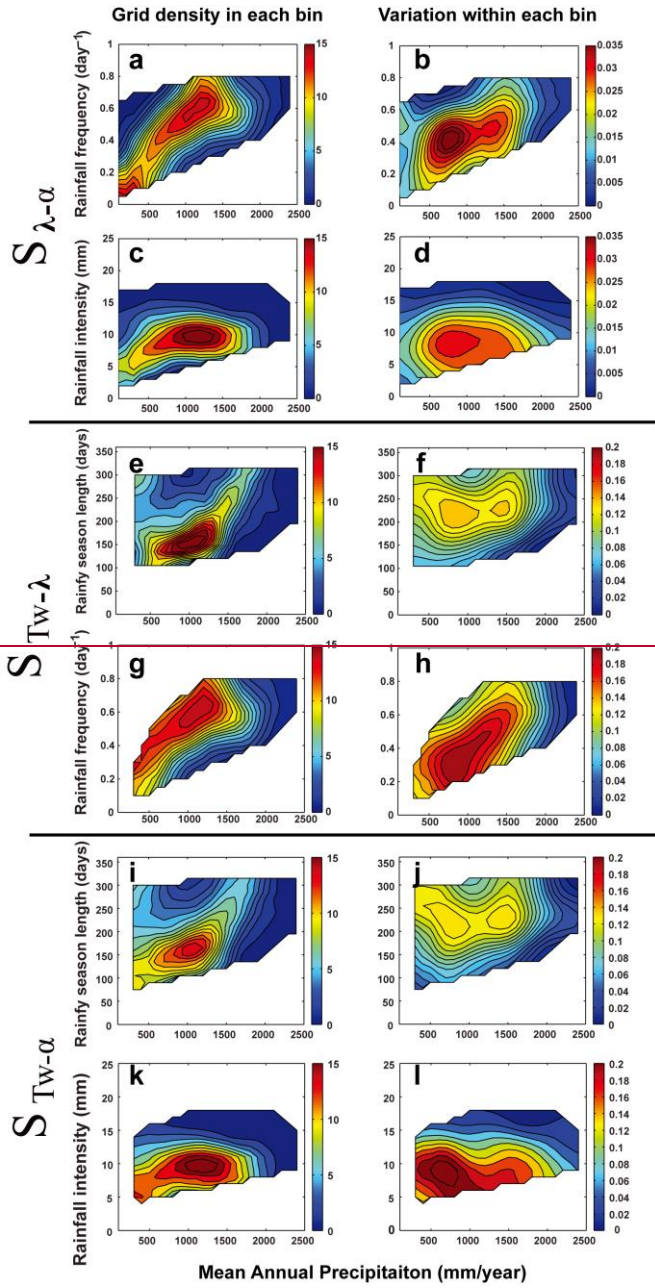


Figure S3. Normalized histograms of three simulated dominating biomes in the three experiments.



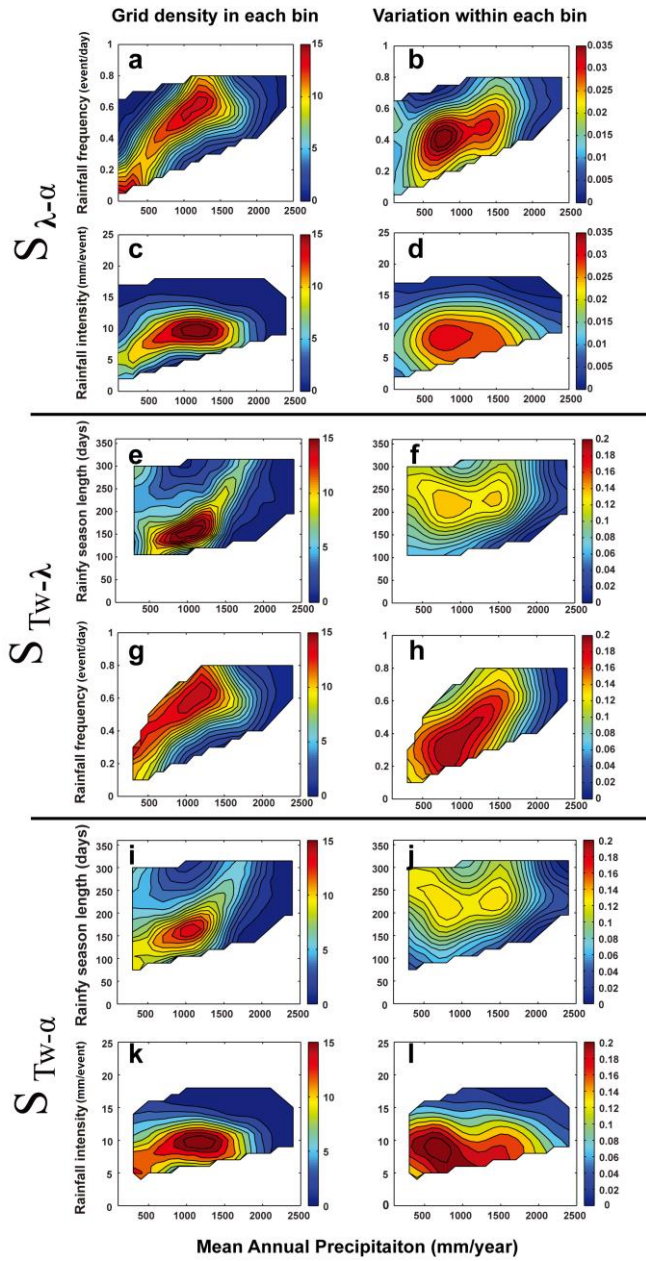


Figure S4. The sample size (n) in each bin (left column) and standard deviation (σ) in each bin (right column), corresponding to [Figure 6](#)[Figure 5](#). In [Figure 6](#)[Figure 5](#) right column, standard deviation (SE) is calculated as $SE = \frac{\sigma}{\sqrt{n}}$.

1 **Continental-scale impacts of intra-seasonal rainfall variability**
2 **on simulated ecosystem responses in Africa**

3
4 Kaiyu Guan^{1,2*}, Stephen P. Good³, Kelly K. Caylor¹, Hisashi Sato⁴, Eric F. Wood¹, and
5 Haibin Li⁵

6
7 ¹Department of Civil and Environmental Engineering, Princeton University, Princeton,
8 NJ, USA

9 ²Department of Environmental & Earth System Science, Stanford University, Stanford,
10 CA 94025, USA

11 ³Department of Geology and Geophysics, University of Utah, Salt Lake City, UT
12 84112, USA

13 ⁴Graduate School of Environmental Studies, Nagoya University, D2-1(510) Furo-cho,
14 Chikusa-ku, Nagoya-city, Aichi 464-8601, Japan

15 ⁵Department of Earth and Planetary Sciences, Rutgers University, Piscataway, NJ
16 08854, USA

17
18 *Corresponding author:

19 Kaiyu Guan

20 Department of Environmental & Earth System Science,
21 Stanford University, Stanford, CA 94025, USA

22 Phone: 609-647-1368, Fax: 650-498-5099

23 Email: kaiyug@stanford.edu

24
25 Running title: Ecological Impacts of Intra-Seasonal Rainfall Variability

26
27 Submitted to *Biogeosciences*

28

29 **Abstract:**

30 Climate change is expected to change intra-seasonal rainfall variability, arising from
31 shifts in rainfall frequency, intensity and seasonality. These intra-seasonal changes are
32 likely to have important ecological impacts on terrestrial ecosystems. Yet, quantifying
33 these impacts across biomes and large climate gradients is largely missing. This gap
34 hinders our ability to better predict ecosystem services and their responses to climate
35 change, esp. for arid and semi-arid ecosystems. Here we use a synthetic weather
36 generator and an independently validated vegetation dynamic model (SEIB-DGVM)
37 to virtually conduct a series of “rainfall manipulation experiments” to study how
38 changes in the intra-seasonal rainfall variability affect continent-scale ecosystem
39 responses across Africa. We generated different rainfall scenarios with fixed total
40 annual rainfall but shifts in: i) frequency vs. intensity, ii) rainy season length vs.
41 frequency, iii) intensity vs. rainy season length. These scenarios were fed into
42 SEIB-DGVM to investigate changes in biome distributions and ecosystem
43 productivity. We find a loss of ecosystem productivity with increased rainfall
44 frequency and decreased intensity at very low rainfall regimes (<400 mm/year) and
45 low frequency (<0.3 event/day); beyond these very dry regimes, most ecosystems
46 benefit from increasing frequency and decreasing intensity, except in the wet tropics
47 (>1800 mm/year) where radiation limitation prevents further productivity gains. This
48 result reconciles seemingly contradictory findings in previous field studies on rainfall
49 frequency/intensity impacts on ecosystem productivity. We also find that changes in
50 rainy season length can yield more dramatic ecosystem responses compared with
51 similar percentage changes in rainfall frequency or intensity, with the largest impacts
52 in semi-arid woodlands. This study demonstrates that not all rainfall regimes are
53 ecologically equivalent, and that intra-seasonal rainfall characteristics play a
54 significant role in influencing ecosystem function and structure through controls on
55 ecohydrological processes. Our results also suggest that shifts in rainfall seasonality
56 have potentially large impacts on terrestrial ecosystems, and these understudied
57 impacts should be explicitly examined in future studies of climate impacts.

58 **Keywords:** rainfall frequency, rainfall intensity, rainfall seasonality, biome

59 distribution, Gross Primary Production (GPP), Africa

60

61 **1. Introduction**

62 Due to increased water holding capacity in the atmosphere as a consequence of global
63 warming (O’Gorman and Schneider, 2009), rainfall is projected to change in intensity
64 and frequency across much of the world (Easterling et al., 2000; Trenberth et al., 2003;
65 Chou et al., 2013), in conjunction with complex shifts in rainfall seasonality (Feng et
66 al., 2013; Seth et al., 2013). These changes possibly indicate a large increase in the
67 frequency of extreme events and variability in rainfall (Easterling et al., 2000; Allan
68 and Soden, 2008), and many of these changes may be accompanied with little changes
69 in total annual rainfall (Knapp et al., 2002; Franz et al., 2010). Meanwhile, regions
70 sharing similar mean climate state may have very different intra-seasonal variabilities,
71 and the ecological significance of intra-seasonal climate variabilities has been largely
72 overlooked previously in terrestrial biogeography (Good and Caylor, 2011). For
73 example, ecosystems in West Africa and Southwest Africa (Figure 1) share similar
74 total annual rainfall, but West Africa has much more intense rainfall events within a
75 much shorter rainy season, while Southwest Africa has a longer and less intense rainy
76 season. The same amount of total rainfall can come in very different ways, which may
77 cause distinctive ecosystem responses and structure. Understanding the impacts of
78 these regional differences in intra-seasonal rainfall variability and their possible future
79 changes on terrestrial ecosystems is critical for maintaining ecosystem services and
80 planning adaptation and mitigation strategies for ecological and social benefits
81 (Anderegg et al., 2013).

82

83 [insert Figure 1]

84

85 The changes in intra-seasonal rainfall characteristics, specifically frequency,
86 intensity and seasonality, have critical significance to ecosystem productivity and
87 structure (Porporato et al., 2001; Weltzin et al., 2003; Williams and Albertson, 2006;
88 Good and Caylor, 2011; Guan et al., 2014), but previous studies on this topic

89 (summarized in Table 1) have their limitations in the following aspects. First, existing
90 relevant field studies mostly focus on a single ecosystem, *i.e.* grasslands, and
91 subsequently only low rainfall regimes have been examined to date (mostly below
92 800mm/year, see Table 1). Grasslands have the largest sensitivity to hydrological
93 variabilities among all natural ecosystems (Scanlon et al., 2005; Guan et al., 2012),
94 however inferences drawn from a single ecosystem are limited in scope and difficult
95 to apply to other ecosystems. Second, even within grasslands, different studies have
96 seemingly contradictory findings (see Table 1), and there is a lack of a comprehensive
97 framework to resolve these inconsistencies. Specifically, whether increased rainfall
98 intensity with decreased rainfall frequency has positive (Knapp et al., 2002; Fay et al.,
99 2003; Robertson et al., 2009; Heisler-White et al., 2009) or negative impacts
100 (Heisler-White et al., 2009; Thomey et al., 2011) on grassland productivity is still
101 under debate. Third, previous relevant studies mostly focus on the impacts of rainfall
102 frequency and intensity (Table 1 and Rodríguez-Iturbe and Porporato, 2004), and
103 largely overlook the possible changes in rainfall seasonality. Rainfall frequency and
104 intensity mostly describe rainfall characteristics within the rainy season, but do not
105 account for the impacts of interplay between rainy season length and dry season
106 length (Guan et al., 2014). For ecosystems predominately controlled by water
107 availability, rainy season length constrains the temporal niche for active plant
108 physiological activities (van Schaik et al., 1993; Scholes and Archer, 1997), and large
109 variations in rainfall seasonality can lead to significant shifts in biome distribution
110 found from paleoclimate pollen records (e.g. Vincens et al., 2007). Given changes in
111 rainfall seasonality have been found in various tropical regions (Feng et al., 2013) and
112 have been projected in future climate (Biasutti and Sobel, 2009; Shongwe et al., 2009;
113 Seth et al., 2013), studies investigating their impacts on terrestrial ecosystems are
114 relatively rare, and very few field studies are designed to address this aspect (Table 1,
115 Bates et al., 2006; Svejcar et al., 2003; Chou et al., 2008). Finally, there is an
116 increasing trend of large-scale studies addressing rainfall variability and ecological
117 responses using satellite remote sensing (Fang et al., 2005; Zhang et al., 2005; Good
118 and Caylor, 2011; Zhang et al., 2013; Holmgren et al., 2013) and flux network data

119 (Ross et al., 2012). These large-scale studies are able to expand analyses to more
120 types of ecosystems and different climate conditions, and provide valuable
121 observation-based insights. However there are very few theoretical modeling works to
122 corroborate this effort. All these above issues call for a comprehensive modeling study
123 to investigate different aspects of intra-seasonal rainfall variability on terrestrial
124 ecosystems spanning large environmental gradients and various biomes.

125 In this paper, we aim to study ecological impacts of intra-seasonal rainfall
126 variability on terrestrial ecosystems. In particular, we design virtual “rainfall
127 manipulation experiments” to concurrently shift intra-seasonal rainfall characteristics
128 without changing total annual rainfall. We focus on the impacts of these different
129 rainfall scenarios on ecosystem productivity (e.g. Gross Primary Production, GPP)
130 and biome distributions in the African continent, simulated by an independently
131 validated dynamic vegetation model SEIB-DGVM (Sato and Ise, 2012). Previous
132 modeling approaches in this topic (Gerten et al., 2008; Hély et al., 2006) designed
133 various rainfall scenarios by rearranging (halving, doubling or shifting) the rainfall
134 amount based on the existing rainfall observations. In contrast to these approaches, we
135 design a weather generator based on a stochastic rainfall model (Rodríguez-Iturbe et
136 al., 1999), which allows us to implement a series of experiments by synthetically
137 varying two of the three rainfall characteristics (rainfall intensity, rainfall frequency,
138 and rainy season length) while fixing total annual rainfall at the current climatology.
139 We choose Africa as our test-bed mostly because the following two reasons: (1) the
140 rainfall regimes and biomes have large gradients varying from extremely dry
141 grasslands to highly humid tropical evergreen forests; (2) Africa is a continent usually
142 assumed to have few temperature constraints (Nemani et al., 2003), which will help to
143 isolate the impacts of precipitation from temperature, as one challenge in attributing
144 climatic controls on temperate ecosystems or Mediterranean ecosystems is the
145 superimposed influences from both temperature and precipitation. The overarching
146 science question we will address is: **How do African ecosystems respond to possible**
147 **changes in intra-seasonal rainfall variability (i.e. rainfall frequency, intensity and**
148 **rainy season length)?**

149

150 [insert Table 1]

151

152 **2. Materials and Methods**

153 **2.1 Methodology overview**

154 Table 1 summarizes previous field-based rainfall manipulation experiments, such as
155 the one that Knapp et al. (2002) did in a grassland that concurrently increasing rainfall
156 frequency and decreasing rainfall intensity while fixing total rainfall. The central idea
157 of our study is to design similar rainfall manipulation experiments but test them
158 virtually in the model domain across large environment gradients. We manipulate
159 rainfall changes through a weather generator based on a parsimonious stochastic
160 rainfall model (Rodriguez-Iturbe et al., 1984). We model the total amount of rainfall
161 during rainy season as a product of the three intra-seasonal rainfall characteristics for
162 the rainy season, rainfall frequency (λ , event/day), rainfall intensity (α , mm/event),
163 and rainy season length (T_w , days) (More details in section 2.3). Thus it is possible to
164 simultaneously perturb two of the rainfall characteristics away from their
165 climatological values while preserving the mean annual precipitation (MAP)
166 unchanged. We then feed these different rainfall scenarios into a well-validated
167 dynamic vegetation model (SEIB-DGVM, section 2.2) to study simulated ecosystem
168 responses. Detailed experiments design is described in section 2.5.

169

170 **2.2 SEIB-DGVM model and its performances in Africa**

171 We use a well-validated vegetation dynamic model SEIB-DGVM (Sato et al., 2007)
172 as the tool to study ecosystem responses to different rainfall variabilities. This model
173 follows the traditional “gap model” concept (Shugart, 1998) to explicitly simulate the
174 dynamics of ecosystem structure and function for individual plants at a set of virtual
175 vegetation patches, and uses results at these virtual patches as a surrogate to represent
176 large-scale ecosystem states. Thus individual trees are simulated from establishment,
177 competition with other plants, to death, which creates “gaps” for other plants to
178 occupy and develop. SEIB-DGVM includes mechanical-based and empirical-based

179 algorithms for land physical processes, plant physiological processes, and plant
180 dynamic processes. SEIB-DGVM contains algorithms that explicitly involve the
181 mechanisms of plant-related water stress (Figure 2; Sato and Ise, 2012). With similar
182 concepts to previous studies (e.g. Milly, 1992; Porporato et al., 2001), the current
183 SEIB-DGVM implements a continuous “water stress factor” (Equation 2) based on
184 the soil moisture status (Equation 1), scaling from 0 (most stressful) to 1 (with no
185 stress), which then acts to scale the stomatal conductance for plant transpiration and
186 carbon assimilation.

$$187 \quad stat_{water} = (S - S_w) / (S_f - S_w) \quad (\text{Equation 1})$$

$$188 \quad \text{Water stress factor} = 2 * stat_{water} - stat_{water}^2 \quad (\text{Equation 2})$$

189 where S , S_w and S_f refer to the fraction of volumetric soil water content within the
190 rooting depth, at the wilting point, and at field capacity, respectively. Figure 2
191 provides a schematic diagram of “water stress factor” from the SEIB-DGVM, and we
192 also include an approximated linear model that has been widely adopted elsewhere
193 (e.g. Milly, 1992; Porporato et al., 2001). The linear model uses an extra variable S^* ,
194 so called “critical point” of soil moisture: when $S > S^*$, there is no water stress (water
195 stress factor = 1); and when $S < S^*$, water stress factor linearly decreases with the
196 decrease of S . Though SEIB-DGVM adopts a quadratic form for “water stress factor”,
197 it essentially functions similarly as the linear model, such that S^* distinguishes two
198 soil moisture regimes that below which there is a large sensitivity of water stress to
199 soil moisture status, and above which there is little water stress. Understanding how
200 this “water stress factor” functions is the key to explain the following results.

201

202 [insert Figure 2]

203

204 SEIB-DGVM allows development of annual and perennial grasses as well as multiple
205 life cycles of grass at one year based on environmental conditions. Multiple life cycles
206 of tree growth per year are possible in theory but rarely happen in simulations (Sato
207 and Ise, 2012). Soil moisture status is the predominant factor to determine LAI of the
208 vegetation layer, which influences maximum daily productivity and leaf phenology.

209 When LAI exceeds 0 for 7 continuous days, dormant phase of perennial vegetation
210 layer changes into growth phase. While when LAI falls below 0 for 7 continuous days,
211 growth phase switches to dormant phase (Sato et al, 2007). SEIB-DGVM also
212 explicitly simulates light conditions and light competition among different PFTs in the
213 landscape based on its simulated 3D canopy structure and radiative transfer scheme
214 (Sato et al, 2007).

215 SEIB-DGVM has been tested both globally (Sato et al., 2007) and regionally for
216 various ecosystems (Sato et al., 2010; Sato, 2009; Sato and Ise, 2012), whose
217 simulated results compare favorably with ground observations and satellite remote
218 sensing measures for ecosystem composition, structure and function. In particular,
219 SEIB-DGVM has been successfully validated and demonstrated its ability in
220 simulating ecosystem structure and function in the African continent (Sato and Ise,
221 2012). Two plant function types (PFTs) of tropical woody species are simulated by
222 SEIB-DGVM in Africa: tropical evergreen trees and tropical deciduous trees. The
223 distribution of these two woody types in the simulation is largely determined by
224 hydro-climatic environments. Tropical evergreen trees only develop in regions where
225 water resources are sufficient all year around, so they can maintain leaves for all
226 seasons; otherwise, tropical deciduous trees could survive and dominate the landscape
227 as they can shed leaves if there is no sufficient water supply in its root zone during the
228 dry season (Sato and Ise, 2012). Trees and grasses coexist in a cell, with the floor of a
229 virtual forest monopolized by one of the two grass PFTs, C₃ or C₄ grass. The
230 dominating grass type is determined at the end of each year by air temperature,
231 precipitation, and CO₂ partial pressure (Sato and Ise, 2012).

232 SEIB-DGVM was run at 1 ° spatial resolution and at the daily step. It was spun-up
233 for 2000 years driven by the observed climate (1970-2000) repeatedly for the soil
234 carbon pool to reach steady state, followed by 200 years simulation driven by the
235 forcings based on the experiment design in Section 2.4. Because our purpose is to
236 understand the direct impacts of intra-seasonal rainfall variability, we turned off the
237 fire component of SEIB-DGVM to exclude fire-mediated feedbacks in the results.
238 Though we are fully aware of the important role of fire in interacting with rainfall

239 seasonality and their influence on African ecosystems (Bond et al., 2005; Lehmann et
240 al., 2011; Staver et al., 2012), studying these interactions is beyond the scope of this
241 work. For the similar reason, we fixed the atmospheric CO₂ concentration at 380
242 ppmv to exclude possible impacts of CO₂ fertilization effects.

243

244 **2.3 Synthetic weather generator**

245 The synthetic weather generator used here has two major components: i) to
246 stochastically generate daily rainfall based on a stochastic rainfall model, and ii) to
247 conditionally sample all other environmental variables from historical records to
248 preserve the covariance among climate forcing variables.

249 The stochastic rainfall model can be expressed as $MAP = \alpha \lambda T_w / f_w$, and we set f_w
250 to be 0.9, i.e. the period including 90% of total annual rainfall is defined as “rainy
251 season” (exchangeable with “wet season” hereafter). In particular, we first use
252 Markham (1970)’s approach to find the center of the rainy season, and then extend the
253 same length to both sides of the center until the total rainfall amount in this temporal
254 window (i.e. “rainy season”) is equal to 90% of the total annual rainfall. Rainy season
255 and dry season have their own rainfall frequency and intensity. Two seasons are
256 separately modeled based on the Market Poisson Process. Here we only focus on and
257 manipulate rainy-season rainfall characteristics in our study, as rainy-season rainfall
258 accounts for almost all the meaningful rainfall inputs for plant use. Thus in the
259 following paper, whenever we mention α or λ , we refer to those during the rainy
260 season.

261 In this rainfall model, any day can be either rainy or not, and a rainy day is
262 counted as one rainy event; rainfall events occur as a Poisson Process, with the
263 parameter $1/\lambda$ (unit: days/event) being the mean intervals between rainfall events, and
264 rainfall intensity α for each rainfall event following an exponential distribution, with α
265 being the mean rainfall intensity per event (Rodríguez-Iturbe et al., 1999). The wet
266 season length is modeled as a beta distribution bounded from 0 to 1, scaled by 365
267 days. All the necessary parameters to fit for the stochastic rainfall model (including
268 the mean and variance of rainfall frequency, intensity and length of wet and dry

269 seasons) were derived from the satellite-gauge-merged rainfall measurement from
270 TRMM 3b42V7 (Huffman et al., 2007) for the period of 1998 to 2012, based on the
271 above assumptions for the rainfall process. Specifically, we applied our definition of
272 “rainy season” to each year of the TRMM rainfall data for per pixel, and calculated
273 the mean and variance of the “rainy season length”, using which we fitted the beta
274 distribution for T_w . For rainfall frequency and intensity, we lumped all the wet or dry
275 season rainfall record together to derive their parameters. The two steps of the
276 synthetic weather generator are described below:

277 **Step 1:** Model the daily rainfall following the Marked Poisson process described
278 above. In particular, for a specific year, we first stochastically generate the wet season
279 length by sampling from the beta distribution, and the dry season length is determined
280 accordingly. Then we generate the daily rainfall for wet and dry season respectively.

281 **Step 2:** Based on the simulated daily rainfall time series in Step 1, we conditionally
282 sample temperature, wind, and humidity from the Global Meteorological Forcing
283 Dataset (GMFD, Sheffield et al., 2006), as well as cloud fraction and soil temperature
284 from the Climate Forecast System Reanalysis (CFSR) from National Centers for
285 Environmental Prediction (NCEP) (Saha et al., 2010). To sample for a specific day, all
286 the historical record within a 21-day time window centered at that specific day makes
287 up a sampling pool. From the sampling pool, we choose the day such that the
288 historical rainfall amount of the chosen day is within $(100-30)\%$ to $(100+30)\%$ of the
289 simulated daily rainfall amount. We then draw all the environmental variables (except
290 rainfall) on that sampled day to the new climate forcing. If we can find a sample from
291 the pool based on the above rule, this sampling is called “successful”. When there is
292 more than one suitable sample, we randomly select one. When there is no suitable
293 sample, we randomly select one day within the pool. The mean “successful” rate for
294 all the experiments and ensembles across Africa is 83%.

295 To test the validity of the synthetic weather generator, we ran SEIB-DGVM using
296 the historical climate record ($S_{\text{climatology}}$) and the synthetic forcing (S_{control}), with the
297 latter generated using the weather generator based on the rainfall characteristics
298 derived from the former. Figure S1 shows that the SEIB-DGVM simulations driven

299 by these two different forcings generate similar biome distributions with a Cohen's
300 Kappa coefficient of 0.78 (Cohen, 1960), and similar GPP patterns in Africa, with the
301 linear fit of annual GPP as: $GPP(S_{\text{control}}) = 1.03 \times GPP(S_{\text{climatology}}) + 0.215$ ($R^2=0.89$,
302 $P < 0.0001$). Both biome and GPP patterns are consistent with observations (Sato and
303 Ise, 2012). These results provide confidence in using the synthetic weather generator
304 and SEIB-DGVM to conduct the further study.

305

306 **2.4 Experiment design**

307 Three experiments are designed as follows:

308 **Exp 1** (Perturbation of rainfall frequency and intensity, termed as $S_{\lambda-\alpha}$ hereafter)
309 Simulations forced by the synthetic forcings with varying λ and α simultaneously for
310 wet season (20% increases of λ and corresponding decreases of α to make MAP
311 unchanged; 20% decreases of λ and corresponding increases of α to make MAP
312 unchanged; no change for dry season rainfall characteristics), while fixing T_w at the
313 current climatology;

314 **Exp 2** (Perturbation of rainfall frequency and rainy season length, termed as $S_{T_w-\lambda}$)
315 Simulations forced by the synthetic forcing with varying T_w and λ simultaneously for
316 wet season (20% increases of T_w and corresponding decreases of λ to make MAP
317 unchanged; 20% decreases of T_w and corresponding increases of λ to make MAP
318 unchanged; no change for dry season characteristics), while fixing α at the current
319 climatology;

320 **Exp 3** (Perturbation of rainy season length and intensity, termed as $S_{T_w-\alpha}$) Simulations
321 forced by the synthetic forcing with varying T_w and α simultaneously for wet season
322 (20% increases of T_w and corresponding decreases of α to make MAP unchanged;
323 20% decreases of T_w and corresponding increases of α to make MAP unchanged; no
324 change for dry season characteristics), while fixing λ at the current climatology.

325 Because λ and T_w have bounded ranges ($\lambda \sim [0, 1]$ and $T_w \sim [0, 365]$), if these two
326 variables after perturbation exceeds the range, we would force their value to be the
327 lower or upper bound, and rearrange the other corresponding rainfall characteristic to
328 ensure MAP unchanged. Each rainfall scenario has six ensemble realizations of

329 synthetic climate forcings to account for the stochasticity of our synthetic weather
330 generator.

331

332 **3. Results**

333 We present the differences in simulated biome distributions of the three experiments
334 (i.e. $S_{\lambda-\alpha}$, $S_{TW-\lambda}$, $S_{TW-\alpha}$) in Figure 3, and their spatial patterns are shown in Figure S2
335 and S3. Differences in simulated annually averaged soil moisture and GPP for each
336 experiment are shown in Figure 4 and 6. These differences represent the simulated
337 ecosystem sensitivity to the slight perturbation of intra-seasonal rainfall characteristics
338 deviating from the current climatology. To further explore how MAP and these
339 rainfall characteristics affect the simulated GPP, Figure 5 shows the difference of
340 simulated GPP as a function of MAP and a perturbed rainfall characteristic in the
341 corresponding experiment. We term Figure 5 as “GPP sensitivity space”, and “positive
342 GPP sensitivity” means that GPP changes at the same direction with MAP or rainfall
343 characteristics, and vice versa for “negative GPP response”. These “GPP sensitivity
344 spaces” are generated based on the aggregated mean GPP in each bin of the rainfall
345 properties. The bin size for MAP, rainfall frequency, rainfall intensity and rainy
346 season length are 100 mm/year, 0.05 event/day, 1 mm/event and 15 days respectively.
347 We also provide the standard error (SE) of the “GPP sensitivity spaces” in each bin to
348 assess their uncertainties, with higher SE meaning larger uncertainties. $SE = \frac{\sigma}{\sqrt{n}}$,
349 where σ and n refer to the standard deviation of GPP values and the sample size in
350 each bin respectively. A series of illustrations in Figure 6 were generalized from the
351 simulated time series, and are used to explain the underlying mechanisms.

352

353 [insert Figure 3; Figure 4; Figure 5]

354

355 **3.1 Ecosystem sensitivity to rainfall frequency and intensity (Experiment $S_{\lambda-\alpha}$)**

356 Experiment $S_{\lambda-\alpha}$ assesses ecosystem responses after increasing rainfall frequency λ
357 and decreasing rainfall intensity α ($\lambda\uparrow$, $\alpha\downarrow$) under a fixed total annual rainfall. The

358 simulated biome distributions show that a small portion of regions are converted from
359 woodland to grassland at low rainfall regime (~500 mm/year), corresponding to a
360 decrease of GPP in these regions. In the high rainfall regime (around 1500 mm/year,
361 Figure 3a), increasing rainfall frequency significantly converts tropical evergreen
362 forests into woodlands. In the intermediate rainfall regime (600-1000 mm/year), there
363 is little change in biome distributions. We further check the spatial patterns of
364 differences in annual mean soil moisture and annual total GPP (Figure 4a and 5b). We
365 find that GPP increases with increasing rainfall frequency across most of the Africa
366 continent, except in the very dry end (in the southern and eastern Africa) and the very
367 wet regions (in central Africa and northeastern Madagascar). This GPP pattern mostly
368 mirrors the soil moisture change in woodlands and grasslands (Figure 4b), except the
369 wet tropics, where the changes of soil moisture and GPP are reversed.

370 Figure 5a shows the GPP sensitivity as a function of MAP and the climatological
371 rainfall frequency, and we find three major patterns:

372 **Pattern 1.1:** Negative GPP sensitivity shows up in the very dry end of MAP regime
373 (MAP<400 mm/year) and with relatively low rainfall frequency ($\lambda < 0.3$ event/day), i.e.
374 GPP decreases with more frequent but less intense rainfall in this low rainfall range.

375 **Pattern 1.2:** Across most rainfall ranges (MAP from 400 mm/year to 1600 mm/year),
376 increasing frequency of rainfall (and simultaneously decreasing rainfall intensity) lead
377 to positive GPP sensitivity. This positive GPP sensitivity peaks at the low range of
378 rainfall frequency (~0.35 event/day) and around the MAP of 1000 mm/year.

379 **Pattern 1.3:** At the high range of MAP (>1800 mm/year) with low rainfall frequency
380 (~0.4 event/day), GPP decreases with increased rainfall frequency.

381 The relationship of GPP sensitivity to MAP and rainfall intensity (Fig. 6c) has no
382 clear patterns as previous ones, mostly because the GPP sensitivity space (Fig. A4c)
383 contains large uncertainties (Fig. A4d, shown as large variance in the data). Thus we
384 will not over-interpret the pattern in Fig. 6c.

385 Pattern 1.1 and Pattern 1.2 can be explained by the illustrative time series in
386 Figure 6a and 6b, respectively. Figure 6a shows that when rainfall events are small
387 and very infrequent, increasing rainfall frequency while decreasing intensity would

388 cause more frequent downcrossings of soil moisture at the wilting point S_w , which
389 subsequently would reduce the effective time of carbon assimilation and plant growth
390 (i.e. when soil moisture is below S_w , plants would be in the extreme water stress and
391 slow down or stop physiological activity). This case only happens where MAP is very
392 low with low frequency and the biome is predominantly grasslands, which explains
393 why negative changes in soil moisture and GPP in Figure 4a and 4b are distributed in
394 those regions. This result also corroborates the field findings of the negative impacts
395 from increasing rainfall frequency in Heisler-White et al.(2009) and Thomey et al.
396 (2011) at low rainfall regimes.

397 Figure 6b provides the hydrological mechanism for the positive sensitivity of soil
398 moisture and GPP with increasing rainfall frequency over the most African continent
399 (Pattern 1.2). Once individual rainfall event has enough intensity and rainfall
400 frequency is enough, downcrossings of S_w would not easily happen. Instead, the
401 accumulative rainy-season soil moisture becomes the dominant control of plant
402 growth, and increasing rainfall frequency has led to a significant increase of soil
403 moisture for plant water use (Figure 4a and 4b). This conclusion drawn from our
404 numerical modeling is consistent with previous findings in Rodríguez-Iturbe and
405 Porporato (2004) based on stochastic modeling. We also find that this positive GPP
406 sensitivity reaches to its maximum in the intermediate total rainfall (~1000 mm/year)
407 and relatively low rainfall frequency (~0.35 event/day), indicating that in these
408 regimes increasing rainfall frequency could most effectively increase soil moisture for
409 plant water use and create marginal benefits of GPP to the increased rainfall frequency.
410 Further increase in large total annual rainfall or rainfall frequency would reduce the
411 sensitivity to water stress with fewer downcrossings of soil moisture critical point S^* ;
412 and once the soil moisture is always ample (i.e. above S^*), the changes in either MAP
413 or rainfall frequency would not alter plant water stress.

414 Pattern 1.3 also shows a negative GPP sensitivity, but its mechanism is different
415 from the previous case of Pattern 1.1. In regions with total rainfall usually more than
416 1800 mm/year, SEIB-simulated tropical forests exhibit radiation-limitation rather than
417 water-limitation during wet season. Increase of rainfall frequency at daily scale would

418 enhance cloud fraction and suppress plant productivity in these regions (Graham et al.,
419 2003). Thus even though soil moisture still increases (Figure 4a), GPP decreases with
420 increased rainfall frequency. This mechanism also explains why tropical evergreen
421 forests shrink its area with increased rainfall frequency (Figure 3a).

422 It is worth noting that the magnitude of GPP changes due to rainfall frequency
423 and intensity is relatively small in most of the woodlands, but can be relatively large
424 for drylands with MAP below 600 mm/year (up to 10-20% of annual GPP). This
425 pattern also explains why only modest changes in biome distribution happen between
426 woodlands and grasslands in $S_{\lambda-\alpha}$ (Figure 3a).

427

428 [insert Figure 6]

429

430 **3.2 Ecosystem sensitivity to rainfall seasonality and frequency (Experiment $S_{T_w-\lambda}$)**

431 Experiment $S_{T_w-\lambda}$ assesses ecosystem responses after increasing rainy season length
432 and decreasing rainfall frequency (i.e. $T_w \uparrow, \lambda \downarrow$) under a fixed total annual rainfall. The
433 simulated biome distribution shows a gain of area in tropical evergreen forests
434 converted from woodlands. The northern Africa has an area increase of woodlands
435 converted from grasslands, and African Horn region has a small expansion of
436 grasslands into woodlands (Figure 3b). Figure 4c and 4d show that increasing rainy
437 season length T_w and decreasing frequency λ would significantly increase annual
438 mean soil moisture and GPP (up to 30%) in most woodland area. Meanwhile
439 decreased soil moisture and GPP are found in the southern and eastern Africa.
440 Tropical evergreen forests show little response. We further explore the GPP sensitivity
441 space in Figure 5e and 5g, and find the following robust patterns (based on small
442 standard errors shown in Figure 5f and 5h):

443 **Pattern 2.1:** The negative GPP sensitivity tends to happen where MAP is mostly
444 below 1000 mm/year with long rainy season length ($T_w > 150$ days) and low rainfall
445 frequency ($\lambda < 0.35$ event/day).

446 **Pattern 2.2:** When MAP and rainfall frequency are large enough (MAP > 1000
447 mm/year and $\lambda > 0.4$ event/day), decreasing λ while increasing T_w would significantly

448 increase GPP. The maximum positive GPP sensitivity happens at the intermediate
449 MAP range (1100-1500 mm/year) and the high rainfall frequency ($\lambda \sim 0.7$ event/day).

450 **Pattern 2.3:** There exists an “optimal rainy season length” for relative changes in
451 ecosystem productivity across large MAP ranges (the white area between the red and
452 blue space in Figure 5e). For the same MAP, any deviation of T_w from the “optimal
453 rainy season length” would reduce GPP. This “optimal rainy season length” follows
454 an increasing trend with MAP until 1400 mm/year.

455 Figure 6c explains the hydrological mechanism for the negative GPP sensitivity
456 in Pattern 2.1. In the situation with low MAP and infrequent rainfall events,
457 decreasing rainfall frequency and expanding rainy season length (i.e. $T_w \uparrow$, $\lambda \downarrow$) would
458 lead to longer intervals between rainfall events and possibly longer excursions below
459 S_w , which would disrupt continuous plant growth and have detrimental effects on
460 ecosystem productivity. It is worth noting that long rainy season in dryland (Figure 5e)
461 is usually accompanied with low rainfall frequency (Figure 5g). The southern African
462 drylands (south of 15 °S) typically fall in this category, and these regions thus have
463 negative GPP sensitivity (Figure 4c and 4d), accompanied by a small biome
464 conversion from woodlands to grasslands (Figure 3b).

465 Figure 6d explains the hydrological mechanisms for the positive GPP sensitivity
466 in Pattern 2.2. When rainfall is ample enough to maintain little or no water stress
467 during rainy season, increasing the interval of rainfall events may introduce little
468 additional water stress but can significantly extend the growing season. This situation
469 mostly happens in woodlands, where limited water stress exists during rainy season,
470 and dry season length is the major constraint for plant growth. Thus the increase of
471 rainy season length extends the temporal niche for plant growth, and leads to a
472 significant woodland expansion to grasslands as well as an expansion of tropical
473 evergreen forests to woodlands (Figure 3b).

474 The little GPP sensitivity in tropical evergreen forest regions is mostly attributed
475 to the long rainy season length in this ecosystem. Thus further increasing T_w may
476 reach to its saturation (365 days) and has little impact to ecosystem productivity. This
477 also explains why the magnitude of GPP sensitivity is much smaller at high MAP

478 range than at the intermediate MAP range.

479 The finding of “optimal rainy season length” across different rainfall regimes
480 (Figure 5e) is consistent with our previous empirical finding about the similar pattern
481 of “optimal rainy season length” for tree fractional cover in Africa derived based on a
482 satellite remote sensing product (Guan et al., 2014). The existence of “optimal rainy
483 season length” fully demonstrates the importance to explicitly consider the non-linear
484 impacts of rainy season length on ecosystem productivity under climate change,
485 which has been largely overlooked before.

486

487 **3.3 Ecosystem sensitivity to rainfall seasonality and intensity ($S_{TW-\alpha}$)**

488 Results of Experiment $S_{TW-\alpha}$ have many similarities with those of $S_{TW-\lambda}$, including the
489 similar changes in biome distributions (Figure 3), soil moisture and GPP patterns
490 (Figure 4e and 4f). We further find that the GPP sensitivity space with MAP and rainy
491 season length for $S_{TW-\alpha}$ (Figure 5i) is also similar with that for $S_{TW-\lambda}$ (Figure 5e). One
492 new finding is that rainfall intensity has little impact on GPP, as the contour lines in
493 Figure 5k are mostly parallel with y-axis (i.e. rainfall intensity).

494 Figure 6e and 6f explain the governing hydrological mechanisms for the patterns
495 of $S_{TW-\alpha}$, which also have many similarities with $S_{TW-\lambda}$. For the negative case (Figure
496 6e), decreasing rainfall intensity and increasing rainy season length in the very low
497 MAP regime may lead to more downcrossings of S_w and interrupt continuous plant
498 growth. The positive case (Figure 6e) is similar as that in Figure 6d, i.e. the
499 repartitioning of excessive wet-season rainfall to the dry season for an extended
500 growing period would significantly benefit plant growth and possible increase tree
501 fraction cover.

502

503 **4. Discussion**

504 In this paper we provide a new modeling approach to systematically interpret the
505 ecological impacts from changes in intra-seasonal rainfall characteristics (i.e. rainfall
506 frequency, rainfall intensity and rainy season length) across biomes and climate
507 gradients in the African continent.

508

509 **4.1 Limitation of the methodology**

510 Though our modeling framework is able to characterize the diverse ecosystem
511 responses to the shifts in different rainfall characteristics, it nevertheless has its
512 limitations. The current rainfall model only deals with the case of single rainy season
513 per year, and approximates the case of double rainy seasons per year to be the single
514 rainy season case. This assumption may induce unrealistic synthetic rainfall patterns
515 in the equatorial dryland regions, in particular the Horn of Africa. Thus the simulated
516 sensitivity of these regions may be less reliable. We also assume that rainfall
517 frequency and intensity are homogenous throughout wet seasons (or dry seasons), but
518 in reality they have seasonal variations. We only consider rainy season length for
519 rainfall seasonality, and neglect the possible temporal phase change; in reality, rainfall
520 seasonality change usually has length and phase shifts in concert. These
521 rainfall-model-related limitations can be possibly overcome by simulating smaller
522 intervals of rainfall processes (e.g. each month has their own α and λ) rather than
523 simulating the whole wet or dry season using one fixed set of α and λ . Besides, only
524 using one ecosystem model also means that the simulated ecosystem sensitivity can
525 be model-specific. Though magnitudes or thresholds for the corresponding patterns
526 may vary depending on different models, we argue that the qualitative results for the
527 GPP sensitivity patterns (e.g. Figure 4 and Figure 5) should hold as the necessary
528 ecohydrological processes have been incorporated in SEIB-DGVM. We also
529 recognize that to exclude fire impacts in the current simulation may bring some
530 limitation for this study, as evidence shows that many savanna regions can be bistable
531 due to fire effects (Staver et al 2011; Hirota et al 2011; Higgins and Scheiter 2012;
532 also see for a possible rebuttal in Hanan et al, 2013). Changes in rainfall regimes not
533 only have direct effects on vegetation productivity, but can also indirectly affect
534 ecosystems through its interactions with fire, with rapid biome shifts being a possible
535 consequence. These feedbacks can be important in situations when the changes in
536 growing season length are related to fuel loads, fuel moisture dynamics and hence fire
537 intensity (Lehmann et al., 2011). Quantifying these fire-rainfall feedbacks will be the

538 important future direction to pursue.

539

540 **4.2 Clarifying the impacts of rainfall frequency and intensity on ecosystem** 541 **productivity**

542 In this modeling study, we provide a plausible answer to possibly resolve the previous
543 debate about whether increasing rainfall intensity (or equivalently decreasing rainfall
544 frequency, i.e. $\lambda \downarrow$, $\alpha \uparrow$) has positive or negative impacts on above-ground primary
545 productivity under a fixed annual rainfall total. We identify that negative GPP
546 sensitivity with increased rainfall frequency is possible at very low MAP range (~ 400
547 mm/year) with relatively low rainfall frequency (<0.35 event/day) (Figure 5a), due to
548 the increased downcrossings of soil moisture wilting point, which restricts plant
549 growth (Figure 6a). This derived MAP threshold (~400 mm/year) is consistent with
550 our meta-analysis based on the previous field studies (Table 1), which shows a
551 threshold of MAP at 340 mm/year separates positive and negative impacts of more
552 intense rainfall on aboveground net primary production (ANPP). Our findings are also
553 consistent with another study about increased tree encroachments with increased
554 rainfall intensity in low rainfall regime (<544mm/year, Kulmatiski and Beard, 2013),
555 which essentially follows the same mechanism as identified in Figure 6a.

556 In addition, we thoroughly investigated the ecosystem responses across a wide
557 range of annual rainfall in Africa. We find that beyond the very low rainfall range
558 (below 400 mm/year), most grasslands and woodlands would benefit from increasing
559 rainfall frequency, which also corroborate the previous large-scale findings about the
560 positive effects of increased rainfall frequency (and decreased rainfall intensity) for
561 tree fractions across the African continent (Good and Caylor, 2011). The only
562 exception happens at the very wet end of MAP (~1800mm/year) where cloud-induced
563 radiation-limitation may suppress ecosystem productivity with increased rainfall
564 frequency. We also find that changes in rainfall frequency and intensity mostly affect
565 grassland-dominated savannas (changes of GPP up to 20%), and the corresponding
566 effects are much smaller in woodlands and have little impact on woodland distribution.
567 Though this work is only based on a single model, it provides a primary assessment

568 for understanding of interactive changes between λ and α in ecosystem functioning,
569 and expands the analysis to a wide range of annual rainfall conditions compared with
570 previous studies (e.g. Porporato et al., 2004).

571

572 **4.3 Ecological importance of rainy season length**

573 The results involving rainy season length (i.e. $S_{T_w-\lambda}$ and $S_{T_w-\alpha}$) provide evidence for
574 the ecological importance of rainfall seasonality. The magnitudes of changes in soil
575 moisture, GPP and biome distribution in $S_{T_w-\lambda}$ and $S_{T_w-\alpha}$ are much larger than those of
576 $S_{\lambda-\alpha}$, with almost one order of magnitude difference. These disproportional impacts of
577 T_w indicate that slight changes in rainy season length could modify biome distribution
578 and ecosystem function more dramatically compared with the same percentage
579 changes in rainfall frequency and intensity. We also notice that $S_{T_w-\lambda}$ and $S_{T_w-\alpha}$ have
580 similar results. This is because that both λ and α describe rainfall characteristics
581 within wet season, while T_w describes rainfall characteristics of both dry season and
582 wet season. Cautions are required that our simplified treatment rainy season length
583 may overestimate its importance, and we did not consider the rainfall phase
584 information here.

585 Given the importance of rainy season length, its ecological impacts under climate
586 change are largely understudied, though substantial shifts in rainfall seasonality have
587 been projected in both Sahel and South Africa (Biasutti and Sobel, 2009; Shongwe et
588 al., 2009; Seth et al., 2013). Here we only address the rainfall seasonality in terms of
589 its length, and future changes in rainfall seasonality may modify their phase and
590 magnitude in concert. The climate community has focused on the increase of extreme
591 rainfall events (Field et al., 2012), which could be captured by the changes in λ or α
592 towards heavier tails in their distribution. However, explicit and systematic
593 assessments and projection on rainfall seasonality changes (including both phase and
594 magnitude) are still limited even in the latest Intergovernmental Panel on Climate
595 Change (IPCC) synthesis reports (Field et al., 2012; Stocker et al., 2013). More
596 detailed studies related to these changes and their ecological implications are required
597 for future hydroclimate-ecosystem research.

598

599 **4.4 Not all rainfall regimes are ecologically equivalent**

600 As Figure 1 gives a convincing example that the same total annual rainfall may arrive
601 in a very different way, our results further demonstrate that ecosystems respond
602 differently to the changes in these intra-seasonal rainfall variability. For example, with
603 similar MAP, drylands in West Africa and Southwest Africa show reversed responses
604 to the same changes in intra-seasonal rainfall variability. As shown in the experiments
605 of $S_{T_w-\lambda}$ and $S_{T_w-\alpha}$, increasing T_w while decreasing λ or α generates slightly positive
606 soil moisture and GPP sensitivity in West Africa (Figure 4c and 4d), but would cause
607 relatively large GPP decrease in Southwest Africa. The prior hydroclimate conditions
608 of these two regions can explain these differences: West Africa has much shorter rainy
609 season with more intense rainfall events; in contrast, Southwest Africa has a long
610 rainy season but many small and sporadic rainfall events. As a result, under a fixed
611 annual rainfall total, slightly increasing rainy season and meanwhile decreasing
612 rainfall intensity would benefit plant growth in West Africa, but the same change
613 would lengthen dry spells in Southwest Africa and bring negative effects to the
614 ecosystem productivity. We further deduce that the rainfall use efficiency (RUE,
615 defined as the ratio of plant net primary production to total rainfall amount) in these
616 two drylands could be different: West Africa may have lower RUE, and the intense
617 rainfall could lead to more infiltration-excess runoff, and thus less water would be
618 used by plants; while Southwest Africa can have higher RUE, because its sporadic
619 and feeble rainfall events would favor grass to fully take the advantage of the
620 ephemerally existed water resources. This conclusion is partly supported by Martiny
621 et al. (2007) based on satellite remote sensing. We further hypothesize that landscape
622 geomorphology in these two drylands may be different and therefore reflect
623 distinctive rainfall characteristics. More bare soil may exist in West Africa grasslands
624 due to intense-rainfall-induced erosion, while Southwest Africa may have more grass
625 fraction and less bare soil fraction. Testing these interesting hypotheses is beyond the
626 scope of this paper, but is worthy the further exploration.

627

628

629 **Acknowledgements:**

630 K. Guan and E. F. Wood acknowledge the financial supports from the NASA NESSF
631 fellowship. S.P. Good and K. K. Caylor acknowledge the financial supports from the
632 National Science Foundation through the Grant EAR-0847368. The authors thank
633 Ignacio Rodríguez-Iturbe for his valuable inputs and discussion.

634

635

636 **References:**

- 637 Anderegg, L. D. L.; Anderegg, W. R. L. & Berry, J. A. (2013), 'Not all droughts are
638 created equal: translating meteorological drought into woody plant mortality', *Tree*
639 *Physiology* **33**, 701-712.
- 640
- 641 Bates, J.; Svejcar, T.; Miller, R. & Angell, R. (2006), 'The effects of precipitation
642 timing on sagebrush steppe vegetation', *Journal of Arid Environments* **64**, 670-697.
- 643
- 644 Biasutti, M. & Sobel, A. H. (2009), 'Delayed Sahel rainfall and global seasonal cycle in
645 a warmer climate', *Geophysical Research Letters* **36**, L23707.
- 646
- 647 Bond, W. J.; Woodward, F. I. & Midgley, G. F. (2005), 'The Global Distribution of
648 Ecosystems in a World without Fire', *New Phytologist* **165**(2), 525-537.
- 649
- 650 Easterling, D. R.; Meehl, G. A.; Parmesan, C.; Changnon, S. A.; Karl, T. R. & Mearns,
651 L. O. (2000), 'Climate Extremes: Observations, Modeling, and Impacts', *Science* **289**,
652 2068-2074.
- 653
- 654 Fang, J.; Piao, S.; Zhou, L.; He, J.; Wei, F.; Myneni, R. B.; Tucker, C. J. & Tan, K.
655 (2005), 'Precipitation patterns alter growth of temperate vegetation', *Geophysical*
656 *Research Letters* **32**, L21411.
- 657
- 658 Fay, P. A.; Carlisle, J. D.; Knapp, A. K.; Blair, J. M. & Collins, S. L. (2003),
659 'Productivity responses to altered rainfall patterns in a C4-dominated grassland',
660 *Oecologia* **137**, 245-251.
- 661
- 662 Feng, X.; Porporato, A. & Rodriguez-Iturbe, I. (2013), 'Changes in rainfall seasonality
663 in the tropics', *Nature Climate Change*.
- 664
- 665 Field, C.; Barros, V.; Stocker, T.; Qin, D.; Dokken, D.; Ebi, K.; Mastrandrea, M.; Mach,
666 K.; Plattner, G.-K.; Allen, S.; Tignor, M. & Midgley, P., ed. (2012), *IPCC, 2012:
667 Managing the Risks of Extreme Events and Disasters to Advance Climate Change
668 Adaptation. A Special Report of Working Groups I and II of the Intergovernmental
669 Panel on Climate Change*, Cambridge University Press, Cambridge, UK, and New
670 York, NY, USA.
- 671
- 672 Franz, T. E.; Caylor, K. K.; Nordbotten, J. M.; Rodríguez-Iturbe, I. & Celia, M. A.
673 (2010), 'An ecohydrological approach to predicting regional woody species distribution
674 patterns in dryland ecosystems', *Advances in Water Resources* **33**(2), 215-230.
- 675
- 676 Gerten, D.; Luo, Y.; Maire, G. L.; Parton, W. J.; Keough, C.; Weng, E.; Beier, C.; Ciais,
677 P.; Cramer, W.; Dukes, J. S.; Hanson, P. J.; Knapp, A. A. K.; Linder, S.; Nepstad, D.;
678 Rustad, L. & Sowerby, A. (2008), 'Modelled effects of precipitation on ecosystem
679 carbon and water dynamics in different climatic zones', *Global Change Biology* **14**,

680 2365-2379.

681

682 Good, S. P. & Caylor, K. K. (2011), 'Climatological determinants of woody cover in
683 Africa', *Proceedings of the National Academy of Sciences of United States of America*
684 **108(12)**, 4902-4907.

685

686 Graham, E. A.; Mulkey, S. S.; Kitajima, K.; Phillips, N. G. & Wright, S. J. (2003),
687 'Cloud cover limits net CO₂ uptake and growth of a rainforest tree during tropical
688 rainy seasons', *Proceedings of the National Academy of Sciences of the United States*
689 *of America* **100(2)**, 572-576.

690

691 Guan, K.; Wood, E. F. & Caylor, K. K. (2012), 'Multi-sensor derivation of regional
692 vegetation fractional cover in Africa', *Remote Sensing of Environment* **124**, 653-665.

693

694 Guan, K.; Wood, E. F.; Medvigy, D.; Pan, M.; Caylor, K. K.; Sheffield, J.; Kimball, J.;
695 Xu, X. & Jones, M. O. (2014), 'Terrestrial hydrological controls on vegetation
696 phenology of African savannas and woodlands', *Journal of Geophysical Research*.

697

698 Hanan, N. P.; Tredennick, A. T.; Prihodko, L.; Bucini, G. & Dohn, J. (2013), 'Analysis
699 of stable states in global savannas: is the CART pulling the horse?', *Global Ecology and*
700 *Biogeography* **23(3)**, 259-263.

701

702 Harper, C. W.; Blair, J. M.; Fay, P. A.; Knapp, A. K. & Carlisle, J. D. (2005), 'Increased
703 rainfall variability and reduced rainfall amount decreases soil CO₂ flux in a grassland
704 ecosystem', *Global Change Biology* **11**, 322-334.

705

706 Heisler-White, J. L.; Blair, J. M.; Kelly, E. F.; Harmoney, K. & Knapp, A. K. (2009),
707 'Contingent productivity responses to more extreme rainfall regimes across a grassland
708 biome', *Global Change Biology* **15(12)**, 2894-2904.

709

710 Hély, C.; Bremond, L.; Alleaume, S.; Smith, B.; Sykes, M. T. & Guiot, J. (2006),
711 'Sensitivity of African biomes to changes in the precipitation regime', *Global Ecology*
712 *and Biogeography* **15**, 258-270.

713

714 Hirota, M.; Holmgren, M.; Nes, E. H. V. & Scheffer, M. (2011), 'Global Resilience of
715 Tropical Forest and Savanna to Critical Transitions', *Science* **334**, 232-235.

716

717 Higgins, S. I. & Scheiter, S. (2012), 'Atmospheric CO₂ forces abrupt vegetation shifts
718 locally, but not globally', *Nature* **488**, 209-212.

719

720 Holmgren, M.; Hirota, M.; van Nes, E. H. & Scheffer, M. (2013), 'Effects of
721 interannual climate variability on tropical tree cover', *Nature Climate Change*.

722

723 Huffman, G. J.; Bolvin, D. T.; Nelkin, E. J.; Wolff, D. B.; Adler, R. F.; Bowman, K. P.

724 & Stocker, E. F. (2007), 'The TRMM Multisatellite Precipitation Analysis (TMPA):
725 Quasi-Global, Multiyear, Combined-Sensor Precipitation Estimates at Fine Scales',
726 *Journal of Hydrometeorology* **8**, 38-55.
727

728 Knapp, A. K.; Fay, P. A.; Blair, J. M.; Collins, S. L.; Smith, M. D.; Carlisle, J. D.;
729 Harper, C. W.; Danner, B. T.; Lett, M. S. & McCarron, J. K. (2002), 'Rainfall
730 Variability, Carbon Cycling, and Plant Species Diversity in a Mesic Grassland', *Science*
731 **298**, 2202-2205.
732

733 Kulmatiski, A. & Beard, K. H. (2013), 'Woody plant encroachment facilitated by
734 increased precipitation intensity', *Nature Climate Change*.
735

736 Lehmann, C. E. R.; Archibald, S. A.; Hoffmann, W. A. & Bond, W. J. (2011),
737 'Deciphering the distribution of the savanna biome', *New Phytologist* **191**, 197-209.
738

739 Markham, C. (1970), 'Seasonality of precipitation in the United States', *Annals of the*
740 *Association of American Geographers* **60(3)**, 593-597.
741

742 Martiny, N.; Camberlin, P.; Richard, Y. & Philippon, N. (2006), 'Compared regimes of
743 NDVI and rainfall in semi-arid regions of Africa', *International Journal of Remote*
744 *Sensing* **27(23)**, 5201-5223.
745

746 Miranda, J.; Armas, C.; Padilla, F. & Pugnaire, F. (2011), 'Climatic change and rainfall
747 patterns: Effects on semi-arid plant communities of the Iberian Southeast', *Journal of*
748 *Arid Environments* **75**, 1302-1309.
749

750 Nemani, R. R.; Keeling, C. D.; Hashimoto, H.; Jolly, W. M.; Piper, S. C.; Tucker, C. J.;
751 Myneni, R. B. & Running, S. W. (2003), 'Climate-Driven Increases in Global
752 Terrestrial Net Primary Production from 1982 to 1999', *Science* **300**, 1560-1563.
753

754 O'Gorman, P. A. & Schneider, T. (2009), 'The physical basis for increases in
755 precipitation extremes in simulations of 21st-century climate change', *Proceedings of*
756 *the National Academy of Sciences of the United States of America* **106(35)**,
757 14773-14777.
758

759 Porporato, A.; Daly, E. & Rodríguez-Iturbe, I. (2004), 'Soil Water Balance and
760 Ecosystem Response to Climate Change', *American Naturalist* **164(5)**, 625-632.
761

762 Porporato, A.; Laio, F.; Ridolfi, L. & Rodríguez-Iturbe, I. (2001), 'Plants in
763 water-controlled ecosystems: active role in hydrologic processes and response to water
764 stress - III. Vegetation water stress', *Advances in Water Resources* **24(7)**, 725-744.
765

766 Robertson, T. R.; Bell, C. W.; Zak, J. C. & Tissue, D. T. (2009), 'Precipitation timing
767 and magnitude differentially affect aboveground annual net primary productivity in

768 three perennial species in a Chihuahuan Desert grassland', *New Phytologist* **181**,
769 230-242.
770

771 Rodr ́guez-Iturbe, I.; Gupta, V. K. & Waymire, E. (1984), 'Scale Considerations in the
772 Modeling of Temporal Rainfall', *Water Resource Research* **20(11)**, 1611-1619.
773

774 Rodr ́guez-Iturbe, I. & Porporato, A. (2004), *Ecohydrology of Water-Controlled*
775 *Ecosystems: Soil Moisture And Plant Dynamics*, Cambridge University Press.
776

777 Rodr ́guez-Iturbe, I.; Porporato, A.; Ridolfi, L.; Isham, V. & Cox, D. R. (1999),
778 'Probabilistic Modelling of Water Balance at a Point: The Role of Climate, Soil and
779 Vegetation', *Proceedings: Mathematical, Physical and Engineering Sciences* **455**,
780 3789-3805.
781

782 Ross, I.; Misson, L.; Rambal, S.; Arneth, A.; Scott, R. L.; Carrara, A.; Cescatti, A. &
783 Genesio, L. (2012), 'How do variations in the temporal distribution of rainfall events
784 affect ecosystem fluxes in seasonally water-limited Northern Hemisphere shrublands
785 and forests?', *Biogeosciences* **9**, 1007-1024.
786

787 Saha, S.; Moorthi, S.; Pan, H.-L.; Wu, X.; Wang, J.; Nadiga, S.; Tripp, P.; Kistler, R.;
788 Woollen, J.; Behringer, D.; Liu, H.; Stokes, D.; Grumbine, R.; Gayno, G.; Wang, J.;
789 Hou, Y.-T.; Chuang, H.-Y.; Juang, H.-M. H.; Sela, J.; Iredell, M.; Treadon, R.; Kleist,
790 D.; Delst, P. V.; Keyser, D.; Derber, J.; Ek, M.; Meng, J.; Wei, H.; Yang, R.; Lord, S.;
791 Dool, H. V. D.; Kumar, A.; Wang, W.; Long, C.; Chelliah, M.; Feng, Y.; Huang, B.;
792 Schemm, J.-K.; Ebisuzaki, W.; Lin, R.; Xie, P.; Chen, M.; Zhou, S.; Higgins, W.; Zou,
793 C.-Z.; Liu, Q.; Chen, Y.; Han, Y.; Cucurull, L.; Reynolds, R. W.; Rutledge, G. &
794 Goldberg, M. (2010), 'The NCEP Climate Forecast System Reanalysis', *Bulletin of the*
795 *American Meteorological Society* **91**, 1015-1057.
796

797 Sato, H. (2009), 'Simulation of the vegetation structure and function in a Malaysian
798 tropical rain forest using the individual-based dynamic vegetation model SEIB-DGVM',
799 *Forest Ecology and Management* **257**, 2277-2286.
800

801 Sato, H. & Ise, T. (2012), 'Effect of plant dynamic processes on African vegetation
802 responses to climate change: analysis using the spatially explicit individual-based
803 dynamic global vegetation model (SEIB-DGVM)', *Journal of Geophysical Research*
804 **117**, G03017.
805

806 Sato, H.; Itoh, A. & Kohyama, T. (2007), 'SEIB-DGVM: A new Dynamic Global
807 Vegetation Model using a spatially explicit individual-based approach', *Ecological*
808 *Modelling* **200(3-4)**, 279-307.
809

810 Sato, H.; Kobayashi, H. & Delbart, N. (2010), 'Simulation study of the vegetation
811 structure and function in eastern Siberian larch forests using the individual-based

812 vegetation model SEIB-DGVM', *Forest Ecology and Management* **259**, 301-311.

813

814 Scanlon, T. M.; Caylor, K. K.; Manfreda, S.; Levin, S. A. & Rodriguez-Iturbe, I. (2005),

815 'Dynamic response of grass cover to rainfall variability: implications for the function

816 and persistence of savanna ecosystems', *Advances in Water Resources* **28**, 291-302.

817

818 Shugart, H. H. (1998), 'Terrestrial ecosystems in changing environments', Cambridge

819 University Press, United Kingdom.

820

821 van Schaik, C. P.; Terborgh, J. W. & Wright, S. J. (1993), 'The Phenology of Tropical

822 Forests: Adaptive Significance and Consequences for Primary Consumers', *Annual*

823 *Review of Ecology and Systematics* **24**, 353-377.

824

825 Scholes, R. J. & Archer, S. R. (1997), 'Tree-Grass Interactions in Savannas', *Annual*

826 *Review of Ecology and Systematics* **28**, 517-544.

827

828 Seth, A.; Rauscher, S. A.; Biasutti, M.; Giannini, A.; Camargo, S. J. & Rojas, M. (2013),

829 'CMIP5 Projected Changes in the Annual Cycle of Precipitation in Monsoon Regions',

830 *Journal of Climate* **26**, 7328-7351.

831

832 Sheffield, J.; Goteti, G. & Wood, E. F. (2006), 'Development of a 50-Year

833 High-Resolution Global Dataset of Meteorological Forcings for Land Surface

834 Modeling', *Journal of Climate* **19**, 3088-3111.

835

836 Shongwe, M. E.; van Oldenborgh, G. J.; van den Hurk, B. J. J. M.; de Boer, B.; Coelho,

837 C. A. S. & van Aalst, M. K. (2009), 'Projected Changes in Mean and Extreme

838 Precipitation in Africa under Global Warming. Part I: Southern Africa', *Journal of*

839 *Climate* **22**, 3819-3837.

840

841 Staver, A. C.; Archibald, S. & Levin, S. A. (2011), 'The Global Extent and

842 Determinants of Savanna and Forest as Alternative Biome States', *Science* **334**,

843 230-232.

844

845 Stocker, T. F.; Qin, D.; Plattner, G.-K.; Tignor, M.; Allen, S. K.; Boschung, J.; Nauels,

846 A.; Xia, Y.; Bex, V. & Midgley, P. M., ed. (2013), *IPCC, 2013: Climate Change 2013:*

847 *The Physical Science Basis. Contribution of Working Group I to the Fifth Assessment*

848 *Report of the Intergovernmental Panel on Climate Change*, Cambridge University

849 Press, Cambridge, United Kingdom and New York, NY, USA..

850

851 Svejcar, T.; Bates, J.; Angell, R. & Miller, R. (2003), 'The influence of precipitation

852 timing on the sagebrush steppe ecosystem. In: Guy, McPherson, Jake, Weltzin (Eds.),

853 Changing Precipitation Regimes & Terrestrial Ecosystems. University of Arizona Press,

854 Tucson, AZ 237pp.', .

855

856 Thomey, M. L.; Collins, S. L.; Vargas, R.; Johnson, J. E.; Brown, R. F.; Natvig, D. O. &
857 Friggens, M. T. (2011), 'Effect of precipitation variability on net primary production
858 and soil respiration in a Chihuahuan Desert grassland', *Global Change Biology* **17**,
859 1505-1515.

860

861 Trenberth, K. E.; Dai, A.; Rasmussen, R. M. & Parsons, D. B. (2003), 'The Changing
862 Character of Precipitation', *Bulletin of American Meterological Society* **84**, 1205-1217.

863

864 Vincens, A.; Garcin, Y. & Buchet, G. (2007), 'Influence of rainfall seasonality on
865 African lowland vegetation during the Late Quaternary: pollen evidence from Lake
866 Masoko, Tanzania', *Journal of Biogeography* **34**, 1274-1288.

867

868 Weltzin, J. F.; Loik, M. E.; Schwinning, S.; Williams, D. G.; Fay, P. A.; Haddad, B. M.;
869 Harte, J.; Huxman, T. E.; Knapp, A. K.; Lin, G.; Pockman, W. T.; Shaw, M. R.; Small,
870 E. E.; Smith, M. D.; Smith, S. D.; Tissue, D. T. & Zak, J. C. (2003), 'Assessing the
871 Response of Terrestrial Ecosystems to Potential Changes in Precipitation', *BioScience*
872 **53(10)**, 941-952.

873

874 Williams, C. A. & Albertson, J. D. (2006), 'Dynamical effects of the statistical
875 structure of annual rainfall on dryland vegetation', *Global Change Biology* **12**,
876 777-792.

877

878 Zhang, X.; Friedl, M. A.; Schaaf, C. B.; Strahler, A. H. & Liu, Z. (2005), 'Monitoring
879 the response of vegetation phenology to precipitation in Africa by coupling MODIS
880 and TRMM instruments', *Journal of Geophysical Research* **110**, **D12103**.

881

882 Zhang, Y.; Moran, M. S.; Nearing, M. A.; Campos, G. E. P.; Huete, A. R.; Buda, A. R.;
883 Bosch, D. D.; Gunter, S. A.; Kitchen, S. G.; McNab, W. H.; Morgan, J. A.; McClaran,
884 M. P.; Montoya, D. S.; Peters, D. P. & Starks, P. J. (2013), 'Extreme precipitation
885 patterns and reductions of terrestrial ecosystem production across biomes', *Journal of*
886 *Geophysical Research: Biogeosciences* **118**, 148-157.

887

Table 1. Summary of previous representative studies on assessing the impacts of rainfall characteristics (i.e. rainfall frequency, intensity and seasonality) on the structure and function of terrestrial ecosystem.

Focus: frequency (freq); intensity (int); seasonality (sea); variation (CV).

Methods: Field Experiments (Field); Remote Sensing (RS); Flux Tower (Flux).

Major Conclusion: increasing rainfall intensity (or decreasing frequency) has positive impacts (int+); increasing intensity (or decreasing frequency) has negative impacts (int-); increasing rainfall CV has positive impacts (CV+); increasing rainfall CV has negative impacts (CV-).

| Focus | Methods | Spatial Scale | Time scale | MAP (mm/year) | Ecosystem type | Major Conclusion | Reference |
|-----------|---------|-------------------------------|-----------------------------|-----------------------|---------------------------------------|--|--------------------------|
| freq; int | RS | Africa continent | intra-annual climatology | [0,3000] | Africa all | (int-) woody cover | Good and Caylor, 2011 |
| freq; int | RS | US | | [163,1227] | US | (int-) ANPP greatest in arid grassland (16%) and Mediterranean forest (20%) and less for mesic grassland and temperate forest (3%) | Zhang et al., 2013 |
| freq; int | RS | Pan-tropics (35°N to 15°S) | inter-annual | [0,3000] | Tropical ecosystems | (CV+) wood cover in dry tropics; (CV-) wood cover in wet tropics | Holmgren et al., 2013 |
| freq; int | RS | Northern China | intra-annual | [100,850] | temperate grassland and forests | (int-) NDVI for temperate grassland and broadleaf forests, not for coniferous forest | Fang et al., 2005 |
| freq; int | Flux | Northern Hemisphere | intra-annual | [393±155,906±243] | shrubland and forest | (int-) GPP, RE and NEP | Ross et al., 2012 |
| seas | RS | Africa continent | climatology | [0,3000] | Africa all | rainy season onset and offset controls vegetation growing season | Zhang et al., 2005 |
| freq; int | Field | plot (Kansas, USA) | intra-annual | 615 | grassland | (int-) ANPP | Knapp et al., 2002 |

| | | | | | | | |
|----------------------------------|-------|---|-------------------------|-----------|-------------------------|--|---|
| (fix MAP) | | | | | | | |
| freq; int (fix MAP) | Field | plot (Kansas, USA) | intra-annual | 835 | grassland | (int-) ANPP | Fay et al., 2003 |
| increase seasonal rainfall | Field | plot(Texas, USA) | intra-annual | 365 | grassland | (int-) ANPP | Robertson et al., 2009 |
| freq; int | Field | plot (Kansas, USA) | intra-annual | [320,830] | grassland | (int-)ANPP for MAP=830mm/yr; (int+)ANPP for MAP=320mm/yr | Heisler-White et al., 2009 |
| freq; int | Field | plot(New Mexico, USA) | intra-annual | 250 | grassland | (int+) ANPP | Thomey et al., 2011 |
| freq; int (fix MAP) | Field | Plot(Kansas, USA) | intra-annual | 834 | grassland | (int-) soil CO2 flux | Harper et al., 2005 |
| freq; int (fix MAP) | Field | plot(Kruger National Park, South Africa) | intra-annual | 544 | sub-tropical savanna | (int+) wood growth; (int-) grass growth | Kulmatiski and Beard, 2013 |
| sea (fix MAP) | Field | plot(Oregon, USA) | intra-annual | [140,530] | grassland | impact biomass and bare soil fraction | Bates et al., 2006; Svejcar et al., 2003 |
| sea | Field | | | | | | |
| freq; int; MAP | Field | plot(South Africa) | intra-annual | [538,798] | grassland | (int-) ANPP | Swemmer et al., 2007 |
| MAP; sea | Field | plot(Spain) | intra-/inter-an nual | 242 | grassland | Mediterranean dryland ecosystem has more resilience for intra- and inter-annual changes in rainfall | Miranda et al., 2008 |

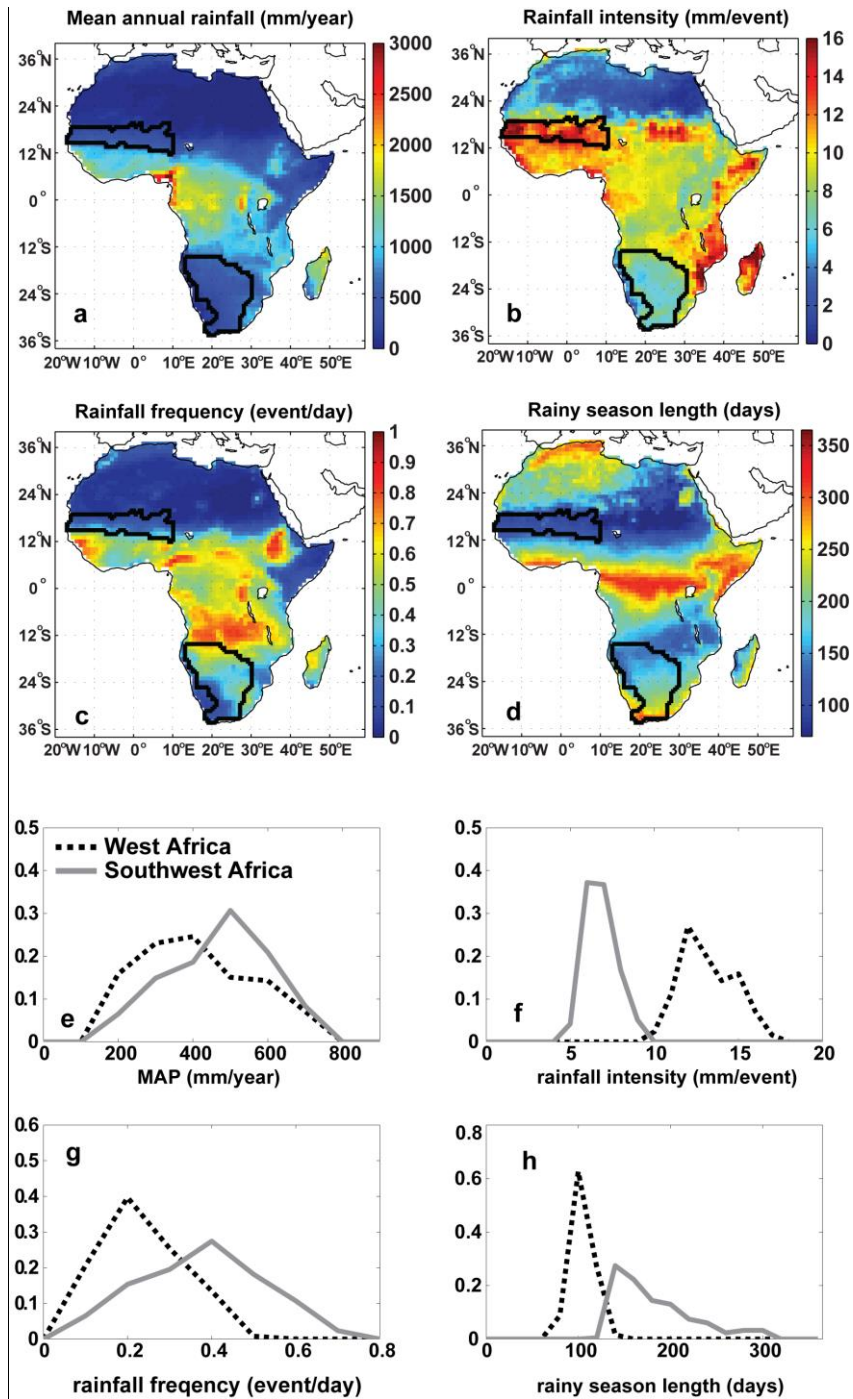


Figure 1. a-b: Spatial pattern of the rainfall characteristics in Africa: a-MAP; b-rainfall intensity; c-rainfall frequency; d-rainy season length. The black-line identified areas refer to two savanna regions in West and Southwest Africa. e-f: Normalized histograms of the rainfall characteristics in two savanna regions of West and Southwest Africa. e-MAP (bin width for the x-axis: 100 mm/year); f-rainfall intensity (bin width for the x-axis: 1 mm/event); g-rainfall frequency (bin width for the x-axis: 0.1 event/day); h-rainy season length (bin width for the x-axis: 20 days).

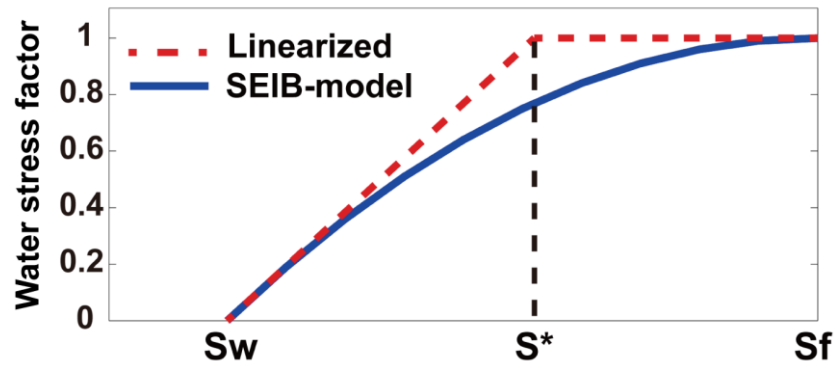


Figure 2. Schematic diagram of water stress factor ranging from 0 (most stressful) to 1 (no stress), which acts to reduce transpiration and carbon assimilation. The red dotted line is based on Porporato et al. (2001) with a reversed sign, and SEIB-DGVM has a nonlinear implementation (blue solid line, Sato and Ise, 2012).

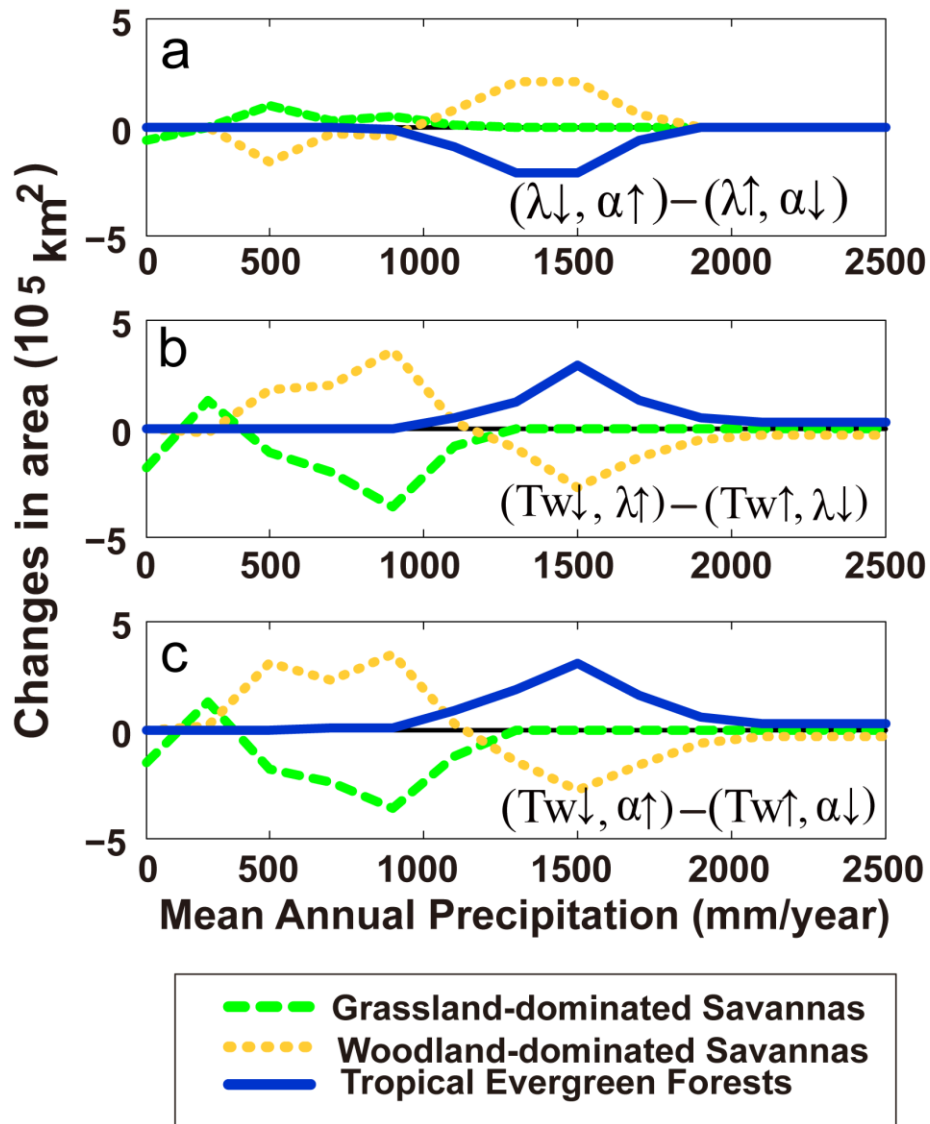


Figure 3. Differences in simulated dominated biomes in the three experiments (i.e. $S_{\lambda-\alpha}$, $S_{Tw-\lambda}$, $S_{Tw-\alpha}$).

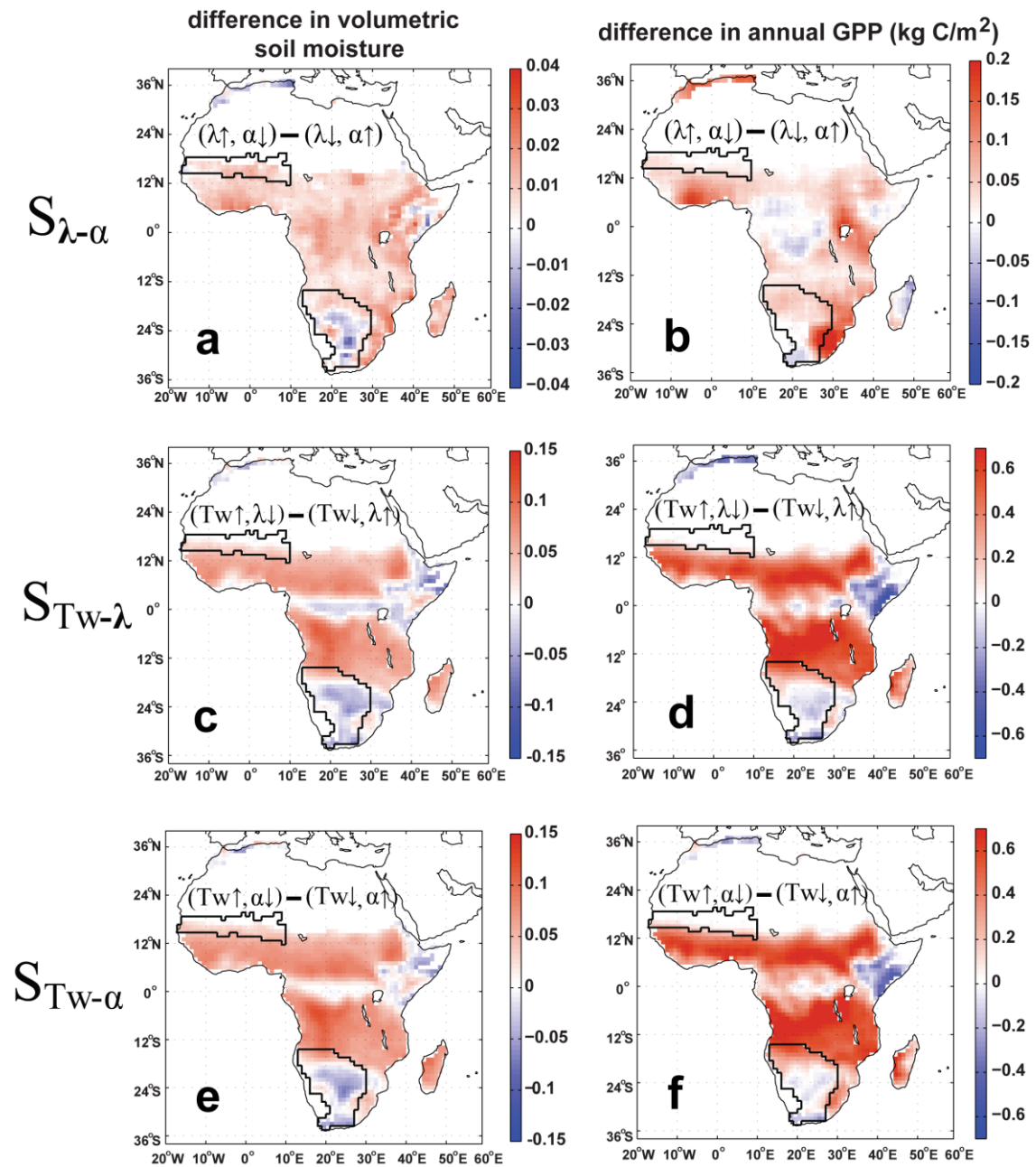


Figure 4. Simulated changes in annual mean soil moisture (0-500mm, first column) and annual mean GPP (second column) for different experiments. Please note that the scales of $S_{\lambda-\alpha}$ is much smaller than those of $S_{TW-\lambda}$ and $S_{TW-\alpha}$. The two areas with black boundaries in each panel are West African grassland and Southwest African grassland associated with Figure 1. The spatial patterns shown here are smoothed by 3*3 smoothing window from the raw data.

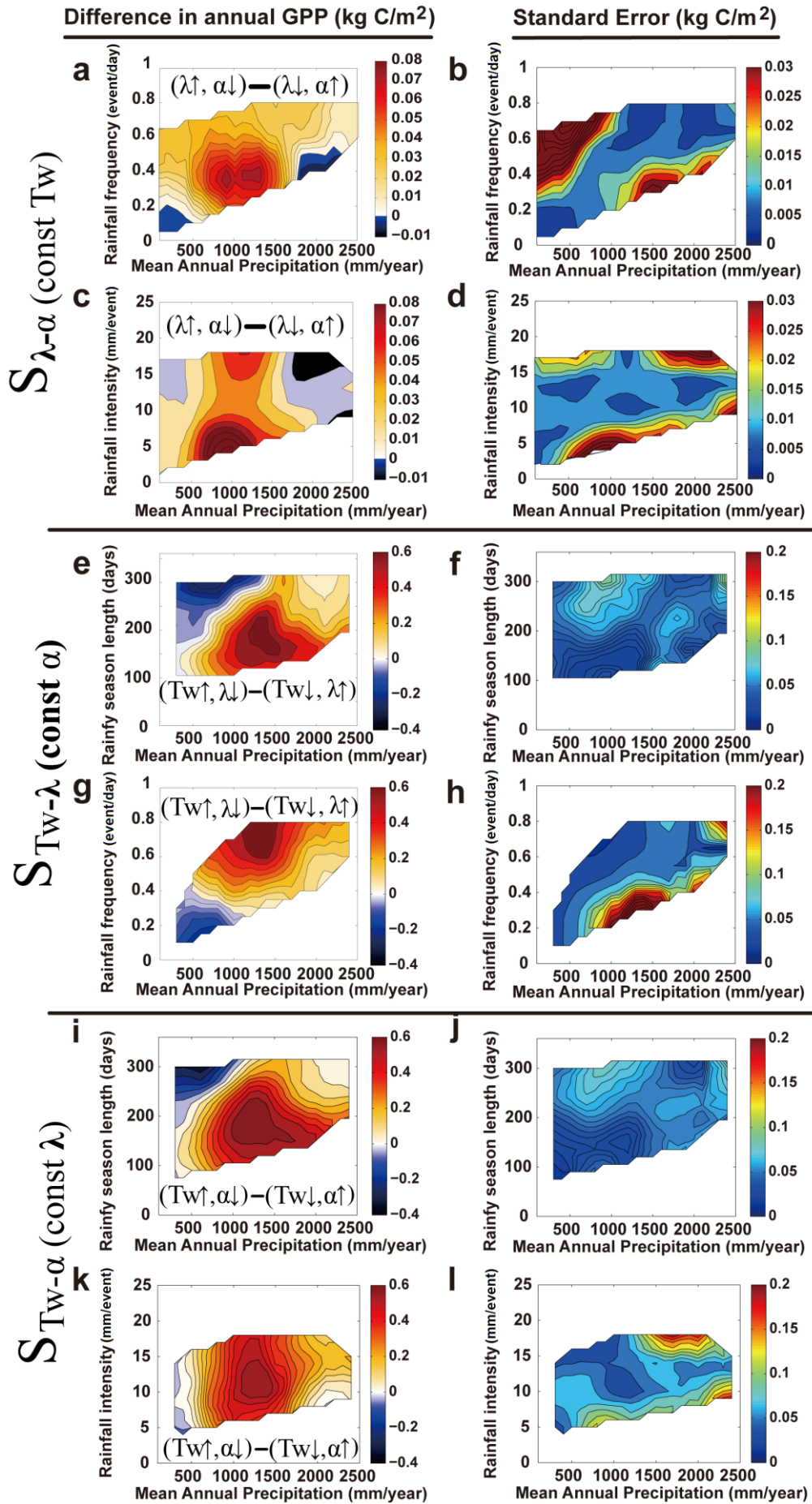


Figure 5. Differences in simulated annual GPP as a function of mean annual precipitation and one of the perturbed rainfall characteristics in all the three experiments (i.e. $S_{\lambda-a}$, $S_{TW-\lambda}$, S_{TW-a}) in the left column. The right column shows the correspondent standard errors (SE, calculated as $SE = \frac{\sigma}{\sqrt{n}}$, where σ refers to the standard deviation within each bin, n is the sample size in each bin, and n and σ are shown in Figure S4), with larger values associated with more uncertainties and requires more caution in interpretation. The contours are based on the binned values, with for each 100 mm/year in MAP, each 0.05 event/day in rainfall frequency, each 1 mm/event in rainfall intensity and each 15 day in rainy season length.

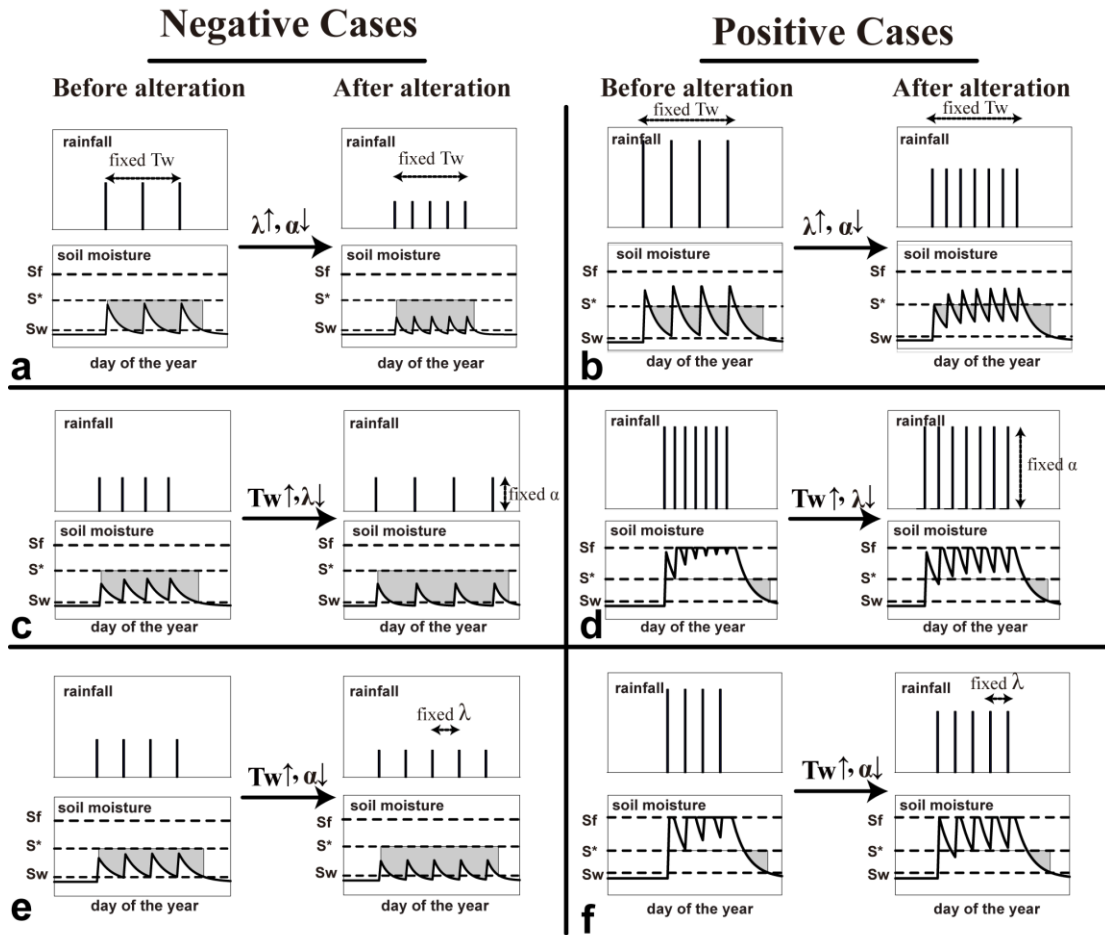


Figure 6. Illustrative time series for hydrological controls on plant root-zone soil moisture dynamics for all the experiments, and these illustrations are generalized based on the simulated time series from the experiments. Both negative and positive cases are shown, and cases with directly hydrological controls are shown (i.e. cloud-induced negative impacts in tropical forests are not shown). The cumulative shaded areas refer to “plant water stress” defined by Porporato et al. (2001).

Supplementary materials:

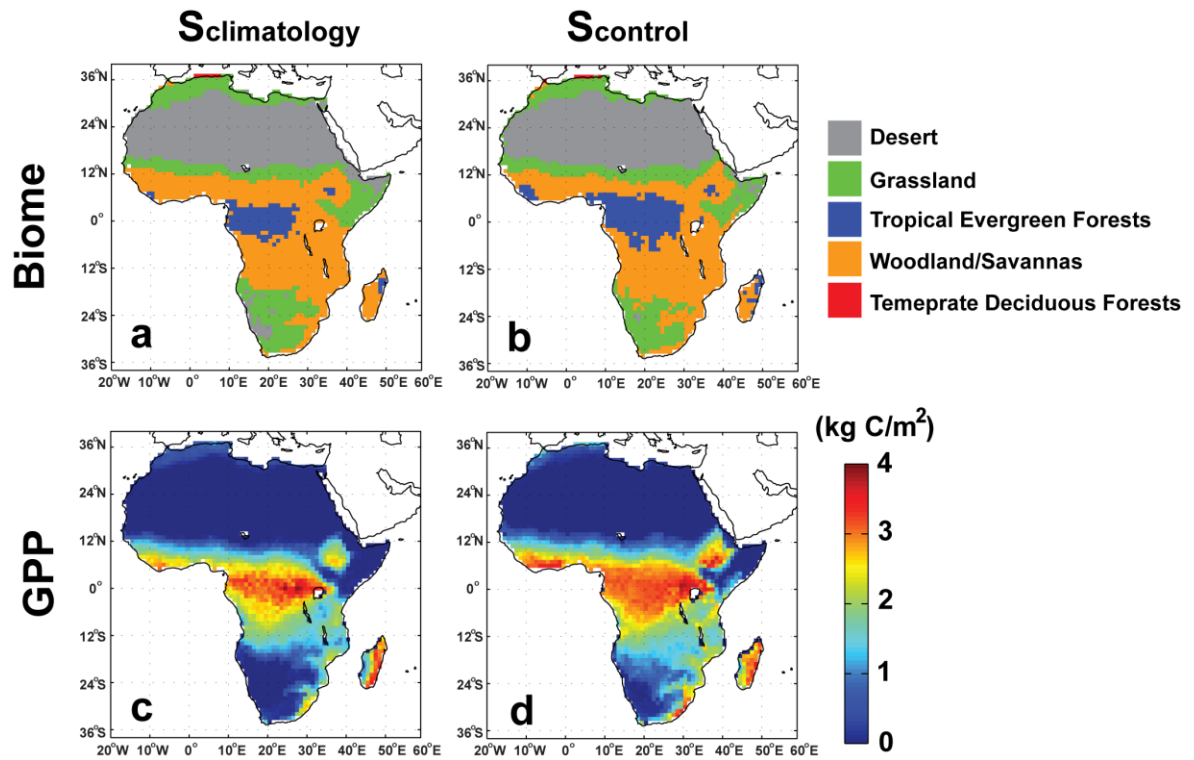


Figure S1. Comparison of biomes and annual GPP between $S_{climatology}$ and $S_{control}$ to test the validity of the synthetic weather generator. The biome definition follows Sato and Ise (2012).

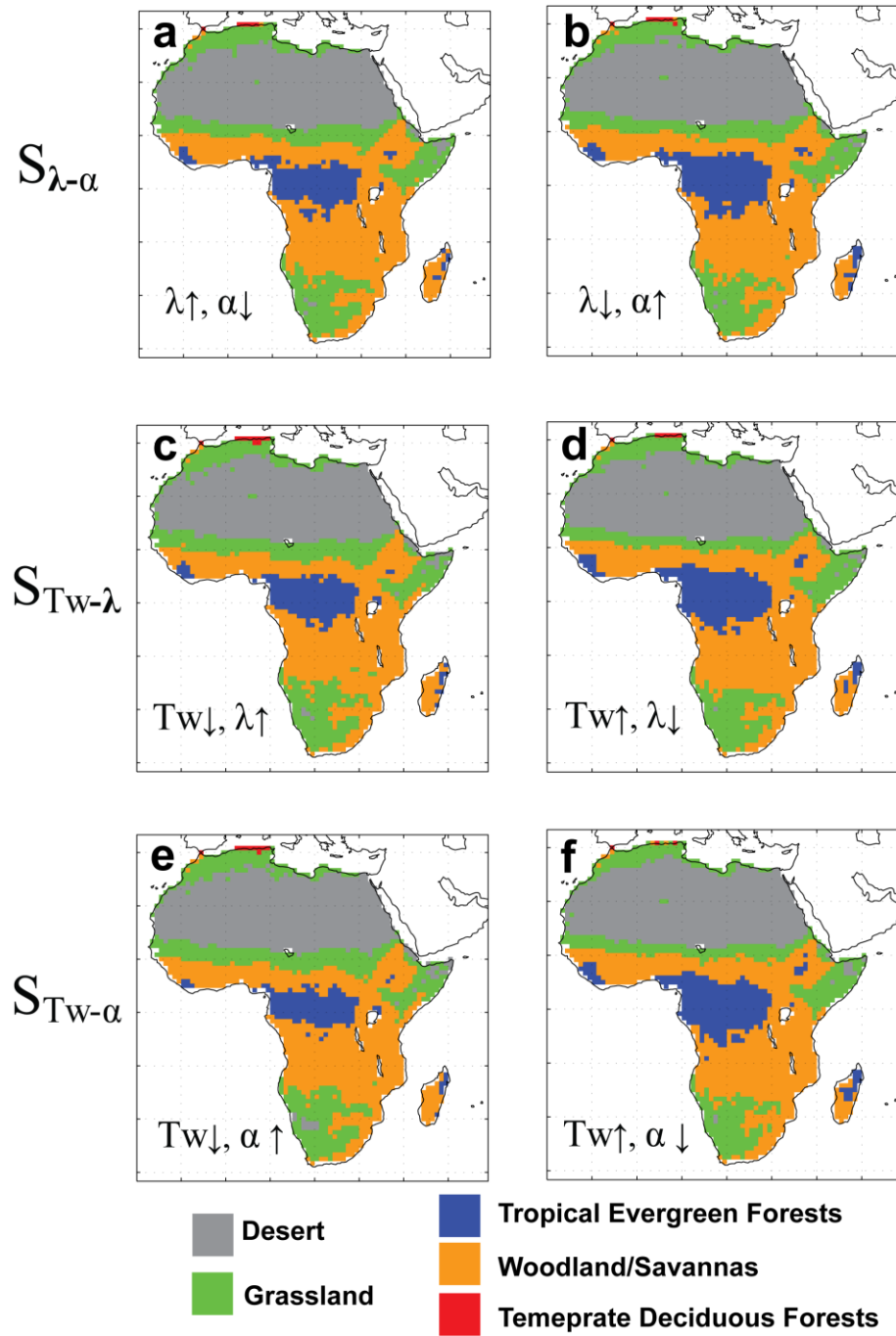


Figure S2. Simulated biomes for different experiments.

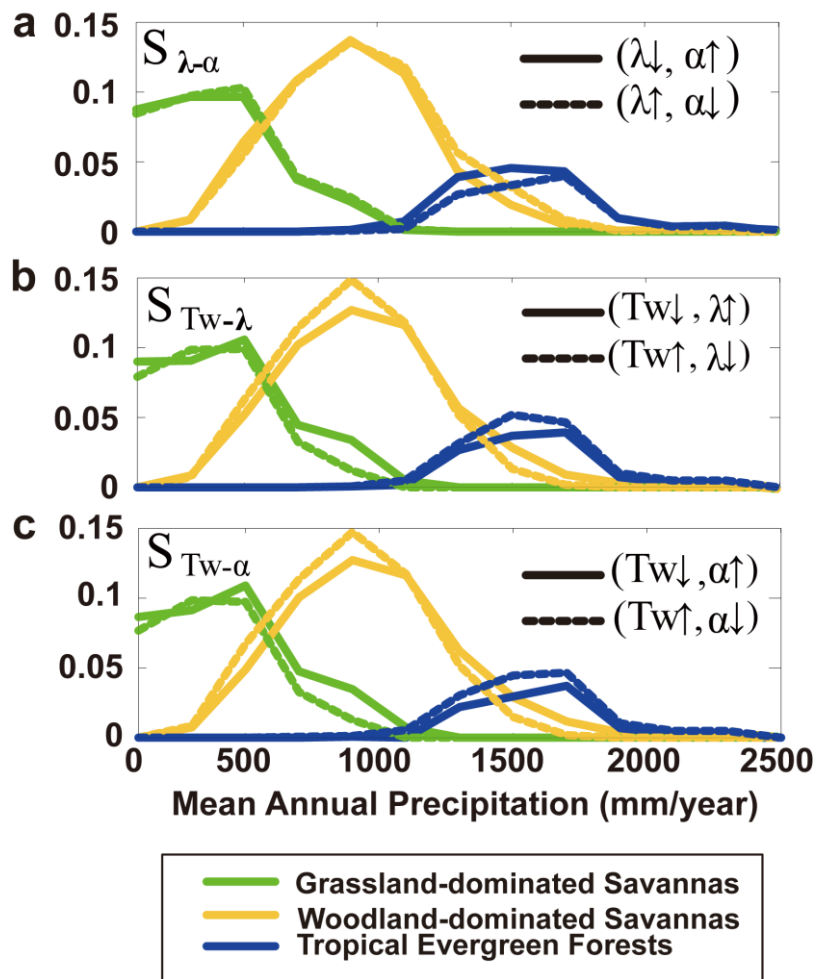


Figure S3. Normalized histograms of three simulated dominating biomes in the three experiments.

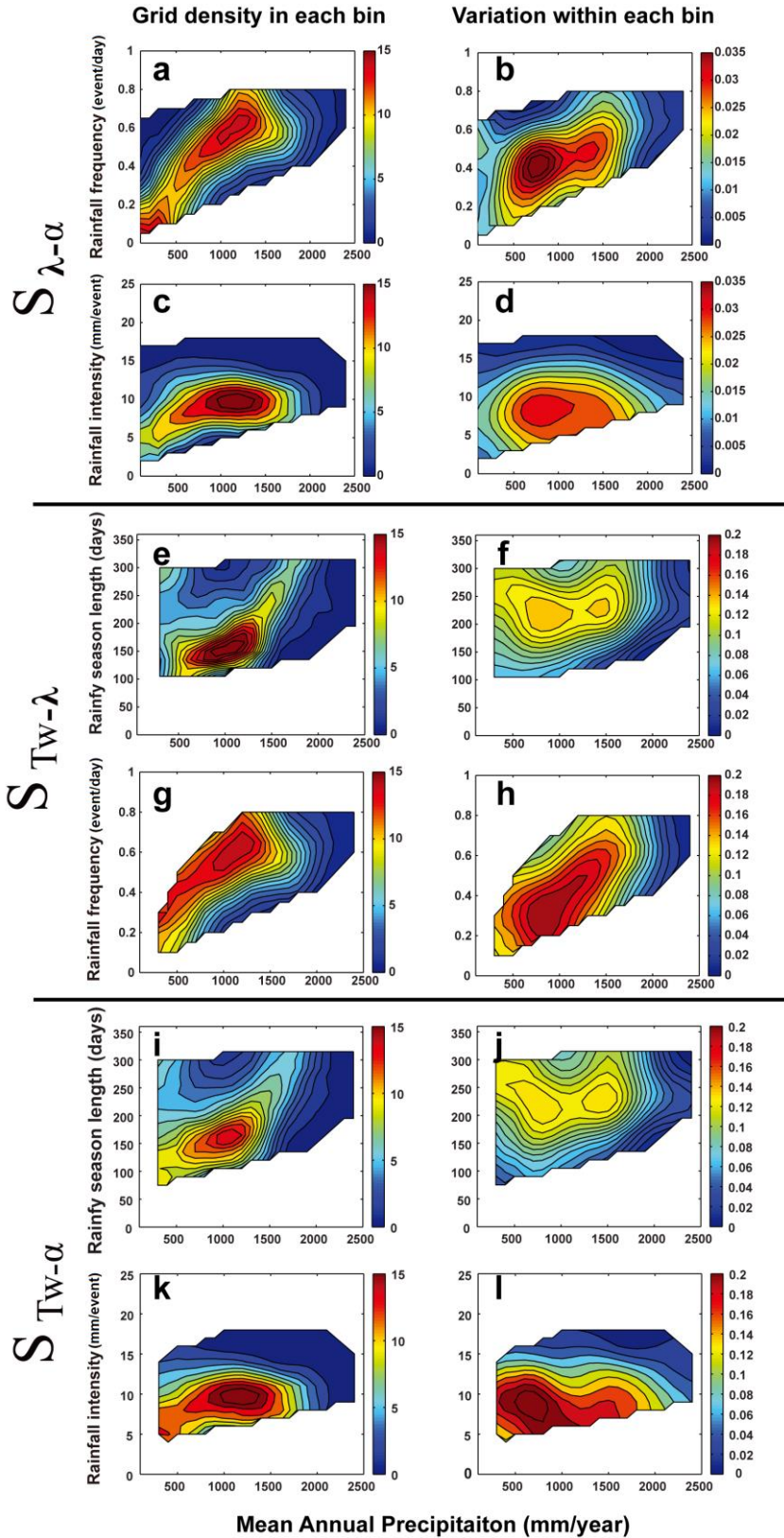


Figure S4. The sample size (n) in each bin (left column) and standard deviation (σ) in each bin (right column), corresponding to Figure 5. In Figure 5 right column, standard deviation (SE) is calculated as $SE = \frac{\sigma}{\sqrt{n}}$.